NKS-448
ISBN 978-87-7893-540-3

Detection of orphan gamma radiation sources in shielded building geometries by mobile gamma spectrometry. A method of using Compton scattered radiation to estimate the shielding mass thickness of common building material

Christopher L. Rääf[1], Robert R. Finck[1], Vikas C. Baranwal[5]
Jonas Boson[6], Antanas Bukartas[1], Marie-Andrée Dumais[5]
Kjartan Guðnason[4], Marjan Ilkov[4], Gísli Jónsson[4]
Mattias Jönsson[1], Simon Karlsson[6]
Marie Lundgaard Davidsdóttir[2], Frode Ofstad[5]
Jan Steinar Rønning[5], Petri Smolander[3]
Mikael Westin[6]

[1]Medical Radiation Physics, ITM, Lund University, Sweden
[2]Danish Emergency Management Agency, Denmark
[3]Radiation and Nuclear Safety Authority, Finland
[4]Icelandic Radiation Safety Authority, Iceland
[5]Geological Survey of Norway, Norway
[6]Geological Survey of Norway, Norway
[7]Swedish Radiation Safety Authority, Sweden

June 2021

Abstract

If nuclear or radioactive materials are out of control (materials out of regulatory control, MORC), authorities must deal with the threatening situation. Gamma-ray sources out of control can have various degrees of shielding. When located in a building the building material shields the source. Information on the shielding of an identified source will provide data to estimate the radiation hazard and assist in securing the source. In a Nordic joint project, a method to assess shielding mass thickness of common building materials in cases with hidden Cs-137 point sources have been studied and experimentally investigated using mobile gamma spectrometry. The method uses detection of Compton scatted photons of different energies in relation to primary photons to obtain approximate information about the mass thickness of shielding material between the source and the detector. These ratios follow the expression of exponential functions of shield mass thickness, provided the shield is composed mainly of materials where Compton interaction dominates. The shielding thickness assessment method is based on previous detector response calibration measurements for well-known shielding geometries, thus determining function parameters. In the experiments, attempts to determine shield thickness from a measured pulse height distribution using various NaI(Tl) spectrometers and applying the exponential function produced values within ±50% of the true value. When applying the method to a HPGe spectrometer, the difference between measured and actual values was less than ±10%.

Key words

Mobile gamma spectrometry, orphan sources, shielding

NKS-448
ISBN 978-87-7893-540-3
Electronic report, June 2021
NKS Secretariat
P.O. Box 49
DK - 4000 Roskilde, Denmark
Phone +45 4677 4041
www.nks.org
e-mail nks@nks.org

Detection of orphan gamma radiation sources in shielded building geometries by mobile gamma spectrometry

A method of using Compton scattered radiation to estimate the shielding mass thickness of common building material

NKS-B SHIELDMORC Final Report 2020
Contract: AFT/B(20)1
May 15, 2021

Christopher L. Rääf[1] (chair), Robert R. Finck[1] (co-chair), Vikas C. Baranwal[5], Jonas Boson[6], Antanas Bukartas[1], Marie-Andrée Dumais[5], Kjartan Guðnason[4], Marjan Ilkov[4], Gísli Jónsson[4], Mattias Jönsson[1], Simon Karlsson[6], Marie Lundgaard Davidsdóttir[2], Frode Ofstad[5], Jan Steinar Rønning[5], Petri Smolander[3], Mikael Westin[6]

[1]Medical Radiation Physics, ITM, Lund University, Sweden
[2]Danish Emergency Management Agency, Denmark
[3]Radiation and Nuclear Safety Authority, Finland
[4]Icelandic Radiation Safety Authority, Iceland
[5]Geological Survey of Norway, Norway
[6]Swedish Radiation Safety Authority, Sweden

Table of contents

About the final report

This is the final report from the NKS/SHIELDMORC activity (Contract: AFT/B(20)1). It presents a method of using mobile gamma spectrometry to estimate the thickness of building-type shielding material that may exist between a point-shaped gamma-ray source and a gamma spectrometer when searching for radiation sources out of regulatory control. The method is based on the fact that a source placed behind shielding material gives rise to an increased amount of Compton scattered radiation from the shield as the thickness of the shield increases counted in relation to the primary radiation penetrating directly through the shield. Lund University has performed gamma spectrometry with NaI(Tl) detectors and HPGe detectors at different distances from Cs-137 sources placed behind common building materials of different thickness to obtain a "knowledge library" that is used to estimate shielding mass thickness for this type of irradiation situation. The intention was to test the method in a joint field experiment where the Nordic participating teams would meet with each laboratory's mobile gamma spectrometers in Barsebäck in Sweden during three days in September 2020. However, the joint experiment could not be performed due to the covid-19 restrictions. Instead, each Nordic team conducted experiments at their home laboratory, led by instructions from Lund University. This report describes the theory and method applied in the "knowledge library" to obtain shield thickness from mobile gamma spectrometry, the instructions for the field experiments and the results and conclusions from the experiments.

Abstract

If nuclear or radioactive materials are out of control (materials out of regulatory control, MORC), authorities must deal with the threatening situation. Gamma-ray sources out of control can have various degrees of shielding. When located in a building the building material shields the source. Information on the shielding of an identified source will provide data to estimate the radiation hazard and assist in securing the source. In a Nordic joint project, a method to assess shielding mass thickness of common building materials in cases with hidden Cs-137 point sources have been studied and experimentally investigated using mobile gamma spectrometry. The method uses detection of Compton scatted photons of different energies in relation to primary photons to obtain approximate information about the mass thickness of shielding material between the source and the detector. These ratios follow the expression of exponential functions of shield mass thickness, provided the shield is composed mainly of materials where Compton interaction dominates. The shielding thickness assessment method is based on previous detector response calibration measurements for well-known shielding geometries, thus determining function parameters. In the experiments, attempts to determine shield thickness from a measured pulse height distribution using various NaI(Tl) spectrometers and applying the exponential function produced values within ±50% of the true value. When applying the method to a HPGe spectrometer, the difference between measured and actual values was less than ±10%.

Summary

The NKS activity SHIELDMORC addresses the problems of mobile detection of shielded gamma-ray sources, which is a very likely scenario when searching for sources out of regulatory control. The project took place for two years 2019-2020 with participants from all the Nordic countries.

In 2019, theoretical Compton scatter calculations were carried out for various shielding materials and distances between a gamma-ray point source and a detector. In addition, experiments with a mobile gamma spectrometer were performed which showed that the amount of Compton scattered photons from a shield in front of the source was depending on the mass thickness of the shield. The experiments also showed that this was only the case with shields containing materials of a low atomic number (2 - 25) where the Compton interaction effect dominates. If the source was shielded or collimated with a material with a high atomic number, such as lead, almost no Compton scattered photons from the shield could be detected in the spectrometer.

In 2020 the project was aimed to set up a “knowledge library” that could be used to determine shielding thickness and activity of shielded Cs-137 sources from pulse height distributions obtained by mobile gamma spectrometry. The aim was also to test its applicability in a joint Nordic field experiment. However, due to the Covid-19 pandemic, the joint field experiment could not be carried out in 2020. Instead, each northern team carried out a portion of the experience at home.

Lund University carried out a number of gamma spectrometry measurements with a NaI(Tl) spectrometer and a HPGe spectrometer using shielding geometries with different building materials, shield thickness and distances. From these measurements a “knowledge library” was set up with functions and parameters describing the relation between a pulse height distribution's count rate ratio from Compton scattered photons and primary photons as a function of shield mass thickness. The method is based on the fact that Compton scattering of photons is the dominant interaction process for photon energies between 150 and 1500 keV in the most common building materials.

In the method, the pulse height distribution from a Cs-137 source is divided into six regions of interest (ROI). These represent recordings of Compton scattered photons in the shield for different scattering angles and of primary photons that penetrated the shield in a direct line of sight between the source and the detector. The count rate of scattered photons in different energy ranges increases exponentially with increasing shield thickness. It has been possible to define a relation (Equation 1) between the net (background subtracted) ratios of the count rates for scattered radiation divided by the count rate for primary photons. Four equations can be configured for a NaI(Tl) detector and three equations for a HPGe detector. This allows for four and three separate calculations of the shield mass thickness for each measured pulse height distribution. The process to do so is described in detail in Appendix A. An excel calculation procedure facilitates the calculations.

When the shield thickness and the distance to the radiation source are known, the activity of the source can be calculated from the count rate of the primary radiation, provided that the detector efficiency is known.

The coefficients in the equation that determine the shielding thickness (Equation 2) from the measurement data depend on the efficiency of the detector. Detectors of the same active volume can be assumed to have approximately the same efficiency. Based on the team's measurements, it can be concluded that this is approximately correct, for 4 litre NaI(Tl) spectrometers and for HPGe detectors with a relative efficiency of 120%. For detectors with other volumes (efficiencies) the coefficients of Equation 2 have to be determined experimentally for each detector.

The “knowledge library” model for determining shield thickness from a measured pulse height distribution using NaI(Tl) detectors produced values within ±50% of the true value when taking all teams and detector volumes into account. For the HPGe detector used by SSM, the difference between the values of the ‘knowledge library' model and the true values was less than 10%. It was found that the slope of the exponential function is dependent on the detector volume. Therefore, greater accuracy can be achieved if the detector ROI selection and exponential function settings are determined individually for each detector instead of using general values for one detector type.

The experimental results of different teams generally revealed some differences between the actual shield thickness and that determined by spectrometry measurements using the “knowledge library”. The differences may be due to different settings of the ROI limits in the spectrometers as they had different numbers of channels. The deviations may also be due to the fact that the shielding geometries varied widely between the different teams' experiments. It would therefore be valuable to carry out complementary joint experiments with the various Nordic mobile systems in order to more closely determine the precision of the method in different shielding conditions.

1. Introduction

1.1 Background

Accidents with lost radioactive sources are rare, but have occurred from time to time. Since 1945, on average, one accident with orphan sources has occurred every two years, which has led to people suffering severe radiation injuries or death (UNSCEAR, 2011). There is also a threat that radioactive sources could be stolen, smuggled and used to intentionally harm people (IAEA, 2007). Authorities must maintain preparedness to deal with threatening situations where nuclear or radioactive material has gotten out of control (material out of regulatory control, MORC). Having the instruments, resources and ability to search for such sources is important to avert possible radiation threats. An important search method is mobile gamma spectrometry, which can be performed with instruments in airplanes, helicopters, and cars and also carried out on foot with portable instrumentation. (Hjerpe *et al*, 2001; Finck and Ulvsand, 2003; Kock *et al*, 2010, Nilsson, 2014).

The ability to detect gamma-ray sources at a distance is limited by the decrease in gamma radiation fluence due to the "inverse distance square law" and the attenuation of the radiation in air and other materials that may be present between the source and the detector. In an NKS-funded project, maximum detection distances for unshielded gamma-ray sources have been investigated through theoretical calculations and practical field experiments. (Rääf et al, 2019). It was shown that the maximum distance at which a source can be detected with a certain probability in mobile gamma spectrometric search depends on several parameters, including the activity of the source, the efficiency of the detection instrument, its speed past the source, the acquisition time interval and the selected alarm level indicating the presence of a source, without too many false positive indications.

Gamma-ray sources out of control can be more or less shielded. A shielded source will be more difficult to detect. It will appear to have lower activity than it really has, because the primary radiation is attenuated in the shield. The situation may pose a potential hazard when the source is going to be retrieved and secured. Information of whether the source is shielded or not, and if it is shielded, having a way to assess the shield thickness, will provide input to estimate the radiation danger and facilitate securing the source.

Determining the shielding of an orphan gamma-ray source requires longer measurement times than needed to simply discover the presence of a source. A moving measuring device may need to make a halt for a while to perform the measurement stationary. Although it takes some time, it is justified as it can provide important information about the source shielding.

1.2 Aim of the project

The SHIELDMORC 2019 project (Rääf et al, 2020) has provided information on how Compton scattered photons from shielded gamma-ray sources contribute to the energy region of a gamma spectrometer's pulse height distribution below the full energy peak. In the present project, measured spectrometric data from Lund University for shielded radiation sources have formed a “knowledge library”, which describes the relation between the shield mass thickness and the count rate ratios in different energy regions for specific NaI(Tl) detectors and HPGe detectors. The objective is to use the “knowledge library” in mobile gamma spectrometry to determine the mass thickness of commonly used building materials between a Cs-137 source and a detector and to investigate the applicability of the method for different spectrometry systems used in the Nordic countries.

2. Theory and method

The method of determining the thickness of radiation shielding material that may be present in connection with a gamma-ray point source is based on comparing the fluence of Compton scattered radiation from the shield with the fluence of primary radiation penetrating the shield. This ratio increases with increasing shield thickness. If the degree of increase is known for various shielding material, it may provide an opportunity to determine the thickness of radiation shields from gamma spectrometry measurements.

2.1 Compton interaction in shielding material

From the theory of photon interaction with matter, it is well known that the probability of Compton scattering per atom is proportional to the atomic number, i.e. the number of electrons per atom. Except for hydrogen, all substances have approximately the same number of electrons per gram of matter. Thus, when counted per unit mass, the Compton interaction is independent of the atomic number of the matter. For photon energies where Compton interaction is the dominant process the probability that a photon of a given energy will undergo Compton scattering will be proportional to the mass thickness (kg/m^2) of the material. Therefore, the mass attenuation coefficient for Compton scattering is constant at a given energy for different materials (except for hydrogen). The mass attenuation coefficient gradually decreases as the photon energy increases (Knoll 2010).

Building materials primarily contain low-atomic-number components. Common substances in building materials include hydrogen (1), carbon (6), oxygen (8), aluminium (13), silicon (14), calcium (20), manganese (25) and iron (26). For these substances (with the exception of hydrogen), Compton scattering is the dominant interaction process for photon energies between 150 keV and 2000 keV.

Figure 1 shows the mass attenuation coefficient for elements with atomic numbers from 1 to 25 for photon energies 100 keV to 2000 keV. From the Figure one can see that the mass attenuation coefficient is nearly constant over the range of atomic numbers at a given energy, except for hydrogen and energies below 150 keV, where the photoelectric effect contributes more significantly.

When the energy of a photon is reduced by a Compton scattering event, the probability of a second Compton event occurring on the scattered photon increases. Thus, as the radiation penetrates more deeply into the shield, its Compton energy spectrum moves towards lower energies. By measuring the energy spectrum after the shield and comparing with the primary (not scattered) fluence through the shield, one should be able to assess the shield mass thickness. The method could be expected to be almost independent of the exact composition of the material, as long as the material does not contain substances with high atomic numbers where photoelectric interaction is the dominating effect.

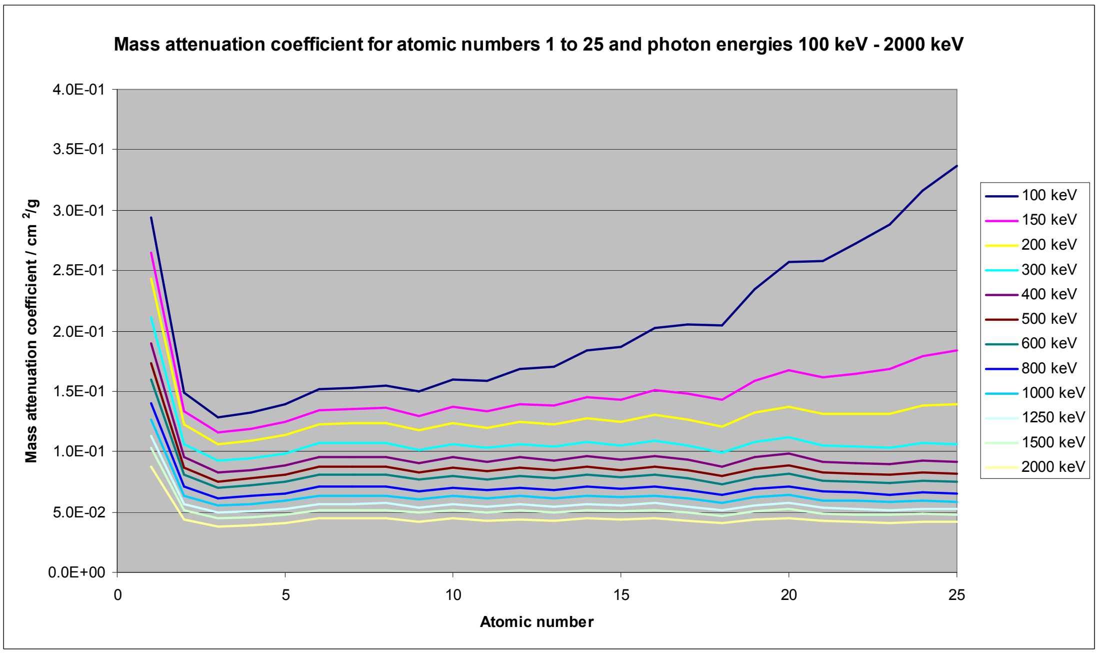

Figure 1. Mass attenuation coefficients for atomic numbers 1 - 25 at photon energies from 100 keV to 2000 keV. Compton scattering of photons is the dominating effect. The mass attenuation coefficients at energies 150 - 2000 keV are nearly constant for atomic numbers 2 - 25, elements that are main components in common building materials. The values are taken from Hubbell and Seltzer (2004).

2.2 Compton scattering angles in shielding material

If a single-scattered Compton photon from the shielding material is to be registered in the detector, then the original photon must leave the source at a certain angle in relation to the source-detector direction. Figure 2 shows examples of this. If the distance between the shield and the detector is long in relation to the size of the detector, the angle of the original photon must be larger than 0 and less than 90 degrees. For a Cs-137 source, the Compton photons emerging from the shield will then have energies ranging between 288 keV and 661 keV. Compton scattered photons with energies lower than 288 keV, are either scattered at least once in material behind the source or are the result of multiple Compton scattering in material somewhere around the source, in the air between the source and detector or in material near the detector.

2.3 Detector response for shield mass thickness

The interaction effects in the detector cause a distortion of the energy distribution of the photons recorded in the detector with respect to the fluence of the photons affecting the detector. This is due, among other things, to the detector's limited energy resolution capability and to the fact that part of the photons interact by Compton scattering in the detector and escape from the detector. The conversion of the pulse height distribution recorded in the gamma spectrometer into the photon fluence impacting on the detector is a complex task. It is not done here. Instead, pulse height distributions are measured with increasing shielding thickness assemblies. Functions describing count rate ratios for different energy regions with respect to shielding thickness are defined and described digitally. This will calibrate the detector response for shield thickness. The response function depends on the detector type, volume and the photon energy of the source. It is here called a “knowledge library”. The thickness of an unknown shield can then be obtained by a gamma spectrometry measurement using the calibrated detector response function from the “knowledge library". The detector response function must be obtained with the natural radiation background subtracted, since only the photon fluence from the radiation source and the shield is to be included in the function.

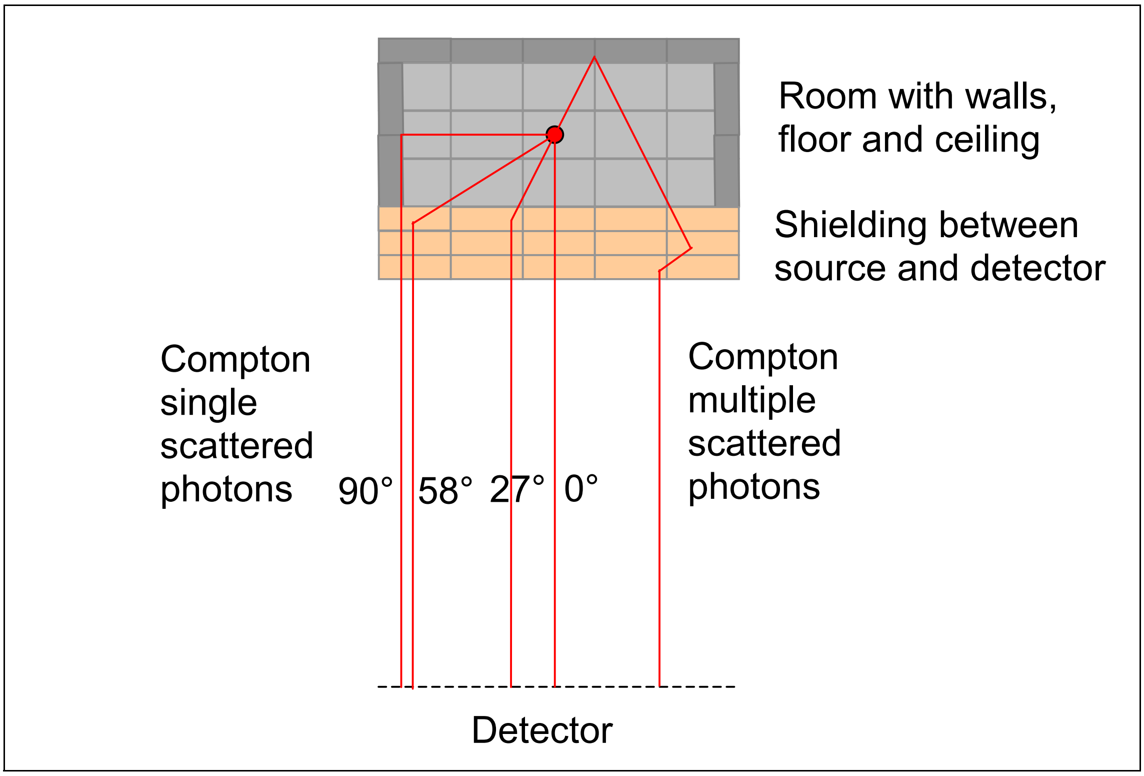

Figure 2. Schematic drawing showing examples of Compton scattering of photons from a gamma ray source placed in a room with floor, ceiling and walls and a shielding material between the source and the detector. Single scattering of photons between 0 and 90 degrees that can reach the detector will take place in the shielding material and the sidewalls. For Cs-137 primary photon energy 662 keV, these photons will have energies between 288 and 662 keV. Single scattered Compton photons in material behind the radiation source will have energies between 184 and 288 keV. Multiple scattered photons can have any energy within the entire range 0 - 662 keV at the detector, but with higher probability at lower energies.

2.4 Using a region-of-interests (ROI) method

The pulse height distribution of a gamma-ray spectrometer may contain hundreds or thousands of channels. To make it easier to use a response function with different spectrometers, the channel region around the full energy peak and parts of the lower energy zones have been divided into regions of interest (ROI). ROIs have fixed energy limits and the count rates within each ROI are summed. The relation between the count rates in the lower energy ROI and the count rate in the full energy peak is used in the response function. Because different spectrometers may have different number of channels, the energy width of a channel may vary. Therefore, the ROI limits expressed in channel numbers may vary from one instrument to another.

In the case of a source with Cs-137 measured by a NaI(Tl) spectrometer, six ROIs are proposed here. Three represent photon energies of Compton scattered photons and three represent combinations of primary and scattered photons. Due to the low energy resolution of a NaI(Tl) spectrometer, it is not possible to obtain a ROI containing only registrations from primary photons. However, by dividing the full energy peak into three sub-components, it is possible to approach the ideal case of recording primary and scattered photons separately. For a gamma spectrometer with an energy width of 3 keV per channel the ROI energy limits have been chosen as ROI A (77-239 keV), ROI B (245-407 keV), ROI C (413-575 keV), ROI PL (581-659 keV), ROI PC (662 keV) and ROI PR (665-743 keV). The full energy peak ROI limits for PL, PC and PR are suitable for a gamma spectrometer that has a NaI(Tl) detector. A high-resolution gamma spectrometer with germanium detector, HPGe, may have narrower PL and PR regions to the left and right of the central channel PC.

The six ROIs represent the following photon energy regions (with limits rounded to whole numbers):

ROI A. 77 - 239 keV, contains Compton scattered photons 110 - 180 degrees in the material behind the source and on its sides, multiple scattered photons and interaction effects in the detector and its surroundings.

ROI B, 245 - 407 keV, contains Compton scattered photons 58 - 110 degrees in the shielding material between the source and detector and in the material surrounding the source, multiple scattered photons and interaction effects in the detector and its surroundings.

ROI C, 413 - 575 keV, contains Compton scattered photons 27 - 58 degrees in the shielding material between the source and detector, multiple scattered photons and interaction effects in the detector and its surroundings.

ROI PL, 581 - 659 keV, contains Compton scattered photons 0 - 27 degrees in the shielding material between the source and detector, primary photons from the source that have penetrated through the shield, some small angle multiple scattered photons and interaction effects in the detector and its surroundings.

ROI PC, 662 keV, contains primary photons from the source, some small angle scattered photons and interaction effects in the detector and its surroundings.

ROI PR, 665 - 743 keV, contains primary photons from the source, a minor contribution of small angle scattered photons and interaction effects in the detector and its surroundings.

Depending on the number of channels and the setting of the gain in a gamma spectrometer the conversion between photon energy and channel number can be set differently for different measuring systems. This makes the translation of energy interval to channel interval more or less rough from system to system. In order to be able to compare the response of multi-channel analyzers with different numbers of channels and gains, the translation from energy interval to channel interval needs to be made as similar as possible for different systems.

Table 1 provides examples of ROIs for different conversion gains and energy widths per channel.

Figure 3 shows how the six ROIs are defined for a pulse height distribution from a Cs-137 source measured by a NaI(Tl) spectrometer.

Table 1. Suggested ROIs with energy interval limits given in keV for detecting primary and scattered photons measured by a gamma spectrometer having 1024, 512 or 256 channels corresponding to channel widths of 3, 6 or 12 keV/channel. The peak area ROI is suitable for a NaI(Tl) spectrometer and divided into three sub-components: left peak area (PL), center channel (PC) and right peak area (PR).

ROI	Energy node (keV)	Compton scattered degree	3 keV/ch (keV)	ROI width chs	6 keV/ch (keV)	ROI width chs	12 keV/ch (keV)	ROI width ch
	74							
A			77-239	55	80-236	27	86-230	13
	242	110						
B			245-407	55	248-404	27	254-398	13
	410	58						
C			413-575	55	416-572	27	422-566	13
	578	27						
PL			581-659	27	584-656	13	590-650	6
PC	662	0	662	1	662	1	662	1
PR			665-743	27	668-740	13	674-734	6
	746							

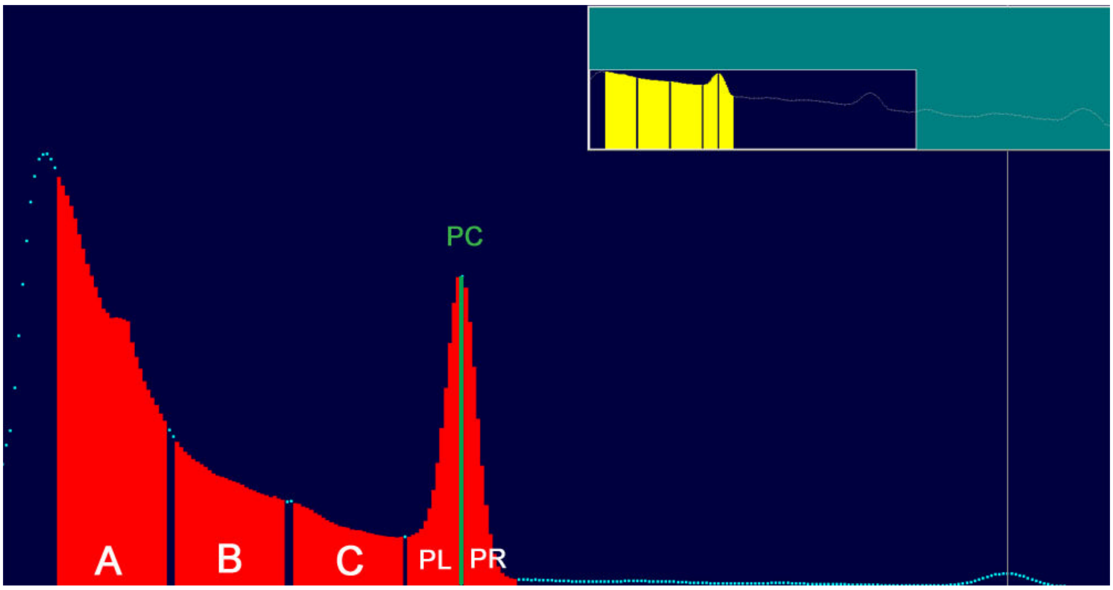

Figure 3. Net (background subtracted) pulse height distribution showing the ROIs defined in Table 1 for a Cs-137 source used in a function for calculating the mass thickness of a shield (kg/m^2) between the source and the detector from a pulse height distribution recorded by a NaI(Tl) spectrometer. The full energy peak is divided into three ROIs (PL, PC and PR). Compton scattered photons from the source and photon interaction effects in the detector are registered in the three ROIs (A, B and C).

2.5 The "knowledge library" function to obtain shield mass thickness

In preparation to find function values for the defined ROIs to determine shield mass thickness from gamma spectrometry data, Lund University performed sets of measurements with a 4 litre NaI(Tl) spectrometer in various geometries. Measurements were performed with different shielding materials commonly used in buildings (wood, clay tiles, concrete blocks) and different shield thickness and distances between the source and the detector. (For the results see Figure LU1 for a 4 litre NaI(Tl) spectrometer and Figure LU2 for a 123% HPGe spectrometer). From these measurements a model (the LU model) was designed that could provide the mass thickness of a shield from the net (background subtracted) count rate ratios of ROI's A/PR, B/PR, C/PR and PL/PR, here denoted as q. It was found that exponential functions, with parameters a and b, could be fitted to provide the net count rate ratios q from the mass thickness x according to

$$q = a\,e^{bx} \tag{1}$$

Solving Equation (1) to obtain the mass thickness x is done by using

$$x = \frac{\ln(q/a)}{b} \tag{2}$$

The values of a and b of the exponential function q for each of four count rate ratios (A/PR, B/PR, C/PR, PL/PR) for the LU model are given in Tables LU1 and LU2. They apply to a 4-litre NaI(Tl) spectrometer and a 123% HPGe spectrometer, respectively.

Each team performed its own gamma spectrometry measurements to see to what extent the LU model using ROI net count rate ratios could describe shield mass thickness according to Equation 2. Measurement procedures and results are described in more detail in the following chapters.

3. Equipment and measurements

As stated in the theory section, for a Cs-137 source, a gamma spectrometer's pulse height distribution is divided into six ROIs, where the first three (A, B, C) represents Compton scattered radiation and the other three represents a combination of Compton and primary radiation from the source (PL, PC, PR). The method for determining the shield thickness is based on ratios between the net (background subtracted) count rates in the first three and the second three ROIs. This must be determined experimentally for specific detectors and varying shield thicknesses. Lund University carried out such determinations as described below. The result forms the "knowledge library" describing the function parameters required to obtain shield mass thickness from a measured pulse height distribution. Each Nordic team then made test measurements in their own country using their mobile gamma spectrometers in geometries with shielded Cs-137 sources to investigate how well the "knowledge library" function can provide the mass thickness of the shields.

3.1 Gamma spectrometers used to obtain the "knowledge library"

Lund University used a 4 litre NaI(Tl) gamma spectrometer (Exploranium) having 512 channels and 5.8 keV/channel conversion gain. The short side of the detector has an area of 10 x 10 cm^2 and the long side is 20 cm, which means that the detector has an uneven angular response. In all measurements, the detector was oriented longitudinally toward the radiation source, resulting in maximum efficiency. The ROI selections for the NaI(Tl) spectrometer are given in Table 2.

In addition a 123% high resolution HPGe spectrometer (Ortec) having 4096 channels and a conversion gain of 0.73 keV/channel. The cylindrical detector has approximately the same diameter as the length along the mantle surface. It provides near uniform efficiency for all angles of incidence except where the cryostat is shielded. The detector was directed so that the incoming photons from the radiation source hit the surface of the mantle. ROI selections for the HPGe spectrometer are given in Table 3.

Table 2. ROI application for the Lund University 4 litre NaI(Tl) spectrometer system (Exploranium) using a conversion gain of 512 channels and setting the energy calibration for Cs-137, 661.66 keV in channel 113.

ROI	Compton scattered degree	Channel numbers	Photon energy keV	Number of channels
Node		13	75	1
ROI A		14-40	81-233	27
Node	110	41-42	238-244	2
ROI B		43-69	250-402	27
Node	58	70-71	408-414	2
ROI C		72-98	420-573	27
Node	27	99	579	1
ROI PL		100-112	585-656	13
ROI PC	0	113	662	1
ROI PR		114-126	667-738	13
Node		127	744	1

Table 3. ROI application for the Lund University 123% HPGe spectrometer system using a conversion gain of 4096 channels and setting the energy calibration for K-40, 1460.86 keV in channel 2000.

ROI	Compton scattered degree	Channel numbers	Photon energy keV	Number of channels
Node		102	74.62	1
ROI A		103-331	75.35-241.80	229
Node	110	332	242.53	1
ROI B		333-561	243.26-409.73	229
Node	58	562	410.46	1
ROI C		563-791	411.19-577.68	229
Node	27	792	578.41	1
ROI PL (NaI)		793-893	579.14-652.16	101
Node		894	652.86	1
ROI PL		895-905	653.63-660.93	11
ROI PC	0	906	661.66	1
ROI PR		907-917	662.39-669.69	11
ROI P		895-917	653.63-669.69	23
Node		918	670.36	1

3.2 The shielding geometry for creation of the "knowledge library"

The "knowledge library" was only created for Cs-137. The Cs-137 point sources had activities 66, 260 and 1200 MBq. Sources were selected depending on shield thickness and distance to the source so that the dead time of the spectrometer was kept low, but which still gave discernible measurement results above the natural background. Acquisition times ranged from tens of minutes to several hours to maintain statistical counting uncertainties at or below 1%. Examples of acquisition times needed to obtain 1% uncertainty in the final result for a 4 litre NaI(Tl)-detector for combinations of source activity, distance and shield thickness is given in Appendix A, Table A.2.

The source was placed in a 'cave' to imitate the location inside a building with a floor, walls and a ceiling. The "cave" was built with concrete tiles and with burnt clay tiles on top of it. The front opening, where the shielding material was placed was somewhat larger than the minimum dimensions of 32 cm wide and 21 cm high to allow Compton photons generated in the front shield up to 60 degrees to reach the spectrometer. Figure 4 shows a photo of the "cave". The dimensions and density of the material used in the shield are given in Table 4.

The distance between the source and the detector was 10 m in most measurements, but a few sets of measurements were made at longer distances, up to 90 m, to check the effect of Compton scattering in the air between the source with shield and the detector.

Table 4. Materials used in the shield for measurements to obtain the "knowledge library"

Material	Dimensions (width, height, thickness)	Density
Concrete tiles	20.0 x 13.3 x 5.0 cm	2270 kg/m^3
Burnt clay tiles	24.5 x 12.0 x 5.0 cm	2095 kg/m^3
Wood beams	120.0 x 12.0 x 4.5 cm	526 kg/m^3

Figure 4. A "cave" built for the source with concrete tiles as "floor" and "walls" and clay tiles as "ceiling". The front opening width should be at least 32 cm and the height at least 21 cm (16 cm above the "floor"). This is to allow Compton scattering in angles between 0 and 60 degrees in the front shield. The source must be placed behind the "front wall" shielding, not more than 7 cm from the inner side of the shielding wall. The plastic cup marks the place for the source.

Figure 5. A shield built with 5 burnt clay tiles in front of the "cave". The tile thickness is 5 cm.

3.3 Teams experimental setups and measurements

The teams performed their measurements at their home location according to the instructions documented in Appendix A.

Radiation shields were generally built with blocks of wood, brick or concrete, i.e. common building materials. Most of the teams utilized one of the materials. The shield thickness was usually varied in steps of 5 cm up to 20 or 30 cm. IRSA, Iceland used a concrete wall. The distance between the source and the detector ranged from 10 to 90 m in the experiments. The air shielding effect was taken into account in the calculation of shield mass thickness. Table 5 lists detectors, shielding materials and geometries used in the experiments.

Details of each team's measurement configuration and shielding geometry are presented in Appendix B.

Table 5. List of the combinations of detector type, shielding material, shield thickness and distances between the source and the detector used by the teams in the SHIELDMORC 2020 experiments.

Team	Detector	Shielding material	Shield thickness / cm	Distance / m
LU model	4 L NaI(Tl)	air only		10
		wood	4.5, 9, 13.5, 18, 22.5, 27, 31.5, 36	10
		clay tiles	5, 10, 15, 20, 25, 30	10
		concrete blocks	5, 10, 15, 20, 25, 30	10
SSM	4 L NaI(Tl)	air only		50
		wood	9, 18, 27, 36	50
		concrete blocks	5, 10, 15, 20, 25, 30	50
DEMA	4 L NaI(Tl)	clay tiles	5, 10, 15, 20, 30	20
STUK	4 L NaI(Tl)	concrete blocks	10, 20, 30	10, 20
IRSA	2 L NaI(Tl)	air only		20
		concrete wall	20	10, 20
NGU	16 L NaI(Tl)	concrete blocks	5, 10, 15, 20, 25, 30	55
LU model	HPGe 123%	air only		50, 90
		wood	4.5, 9, 13.5, 18, 22.5, 27, 31.5, 36	30
		clay tiles	5, 10, 15, 20, 25, 30	30, 50
SSM	HPGe 120%	air only		50
		wood	9, 18, 27, 36	50
		concrete blocks	5, 10, 15, 20, 25, 30	50

4. Results and discussion

The results presented here are the model parameters in the ”knowledge library” that make it possible to determine shield thickness from gamma spectrometry measurements and the results from the individual teams' test measurements for different shields using the model from the “knowledge library".

4.1 Examples of measured shielding results from Lund University

Results from shielding measurements with a Cs-137 point source at 10 m distance and different thickness of concrete shielding using a 4 litre NaI(Tl) spectrometer is shown in Fig 6. The pulse height distribution is normalized so that net (background subtracted) count rate at 662 keV is set to 100 for all measurements. In this way one can see the increased contribution of scattered radiation to lower energies with increased shielding thickness.

There is also a small contribution of scattered radiation from the Compton interaction with materials on the side of the detector and behind the detector. These contributions are nearly insignificant compared with the number of photons from Compton scattering in the shield in front of the source. This is because scattered photons from the side and back have lower energy and are more easily absorbed in the shield in front of the source so that only a small percentage reaches the detector.

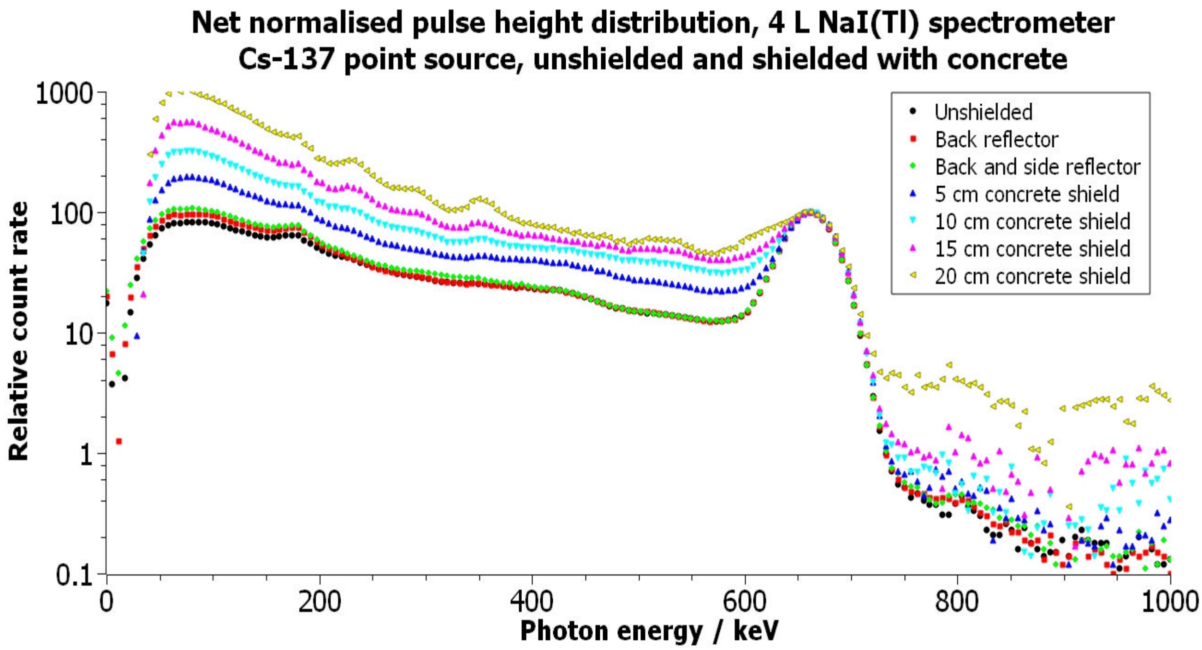

Figure 6. Net (background subtracted) normalised pulse height distribution of photons registered from a Cs-137 point source with varying thickness of concrete shielding between the source and a 4 litre NaI(Tl)-spectrometer. The source-detector distance is 10 m. The maximum count rate in the center channel (661.66 keV) of the full energy peak is set to 100 for all measurements. Using concrete tiles behind the source and on its sides increases the registrations of Compton photons (single and multiple scattered) from the unshielded source for initial scattering angles between 90 and 180 degrees, producing photons with energies below 288 keV (denoted as Back reflector and Back and side reflector).

Net normalized count rate results using a 123% HPGe spectrometer at 50 m distance and different thickness (5 - 30 cm) of burnt clay brick as shielding (Photo in fig 5) is shown in Fig 7. The larger statistical fluctuation in count rates compared to the pulse height distribution obtained by NaI(Tl) spectrometry is due to lower efficiency of the HPGe spectrometer and use of shorter measurement times.

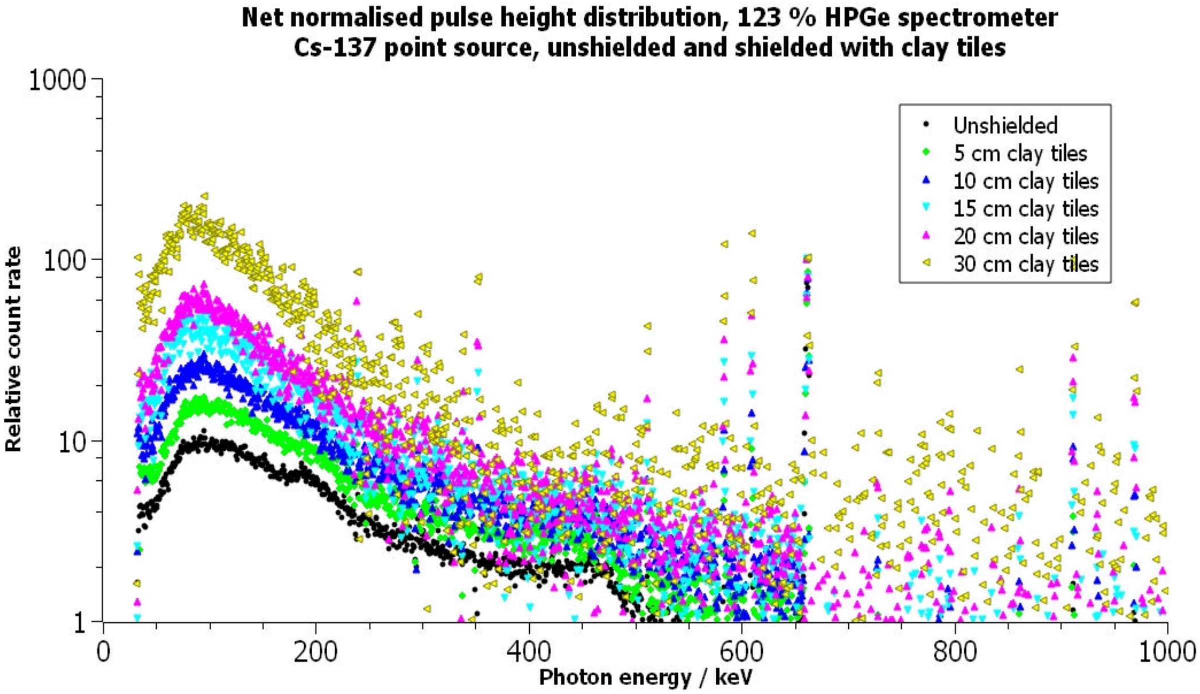

Figure 7. Net (background subtracted) normalized pulse height distribution of photons registered from a Cs-137 point source with varying thickness of burnt clay tiles shielding between the source and a 123% HPGe spectrometer. The source-detector distance is 50 m. The maximum count rate in the center channel of the full energy peak (661.66 keV) is set to 100 for all measurements. Due to some gain drift when measuring the background, remnants of full energy peaks from naturally occurring radionuclides are seen. Registrations for photon energies higher then the full energy peak of Cs-137 are due to low-probability pile-up pulses having high statistical uncertainty.

4.2 The “knowledge library” for determining shield thickness

From a series of shielding measurements on building materials with a Cs-137 point source, Lund University has calculated quotients between net count rates for Compton scattered photons (ROI A, B, C and PL) and primary photons (ROI PR). These quotients provided straight lines in a semi-logarithmic diagram as a function of the mass thickness of the shield. See Fig LU1 for the 4 litre NaI(Tl) spectrometer and Fig LU2 for the 123% HPGe spectrometer.

The A/PR, B/PR, C/PR and PL/PR quotients were fitted to exponential functions as a function of the shield thickness according to Equation 1.

The values of the coefficients *a* and *b* are given in Table LU1 for the 4 litre NaI (Tl) spectrometer and in the Table LU2 for the 123% HPGe spectrometer. The coefficients are valid for all types of building material having main components up to atomic number 26 (iron), presuming that the source is not shielded by high atomic number material such as lead.

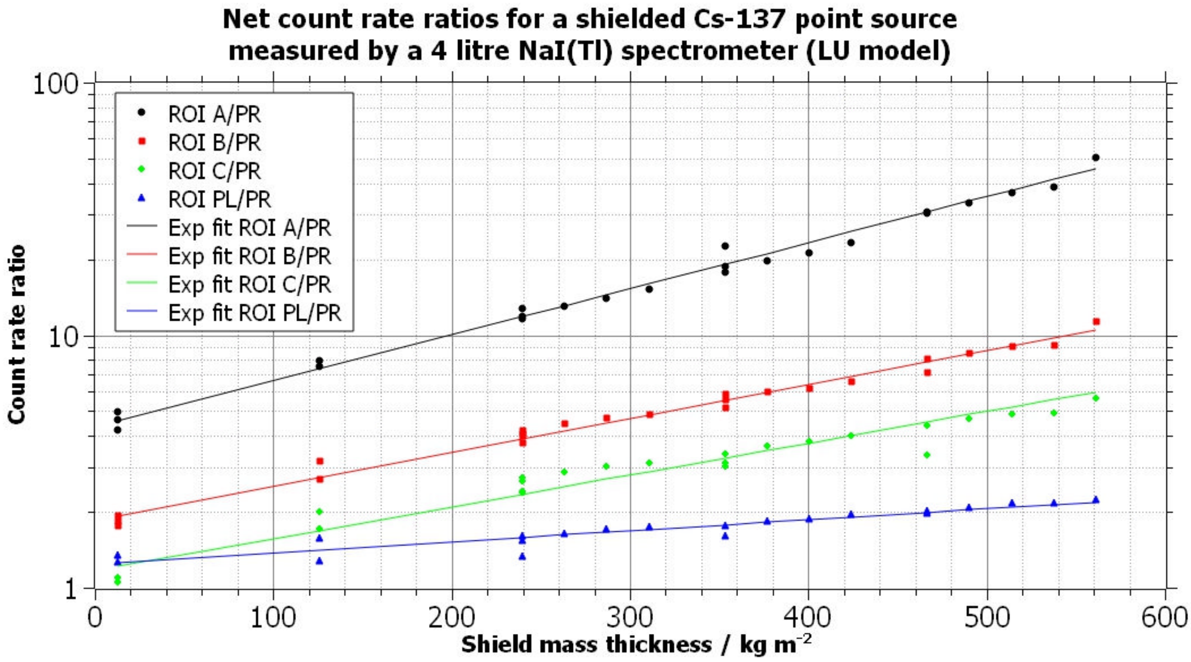

Figure LU1. Net (background subtracted) count rate ratios A/PR, B/PR, C/PR and PL/PR as functions of shield mass thickness for registrations in the ROI photon energy intervals A, B, C, PL and PR according to the definition in Table 1 (and approximated according to Table 2). The straight lines are fitted exponential functions to measured values. The coefficients are given in Table LU1. Functions are valid for measurements with a 4 litre NaI(Tl)-spectrometer with its elongated (0.04 m^2) side facing the source. The mass thickness of the air between the source and the detector is included in the shield mass thickness values.

Table LU1. Coefficients *a* and *b* in Equation 1 and 2 for obtaining the shield mass thickness (kg/m^2) from the measured ROI net cps quotients *q* when using a 4 litre NaI(Tl) spectrometer (LU model).

ROI net cps quotient type for *q*	*a*	*b*
ROI A/PR	4.32	0.0042
ROI B/PR	1.85	0.0031
ROI C/PR	1.17	0.0029
ROI PL/PR	1.24	0.0010

Table LU1 was obtained with a NaI(Tl) spectrometer with 512 channels and a conversion gain of 5.8 keV per channel. Spectrometers with different channel divisions may have a slightly different ROI adjustment. Thus, parameter values could be slightly different.

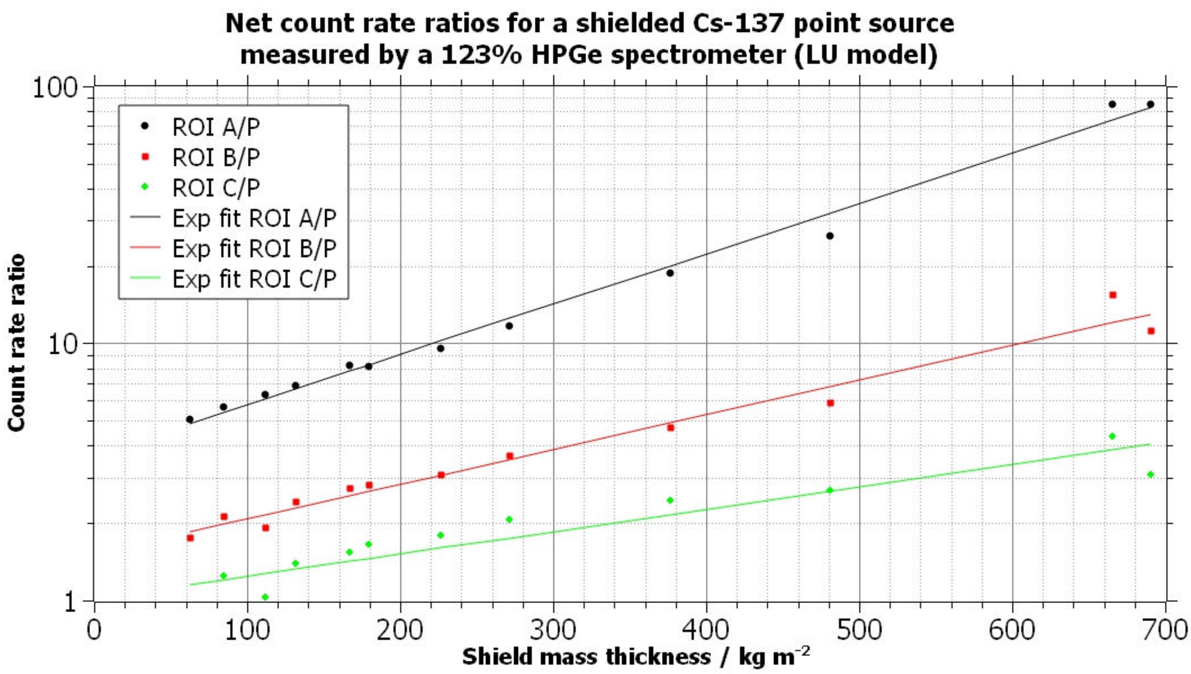

Figure LU2. Net (background subtracted) count rate ratios A/P, B/P and C/P as functions of shield mass thickness for registrations in the ROI photon energy intervals A, B, C and P according to the definition in Table 3. The straight lines are fitted exponential functions to measured values. The coefficients are given in Table LU2. Functions are valid for measurements with a 123% HPGe-spectrometer with its cylindrical mantle side facing the source. The mass thickness of the air between the source and the detector is included in the shield mass thickness values.

Table LU2. Coefficients *a* and *b* in Equation 2 for obtaining the shield mass thickness (kg/m^2) from the measured ROI net cps quotients *q* when using a 123% HPGe spectrometer (LU model).

ROI net cps quotient type for *q*	*a*	*b*
ROI A/P	3.68	0.0045
ROI B/P	1.52	0.0031
ROI C/P	1.02	0.0020

4.3 How to obtain the mass thickness of the shielding material for a Cs-137 source using gamma spectrometry and the "knowledge library" function

Equation 2 is used to obtain the mass thickness *x* where *q* represents the quotients of net ROI count rates (A/PR, B/PR, C/PR, PL/PR). Parameters and *a* and *b* are taken from Table LU1 (for a 4 litre NaI(Tl) spectrometer) or the Table LU2 (for a 123% HPGe-spectrometer. The complete procedure for obtaining shield mass thickness from gamma spectrometry data is described in Appendix A. An Excel program was created to facilitate the computation.

The procedure will provide four values of the mass thickness x (three for HPGe) which should be roughly equal. If not, the shielding geometry may somehow deviate from the type of configuration used as the basis for the "knowledge library". The ratios C/PR and PL/PR (or C/P for HPGe) are probably the ones that best represent the mass thickness of the shield because these ratios mainly represent single scattered photons between 0 and 58 degrees (27 - 58 degrees for HPGe).

4.4 Results from the team's experiments using the "knowledge library" function

All participating teams made shielding measurements at their own home site during the autumn 2020, generally using one type of building material and a few distances. How well the different teams' measurement results matched the LU "knowledge library" model can be interpreted from Figures 8 - 14 where the quotas q are plotted against the shield mass thickness x and the LU model is represented by the dashed lines in the diagrams.

SSM results (Fig 8 and 9) for the two 4 litre NaI(Tl) detectors (marked L and R) are in approximate agreement with the LU model for larger shield thickness with ±10% deviation from the true value for concrete blocks between 15 and 30 cm thickness. The deviation from the true value was larger for low shield thickness, which may depend on the background not being fully representative due to a rain shower just before the measurements. SSM results (Fig 14) of shield thickness measured by the 120% HPGe detector using the LU model were in good agreement with and the true values.

DEMA results (Fig 10) for a 4 litre NaI(Tl) detector showed 5 - 40% overestimation of the shield thickness of clay tiles 15 - 30 cm compared to the true value when using the LU model. For thinner shield the overestimation was 20 - 50%. This was when using the ROI's A, B, and C in relation to ROI PR. When using the relation PL/PR the overestimation of shield thickness was much larger. This may probably be due to some difference in the selected boundaries for the PL and PR ROIs compared to those used by LU. The model outcome is very sensitive to small changes in these boundaries.

STUK results (Fig 11) for a 4 litre NaI(Tl) detector showed 5 - 25% underestimation of the shield thickness for concrete blocks of thickness 20 - 30 cm compared to the true value when using the LU model and 5 - 60% underestimation for 10 cm. The reason for this may be a high dead-time of 10% that may have distorted the pulse height distribution to some extent. There may also be some small difference in detector efficiency or ROI boundaries between the STUK and LU spectrometers. The underestimation is largest for the ROI A/PR ratio. For the ROI PL/PR ratio the STUK measurements using the LU model are close to the true value.

IRSA results (Fig 12) for two 2 litre NaI(Tl) detectors showed an underestimation of about 15% for the first detector and about 35% for the second detector compared to the true value of a 20 cm concrete wall when using the LU model. There may be several reasons for the deviation. Lund University's model is based on measurement data from a detector with a volume of 4 litres. Detectors with 2-litre volumes have a slightly different relative efficiency over the energy range of the recorded photons. It affects the relationship between the count rates in the different ROIs. Furthermore, the shielding geometry in the experiment is somewhat different from the geometry for which the model was developed. Exactly how it may affect the validity of the model has not yet been possible to investigate.

NGU results (Fig 13) for a 16 litre NaI(Tl) detector showed about 10% overestimation of the shield thickness for concrete blocks of thickness 10 - 20 cm compared to the true value when using the LU model for a 4 litre NaI(Tl) detector. The overestimation was larger, about 45% for thickness 25 and 30 cm. The explanation for this may be that the efficiency curve of the 16 litre detector (consisting of four 4 litre detectors close to each other) is somewhat steeper with increasing photon energy than the efficiency curve for a single 4 litre detector, thereby increasing the q-ratios of scattered to primary photon count rates A/PR, B/PR and C/PR.

Different local conditions could have played a role as well in the observed deviation. However, more detailed measurements must be performed to verify this.

The conclusion one can draw from all teams' measurements of shield mass thickness is that the LU model applying the exponential function appears to provide a reasonable value of the shield thickness for mass thickness 100 - 700 kg/m^2 if it is used with detectors of the same volume as it was calibrated for. For other detector volumes, the slope of the exponential function q in Equation 1 increases with increasing detector volume, i.e. the coefficient b increases. Detectors with other volumes than in the LU model should have their own coefficients determined for the exponential function. This was tested by calculating each team’s individual coefficients a and b by fitting their measurement data to Equation 1. The values are given in Table 6 for NaI(Tl) detectors and Table 7 for a HPGe detector (only used by SSM) together with the LU model values (in bold).

For each team the exponential function based on the team's detector-specific parameters a and b is shown graphically in Fig 8 - 14. Dotted lines in the diagrams represent the exponential function using the LU model. By comparing the slopes of the lines for each team with the slope of the LU model, one can get an approximate picture of how well different teams measurement data can be represented by the LU model.

Table 6. Coefficients a and b in the expression for determining the shield mass thickness $x = \ln(q/a)/b$ where q is the respective measured count rate ratios of ROIs A/PR, B/PR, C/PR and PL/PR, as obtained in the experimental measurements by IRSA/GR, SSM, DEMA, STUK and NGU compared to the coefficients in the Lund University (LU model). Detector type NaI(Tl).

		ROI A/PR		ROI B/PR		ROI C/PR		ROI PL/PR	
Team	NaI(Tl) detector volume	*a*	*b*	*a*	*b*	*a*	*b*	*a*	*b*
IRSA	2 litre	4.65	0.0022	1.67	0.0026	0.82	0.0032	1.02	0.0012
LU model	**4 litre**	**4.32**	**0.0042**	**1.85**	**0.0031**	**1.17**	**0.0029**	**1.24**	**0.0010**
SSM (L)	4 litre	2.81	0.0048	1.42	0.0039	1.11	0.0026	1.14	0.0012
SSM (R)	4 litre	2.92	0.0048	1.38	0.0040	1.10	0.0026	1.13	0.0012
DEMA	4 litre	4.54	0.0045	2.27	0.0031	1.68	0.0023	1.75	0.0010
STUK	4 litre	1.57	0.0052	1.32	0.0035	1.20	0.0022	1.18	0.0011
NGU	16 litre	1.92	0.0062	1.03	0.0054	0.92	0.0036	1.33	0.0013

Table 7. Coefficients a and b in the expression for determining the shield mass thickness $x = \ln(q/a)/b$ where q is the respective measured count rate ratios of ROIs A/P, B/P and C/P, as obtained in the experimental measurements by SSM compared to the coefficients in the Lund University (LU) model. Detector type HPGe.

		ROI A/P		ROI B/P		ROI C/P	
Team	HPGe detector efficiency	*a*	*b*	*a*	*b*	*a*	*b*
LU model	**123%**	**3.68**	**0.0045**	**1.52**	**0.0031**	**1.02**	**0.0020**
SSM	120%	3.50	0.0047	1.50	0.0033	1.01	0.0019

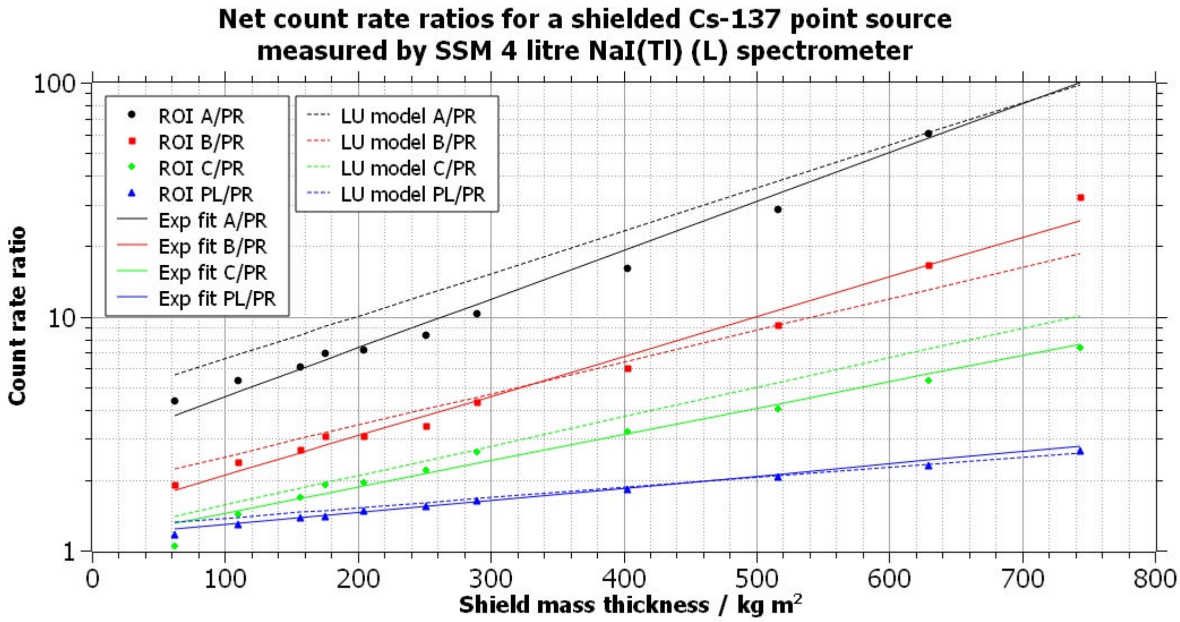

Figure 8. SSM experimentally obtained net (background subtracted) count rate ratios of ROI's A/PR, B/PR, C/PR and PL/PR as functions of shield mass thickness compared to modelled data from Lund University (LU model …, dotted lines). The photon energy intervals of ROI's A, B, C, PL and PR are valid for a Cs-137 point source and defined in the main report. Experimental data sets (marked ROI …) for a 4 litre NaI(Tl) detector are fitted to exponential expressions (coefficients given in Table 6) and shown as straight lines (Exp fit …) in the semi logarithmic diagram.

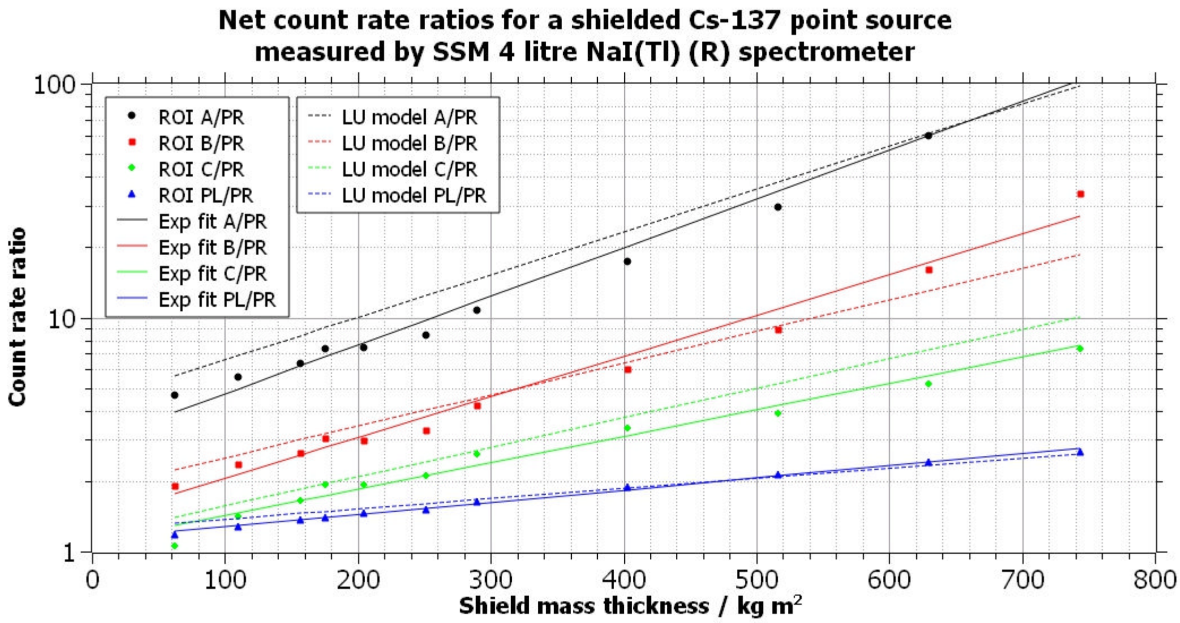

Figure 9. SSM experimentally obtained net (background subtracted) count rate ratios of ROI's A/PR, B/PR, C/PR and PL/PR as functions of shield mass thickness compared to modelled data from Lund University (LU model …, dotted lines). The photon energy intervals of ROI's A, B, C, PL and PR are valid for a Cs-137 point source and defined in the main report. Experimental data sets (marked ROI …) for a 4 litre NaI(Tl) detector are fitted to exponential expressions (coefficients given in Table 6) and shown as straight lines (marked Exp fit …) in the semi logarithmic diagram.

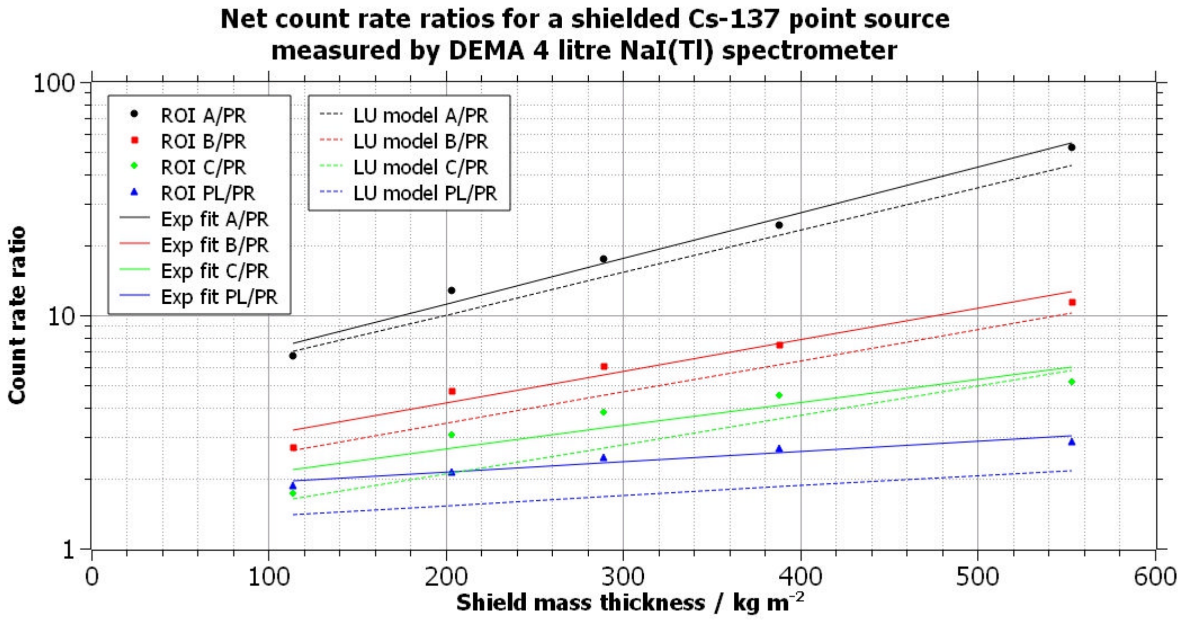

Figure 10. DEMA experimentally obtained net (background subtracted) count rate ratios of ROI's A/PR, B/PR, C/PR and PL/PR as functions of shield mass thickness compared to modelled data from Lund University (LU model …, dotted lines). The photon energy intervals of ROI's A, B, C, PL and PR are valid for a Cs-137 point source and defined in the main report. Experimental data sets (marked ROI …) for a 4 litre NaI(Tl) detector are fitted to exponential expressions (coefficients given in Table 6) and shown as straight lines (marked Exp fit …) in the semi logarithmic diagram.

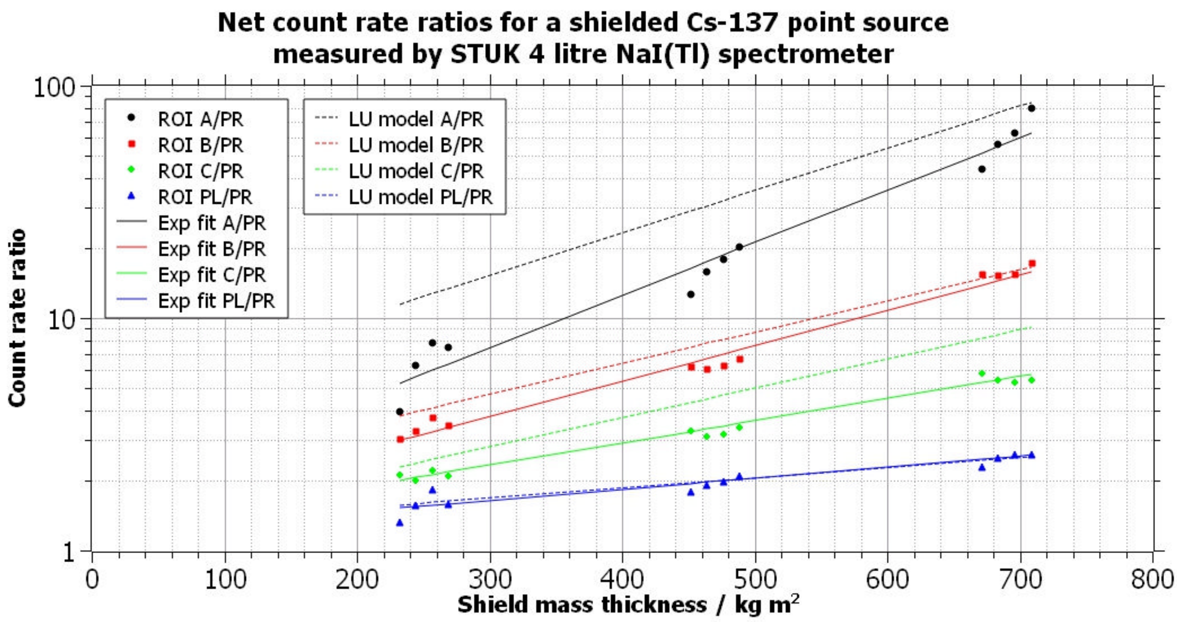

Figure 11. STUK experimentally obtained net (background subtracted) count rate ratios of ROI's A/PR, B/PR, C/PR and PL/PR as functions of shield mass thickness compared to modelled data from Lund University (LU model …, dotted lines). The photon energy intervals of ROI's A, B, C, PL and PR are valid for a Cs-137 point source and defined in the main report. Experimental data sets (marked ROI …) for a 4 litre NaI(Tl) detector are fitted to exponential expressions (coefficients given in Table 6) and shown as straight lines (marked Exp fit …) in the semi logarithmic diagram.

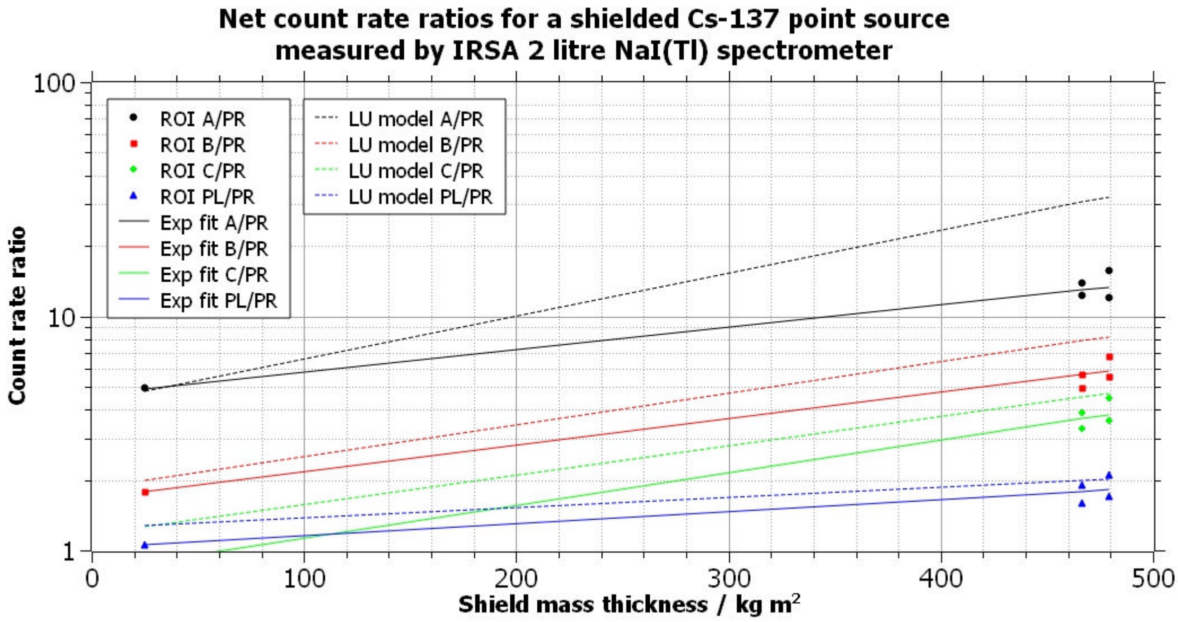

Figure 12. IRSA experimentally obtained net (background subtracted) count rate ratios of ROI's A/PR, B/PR, C/PR and PL/PR as functions of shield mass thickness compared to modelled data from Lund University (LU model …, dotted lines). The photon energy intervals of ROI's A, B, C, PL and PR are valid for a Cs-137 point source and defined in the main report. Experimental data sets (marked ROI …) for a 2 litre NaI(Tl) detector are fitted to exponential expressions (coefficients given in Table 6) and shown as straight lines (marked Exp fit …) in the semi logarithmic diagram.

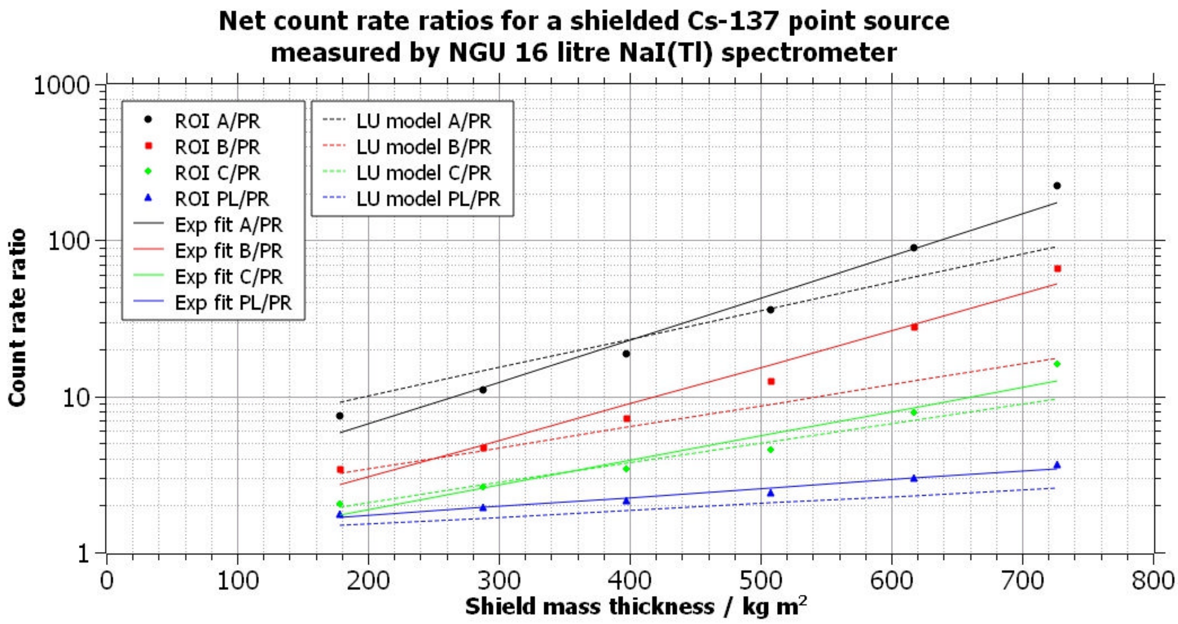

Figure 13. NGU experimentally obtained net (background subtracted) count rate ratios of ROI's A/PR, B/PR, C/PR and PL/PR as functions of shield mass thickness compared to modelled data from Lund University (LU model …, dotted lines). The photon energy intervals of ROI's A, B, C, PL and PR are valid for a Cs-137 point source and defined in the main report. Experimental data sets (marked ROI …) for a 16 litre NaI(Tl) detector are fitted to exponential expressions (coefficients given in Table 6) and shown as straight lines (Exp fit …) in the semi logarithmic diagram.

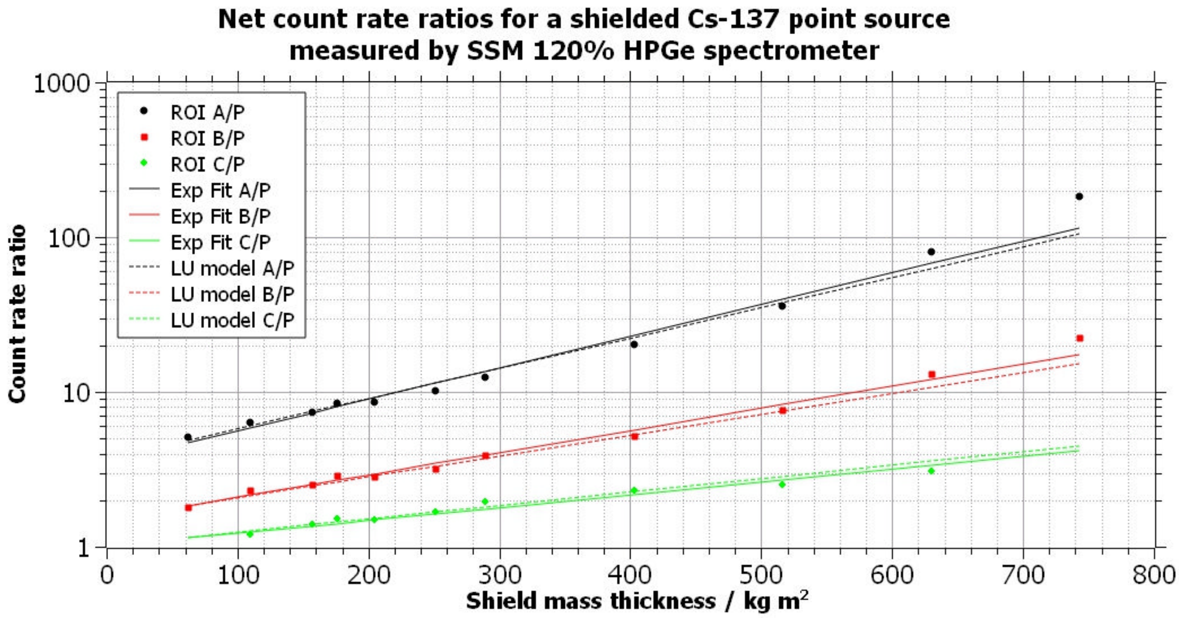

Figure 14. SSM experimentally obtained net (background subtracted) count rate ratios of ROI's A/P, B/P and C/P as functions of shield mass thickness compared to modelled data from Lund University (LU model …, dotted lines). The photon energy intervals of ROI's A, B, C, and P are valid for a Cs-137 point source and defined in the main report. Experimental data sets (marked ROI …) for a 120% HPGe detector are fitted to exponential expressions (coefficients given in Table 6) and shown as straight lines (marked Exp fit …) in the semi logarithmic diagram.

5. Conclusions

Lund University (LU) made a number of gamma-ray spectrometry measurements of Cs-137 point sources using wood, clay tiles and concrete blocks as shielding material between the source and the detector. Based on pulse height distributions, three ROIs for scattered radiation and three ROIs for primary radiation were defined. It was found that the net (background subtracted) count rate ratios for Compton scattered to primary photons from the source could be described by exponential functions of shield mass thickness. Function parameters were determined for a 4-liter NaI(Tl) spectrometer and a 123% HPGe spectrometer. The exponential functions and its parameters defined the LU “knowledge library” model.

All Nordic teams performed field gamma spectrometry using Cs-137 point sources behind shields (burnt clay tiles or concrete) at their home site. This was in order to test the hypothesis of an exponential relation between the ratio of the detector count rate from scattered radiation to the count rate from primary radiation as a function of the mass thickness of the shield between the source and the detector. The hypothesis was found fairly true for shield mass thickness values 200 - 700 kg/m^2. By knowing the parameters of the exponential functions, it was possible to roughly estimate the shield thickness from a measured pulse height distribution if the shield did not contain high atomic number material.

How well the shield thickness of building material can be determined by a procedure like the Lund University (LU) “knowledge library” model depends on a number of things. These are mainly: (1) an appropriate choice of energy regions (ROIs) for the detector’s registration of scattered and primary radiation, (2) a proper calibration of the detector's pulse height distribution for scattered radiation for varying shield thickness, (3) a precise knowledge of the background at the site without the source and (4) a constant energy calibration of the spectrometer during all measurements.

The LU “knowledge library” model for determining shield thickness from a measured pulse height distribution using NaI(Tl) detectors produced values within ±50% of the true value when taking the results from all teams and detector volumes into account. For the HPGe detector used by SSM, the difference between the values of the LU model and the real values was less than 10%. It was found that the slope of the exponential function is dependent on the detector volume. Therefore, greater accuracy may be achieved if the detector’s ROI selection and exponential function parameters are determined individually for each detector instead of using general values.

A problem with the LU method is that it is necessary to know in advance the natural radiation background at the site, as it must be subtracted from the measurements with the radiation source in place. This complicates its use in a real situation. However, it may be possible to use the information in the pulse height distribution for higher photon energies than the primary energy to construct a background for lower energies that can be used in the subtraction. This will require development and testing to determine if such a method is possible.

The LU model has only been tested on a small number of shielding geometries and the teams have built their own geometries at their home site with different local condition (e.g. humidity and terrain), which added uncertainties in the comparisons between the results of different detectors. It would be desirable to carry out measurements with the team’s different detectors on the exact same shielding geometries and at the same location in order to be able to better map the basic uncertainties in the method. It remains to be determined if the LU method also works for the large variation in shielding geometry in real buildings of different types.

Acknowledgement

The authors thank Barsebäck Kraft AB for the access to the zones for certain parts of the experimental measurements. Thanks also to the family of Abbekås Åkeri AB for the kindness of making ground surfaces available for the measurement of shielded radiation sources.

The experiments made by Lund University were carried out with measuring equipment financed by the Swedish Radiation Protection Authority (SSI) and The Swedish Radiation Safety Authority (SSM).

NKS conveys its gratitude to all organizations and persons who by means of financial support or contributions in kind have made the work presented in this report possible.

Disclaimer

References

R.R. Finck, T.Ulvsand. Search for orphan gamma radiation sources, Experiences from the Barents Rescue 2001 exercise. Proceedings, Security of Radioactive Sources held at IAEA, Vienna, Austria, 10-13 March 2003. IAEA, Vienna, pp 123 – 137, 2003.

Thomas Hjerpe, Robert R. Finck, and Christer Samuelsson. 2001. Statistical Data Evaluation in Mobile Gamma Spectrometry: An Optimization of On-Line Search Strategies in the Scenario of Lost Point Sources, Health Physics Vol 80 No 6, pp 563 – 570, 2001.

Hubbell and Seltzer, Tables of X-Ray Mass Attenuation Coefficients and Mass Energy-Absorption Coefficients (version 1.4). [Online] Available: http://physics.nist.gov/xaamdi [2004, July 12]. National Institute of Standards and Technology, Gaithersburg, MD, 2004.

IAEA, Combating Illicit Trafficking in Nuclear and Other Radioactive Material, IAEA Nuclear Security Series No. 6, Technical Guidance, Vienna, 2007.

G.F. Knoll, Radiation Detection and Measurement, 4:th edition. John Wiley & Sons Inc, 2010.

Peder Karl-Johan Kock; Robert R Finck; Jonas M Nilsson; Karl Östlund; Christer Samuelsson. A Deviation Display Method for Visualising Data in Mobile Gamma-ray Spectrometry, Applied Radiation and Isotopes, Volume 68, Issue 9, pp 1832-1838, 2010.

Jonas Nilsson, Karl Östlund, Joakim Söderberg, Sören Mattsson, Christopher Rääf. Tests of HPGe- and scintillation-based backpack γ-radiation survey systems. Journal of Environmental Radioactivity 135:54–62 (2014).

H. Toivonen, M. Granström, G. Ågren, G. Jónsson, B. Møller, P. Roos, H. Ramebäck, Activity estimation of shielded or hidden radionuclides in emergency conditions, Nordic Nuclear Safety Research, Report NKS-399, Dec 2017.

Christopher L. Rääf (chair), Robert R. Finck (co-chair), Antanas Bukartas, Gísli Jónsson, Sune Juul Krogh, Simon Karlsson, Morten Sickel, Petri Smolander, Jonas Wallin, Robin Watson. AUTOMORC – Improvement of automatic methods for identification of radioactive material out of regulatory control (MORC) by mobile gamma spectrometric search experiments. Nordic Nuclear Safety Research, Report NKS-422, March 2019.

Christopher L. Rääf (chair), Robert R. Finck (co-chair), Vikas C. Baranwal, Antanas Bukartas, Marie-Andrée Dumais, Kjartan Guðnason, Yvonne Hinrichsen, Gísli Jónsson, Mattias Jönsson, Peder Kock, Sune Juul Krogh, Simon Karlsson, Frode Ofstad, Jan Steinar Rønning, Petri Smolander, Kasra Tazmani, Mikael Westin, SHIELDMORC – Detection distances and methods to locate orphan gamma radiation sources in shielded building geometries by mobile gamma spectrometry, Nordic Nuclear Safety Research, Report NKS-433, March 2020.

UNSCEAR. Sources and Effects of Ionizing Radiation: United nations Scientific Committee on the Effects of Atomic Radiation 2008 Report, Volume II, Scientific Annex C, Radiation Exposures in Accidents, United Nation Publication, April 2011.

APPENDIX A

A.1 Verifying the “knowledge library” method for shielding thickness assessment. Recommended experiment for the Nordic teams to perform at home during autumn 2020

As part of the NKS/SHIELDMORC 2020 project, it was recommended that each Nordic team should carry out at least one shielding measurements at home and analyze measurement data as described below:

A.1.1 Measurement procedure at the home site

The measurements can be performed in one of two proposed ways:

Either:

(I) Perform shielding measurements according to the previously sent description dated 2020-08-25 with a Cs-137 source and use shielding materials that are built up to a few different thicknesses.

Or:

(II) Carry out at least one shielding measurement using an existing building where the Cs-137 source is placed inside an outer wall of the building and spectrometry measurement is made outside the building at least 10 meters away from the wall.

Regardless of whether method I or II is used, the following steps need to be performed:

1. In the gamma spectrometer, set the ROIs for the areas A, B, C, PL, PC and PR with guidance from Table 1 (in the main report). Depending on how the gain is set, the number of channels in the ROI areas will be different for different teams and spectrometers. The nodes (in channels) between ROIs should be as small as possible, preferably only one channel width. Note that the maximum value of the full energy peak for Cs-137 of 662 keV is a node. This divides the peak into a left ROI (PL) and a right ROI (PR). It is important that no gain shift takes place during or between measurements.

2. Calculation of shield thickness from measurement data is done with the table in the Excel diagram "Shield-thickness-calc.xls". The table applies to measurement with a 4 liter NaI(Tl)-spectrometer. Presumably it also applies approximately to other volumes of NaI(T1)-crystals. Before starting measurements, familiarize yourself with the input data to be entered in the table. All boxes for input are marked with a black frame. The rest of the table data are calculated automatically. A picture of the Excel table “Shield-thickness-calc” is given below in Table A.1.1, An example of filled-in measurement data is shown in Table A.1.2.

3. Decide where to perform the measurement experiment and put the detector in place. The measurements should be done stationary. Do not move the detector between measurements. The experiment is performed to be able to verify the calculation model with the use of data from a "knowledge library". This is sensitive to gain shifts during measurements. It is therefore important that gain shifts are minimized during and between measurements. Even such small gain shifts as 1 - 2 channels impairs the precision and possibilities of verifying the model.

4. Any common building material (concrete, clay tiles, wood, gypsum etc.) can be used as a shield, but not high-Z material such as lead. Determine the density (kg/m^3) and thickness (m) of the shielding material to be used in the experiment.

5. Measure the natural background at the site for at least one hour. Before starting the measurement, make sure that the radiation source to be used later is so shielded and at such a long distance that it cannot affect the background measurement the slightest.

6. From the measured pulse height distribution of the background, obtain the ROI counts in the areas A, B, C, PL and PR and divide the counts by the acquisition time (s) to get the count rates (s^{-1}) in the ROI areas. Fill in the count rate values in the Excel table "Shield-thickness-calc.xls" (Cells B16:B19).

7. Put the radiation source in place behind the shielding material. Measure the pulse height distribution during the time recommended in section A.2 below, which gives about 1 percent uncertainty. Should this not be possible, a shorter acquisition time may be accepted.

8. From the measured pulse height distribution with the source, obtain the ROI counts in the areas A, B, C, PL and PR and divide the counts by the acquisition time (s) to get the count rates (s^{-1}) in the ROI areas. Fill in the count rate values in the Excel table "Shield-thickness-calc.xls" (Cells C16:C19). The Excel routine automatically calculates four variants of the mass thickness of the shield and an average value of these.

9. To compare the shield mass thickness obtained by gamma spectrometry with the true value, fill in the true value of the thickness (m) of the shield (Cell B12), the density (kg/m^3) of the shield (Cell C12) and the source-detector distance (m) (Cell E12). Observe the units to be used. The deviation between measured and true values are then shown (Cells H16:19) and its average (Cell H21).

10. Repeat steps 7 - 9 if additional measurements are made with a different shield thickness.

11. Write a short description of the measurements and send this together with completed Excel tables with calculated shield mass thicknesses by email to robert.finck@med.lu.se. Lund University will compile the team's data for the final report to NKS for SHIELDMORC in December 2020.

Table A.1.1 Copy of the Excel table “Shield-thickness-calc.xls” for calculation of mass shield thickness from gamma spectrometric analysis.

Calculation of shield mass thickness from gamma spectrometry on a shielded Cs-137 point source with a mobile 4 litre NaI(Tl)-spectrometer. Comparison with observed data.

Report from team:	
Describe shield material:	

Observed data without gamma spectrometry					
Shield thickness observed (m)	Shield material density (kg/m^3)	Shield mass thickness (kg/m^2)	Source detector distance (m)	Air mass thickness (kg/m^2)	Total mass thickness (kg/m^2)

	Measured by gamma spectrometry			Calculated by the "knowledge library" model			
ROI	Background count rate (/s)	Measured gross count rate (/s)	Net count rate (/s)	ROI */PR ratios	Total mass thickness by model (kg/m^2)	Shield mass thickness by model (kg/m^2)	Deviation from observed (%)
A							
B							
C							
PL							
PC							
PR				Average			

Table A.1.2. Example of observed and measured data filled in the “Shield-thickness-calc.xls” calculation table.

Calculation of shield mass thickness from gamma spectrometry on a shielded Cs-137 point source with a mobile 4 litre NaI(Tl)-spectrometer. Comparison with observed data.

Report from team:	Lund University test measurement
Describe shield material:	Concrete tiles

Observed data without gamma spectrometry					
Shield thickness observed (m)	Shield material density (kg/m^3)	Shield mass thickness (kg/m^2)	Source detector distance (m)	Air mass thickness (kg/m^2)	Total mass thickness (kg/m^2)
0.15	2271.00	340.65	10.00	12.43	353.08

	Measured by gamma spectrometry			Calculated by the "knowledge library" model			
ROI	Background count rate (/s)	Measured gross count rate (/s)	Net count rate (/s)	ROI */PR ratios	Total mass thickness by model (kg/m^2)	Shield mass thickness by model (kg/m^2)	Deviation from observed (%)
A	640.29	1219.76	579.47	18.814	350.32	337.89	-0.8
B	191.70	353.47	161.77	5.252	336.60	324.17	-4.8
C	97.30	191.40	94.10	3.055	330.98	318.55	-6.5
PL	38.68	93.50	54.82	1.780	361.43	349.00	2.5
PC			0.00				
PR	26.39	57.19	30.80	Average	344.83	332.40	-2.4

A.2 Combinations of photon source activity, measuring distance, shielding thickness and acquisition times needed to obtain enough statistical accuracy to obtain a “knowledge library” for the NKS/SHIELDMORC project.

A.2.1 Background and short theory

Determination of shield thickness by measuring primary and scattered radiation from a gamma-emitting source is based on the probability of Compton interaction in matter being proportional to the electron density. For materials with a relatively low atomic number, Compton interactions in a radiation shield become approximately proportional to the mass thickness of the shield (kg/m^2). By comparing measurement data for the primary photon fluence that has passed through the shield with the photon fluence for Compton scattered photons in the shield for a few different energy ranges, it is possible to approximately estimate the mass thickness of the shield. Since a gamma spectrometer does not measure the photon fluence directly, but produces a pulse height distribution, which is different from the gamma spectrum due to the interaction in the detector, the spectrometer's measurement data for primary radiation and scattered radiation must be obtained in practice, as it is complicated to theoretically calculate the conversion from pulse height distribution to photon fluence over the whole energy spectrum.

The practical shielding measurements provide a shortcut to determining the thickness of the radiation shield. Once the measurements have been made, the result can be used as a "knowledge library" to assess similar shielding geometries from pulse height measurement data. To be useful, the measurements must be made with sufficient statistical accuracy.

A.2.2 Tables of minimum acquisition times

Below, tables show combinations of the source activity, the source-detector distance, the shield thickness (in kg/m^2) and the acquisition time required to achieve about 1 percent uncertainty in the measurements. The tables apply to Cs-137 and common building materials such as clay brick, concrete and wood.

The natural background (without radiation source) must be measured on site (at least one hour). The energy drift in the pulse height distribution must be kept minimal. Already a couple of channels of drift leads to a significant increase in the error in the measurements, if not corrected.

The division of the pulse height distribution into different energy ranges (ROI) is described in the theory section in the main part of this document. As long as sufficient statistical accuracy has been achieved in the measurements of the pulse height distribution, post-analyzes can be performed with different settings of ROI. It is thus important to save the entire pulse height distribution for each individual measurement.

Measurements should be made with the source in place without a shield and with a shield where the thickness of clay brick or concrete is varied in steps of 5 or 10 cm up to 30 cm (corresponds to approximate range 0 - 650 kg/m^2) and optional with wood up to 50 cm (corresponds to approximate range 0 - 260 kg/m^2).

About 30000 net counts are needed in the full energy peak of 662 keV to obtain a statistical uncertainty of about 1% in the final results, after processing ROI data. Acquisition times in Table A.2.1 - A.2.8 are given with this prerequisite.

Table A.2.1 Acquisition time (s) needed to obtain about 1% uncertainty in the final result for a 4 L NaI(Tl)-detector. No shielding material between the source and the detector.

Distance	Cs-137 source activity (MBq)					
(m)	10	30	100	300	1000	3000
10	195	65	20	*	*	*
20	860	290	85	30	10	*
30	2100	700	210	70	20	*
40	7200	2300	720	240	70	15
50	*	3800	1100	380	115	40

* Not practically feasible

Table A.2.2 Acquisition time (s) needed to obtain about 1% uncertainty in the final result for a 4 L NaI(Tl)-detector with 10 cm clay brick or concrete shielding (≈220 kg/m2)

Distance	Cs-137 source activity (MBq)					
(m)	10	30	100	300	1000	3000
10	920	300	90	30	10	*
20	4000	1400	400	140	40	15
30	10000	3300	1000	330	100	30
40	*	6500	2000	650	200	65
50	*	*	3400	1100	340	110

* Not practically feasible

Table A.2.3 Acquisition time (s) needed to obtain about 1% uncertainty in the final result for a 4 L NaI(Tl)-detector with 20 cm clay brick or concrete shielding (≈440 kg/m2)

Distance	Cs-137 source activity (MBq)					
(m)	10	30	100	300	1000	3000
10	4300	1400	430	140	40	15
20	*	6300	1900	630	190	65
30	*	*	4700	1600	470	160
40	*	*	9200	3100	1920	310
50	*	*	*	5300	1600	530

* Not practically feasible

Table A.2.4 Acquisition time (s) needed to obtain about 1% uncertainty in the final result for a 4 L NaI(Tl)-detector with 30 cm clay brick or concrete shielding (≈660 kg/m2)

Distance	Cs-137 source activity (MBq)					
(m)	10	30	100	300	1000	3000
10	*	6800	2000	680	200	70
20	*	*	8900	3000	900	300
30	*	*	*	7400	2200	740
40	*	*	*	*	4300	1500
50	*	*	*	*	7500	2500

* Not practically feasible

Table A.2.5 Acquisition time (s) needed to obtain about 1% uncertainty in the final result for a 16 L NaI(Tl)-detector. No shielding material between source and detector.

Distance	Cs-137 source activity (MBq)					
(m)	10	30	100	300	1000	3000
10	50	15	5	*	*	*
20	220	70	20	*	*	*
30	540	180	55	20	*	*
40	1100	350	110	35	10	*
50	1800	600	180	60	20	*
60	2900	960	290	100	30	10
70	4300	1400	430	140	40	15
80	6200	2100	620	210	60	20
90	8600	2900	860	290	90	30
100	*	3900	1200	390	120	40

* Not practically feasible

Table A.2.6 Acquisition time (s) needed to obtain about 1% uncertainty in the final result for a 16 L NaI(Tl)-detector with 10 cm clay brick or concrete shielding (≈220 kg/m2)

Distance	Cs-137 source activity (MBq)					
(m)	10	30	100	300	1000	3000
10	230	80	25	10	*	*
20	1000	340	100	35	10	*
30	2500	840	250	85	25	8
40	5000	1700	500	170	50	16
50	8500	2800	850	280	85	30
60	*	4500	1400	450	140	45
70	*	6700	2000	670	200	70
80	*	9700	2900	970	290	100
90	*	*	4100	1400	400	140
100	*	*	5500	1800	550	180

* Not practically feasible

Table A.2.7 Acquisition time (s) needed to obtain about 1% uncertainty in the final result for a 16 L NaI(Tl)-detector with 20 cm clay brick or concrete shielding (≈440 kg/m2)

Distance (m)	Cs-137 source activity (MBq)					
	10	30	100	300	1000	3000
10	1100	360	110	40	11	*
20	4800	1600	480	160	50	16
30	*	4000	1200	400	120	40
40	*	7800	2300	780	230	80
50	*	*	4000	1300	400	130
60	*	*	6300	2100	630	210
70	*	*	9500	3200	950	320
80	*	*	*	4600	1400	460
90	*	*	*	6400	1900	640
100	*	*	*	8600	2600	860

* Not practically feasible

Table A.2.8 Acquisition time (s) needed to obtain about 1% uncertainty in the final result for a 16 L NaI(Tl)-detector with 30 cm clay brick or concrete shielding (≈660 kg/m2)

Distance (m)	Cs-137 source activity (MBq)					
	10	30	100	300	1000	3000
10	5100	1700	510	170	50	20
20	*	7500	2300	750	230	75
30	*	*	5600	1900	560	190
40	*	*	*	3600	1100	370
50	*	*	*	6630	1900	630
60	*	*	*	9900	3000	990
70	*	*	*	*	4500	1500
80	*	*	*	*	6400	2100
90	*	*	*	*	9000	3000
100	*	*	*	*	*	4100

* Not practically feasible

A.2.2 Example of how to use the Tables A.2.1 -A.2.8.

Presume that you have a 4 L NaI(Tl)-detector and a 300 MBq Cs-137 source. In order not to change the source detector distance during measurements, you could place the source at 30 m distance. For the first measurement without a shield between the source and detector (only air shielding) you need 70 s acquisition time (Table A.2.1). For 10 cm burnt clay tile shielding you need 330 s acquisition time (Table A.2.2). For 20 cm shielding you need 1600 s acquisition time (Table A.2.3) and for 30 cm shielding you need 7400 s acquisition time (Table A.2.4), i.e. a little more then two hours.

Tables A.2.5 - A.2.8 are for a 16 L NaI(Tl)-detector. For about the same measuring times as a 4 L NaI(Tl)-detector, a 300 MBq source should be placed at 50 m distance. A 1000 MBq source should be placed at 80 m.

APPENDIX B

B.0 Reports from shielding measurements made by each team at their home location during autumn 2020.

Due to the covid-19 pandemic restrictions imposed by the laws of participating countries, joint field experiments in Sweden could not be carried out as originally planned. Instead, each team conducted its own experiments with the equipment available at their home laboratory. In the following, the measurement results from the individual teams' experiments at home are presented.

B.1 Report from Danish Emergency Management Agency (DEMA) shielding measurements for SHIELDMORC 2020

B.1.1 Description of shielding set-up and geometry

Clay tiles were used as shielding material. The dimension of each tile was 5.4 cm x 10.8 cm x 22.8 cm. The density was 1650 kg/m3 (+/- 10%). The Cs-137 source activity was 300 MBq. The distance between the source and the detector was 20 m.

B.1.2 Description of measuring equipment

The gamma spectrometer used, was a car borne gamma spectrometer, from RSI. The detector used for the SHIELDMORC measurements was a 4L NaI(Tl)-crystal with 1024 channels. The rectangular detector was placed such that the longer side was oriented towards the source. The acquisition times are listed in Table B.1.1.

Table B.1.1. Acquisition times for the DEMA shielding measurements

Measurement	Acquisition time (s)
Background	3472
Source without shielding	37
Source with 5 cm clay tile shielding	148
Source with 10 cm clay tile shielding	147
Source with 15 cm clay tile shielding	363
Source with 20 cm clay tile shielding	643
Source with 30 cm clay tile shielding	3024

B.1.3 ROI set-up

The ROI setup was done according to Table B.1.2

Table B.1.2 The ROI setup for the DEMA shielding experiment

ROI	Energy node (keV)	Energy interval (keV)	Channel interval	Number of channels
	74			
A		75 - 240	25 - 80	55
	242			
B		243 - 408	81 - 136	55
	410			
C		441 - 576	137 - 192	55
	578			
PL		579 - 660	193 - 220	27
PC	662	663	221	1
PR		666 - 747	222 - 249	27

B.1.4 Results

Results of calculated shield thickness from measured ROI count rate ratios using the LU exponential model compared to true values is given in Fig B.1.1.

Report from team:	DEMA
Describe shield mater	Clay tiles, thickness 5.4 cm

Observed data without gamma spectrometry

Shield thickness observed (m)	Shield material density (kg/m³)	Shield mass thickness (kg/m²)	Source detector distance (m)	Air mass thickness (kg/m²)	Total mass thickness (kg/m²)
0.054	1650.00	89.10	20.00	24.86	113.96

ROI	Measured by gamma spectrome: Background count rate (/s)	Measured gross count rate (/s)	Net count rate (/s)	ROI */PR ratios	Calculated by the "knowledge library" mode: Total mass thickness by model (kg/m²)	Shield mass thickness by model (kg/m²)	Deviation from observed (%)
A	644.88	2925.30	2280.42	6.700	104.50	79.64	-10.6
B	181.94	1110.37	928.43	2.728	125.27	100.41	12.7
C	83.03	670.45	587.42	1.726	134.06	109.20	22.6
PL	31.84	663.08	631.24	1.855	402.59	377.73	323.9
PC	0.81	47.31	46.50				
PR	21.06	361.41	340.35	Average	191.60	166.74	87.1

Report from team:	DEMA
Describe shield mater	Clay tiles, thickness 10.8 cm

Observed data without gamma spectrometry

Shield thickness observed (m)	Shield material density (kg/m³)	Shield mass thickness (kg/m²)	Source detector distance (m)	Air mass thickness (kg/m²)	Total mass thickness (kg/m²)
0.108	1650.00	178.20	20.00	24.86	203.06

ROI	Measured by gamma spectrome: Background count rate (/s)	Measured gross count rate (/s)	Net count rate (/s)	ROI */PR ratios	Calculated by the "knowledge library" mode: Total mass thickness by model (kg/m²)	Shield mass thickness by model (kg/m²)	Deviation from observed (%)
A	644.88	1974.96	1330.08	12.778	258.21	233.35	30.9
B	181.94	678.59	496.65	4.771	305.62	280.76	57.6
C	83.03	404.23	321.20	3.086	334.41	309.55	73.7
PL	31.84	254.59	222.75	2.140	545.66	520.80	192.3
PC	0.81	14.89	14.08				
PR	21.06	125.15	104.09	Average	360.98	336.12	88.6

Report from team:	DEMA
Describe shield mater	clay tiles, thickness 16.2 cm

Observed data without gamma spectrometry

Shield thickness observed (m)	Shield material density (kg/m³)	Shield mass thickness (kg/m²)	Source detector distance (m)	Air mass thickness (kg/m²)	Total mass thickness (kg/m²)
0.16	1650.00	267.30	20.00	24.86	292.16

ROI	Measured by gamma spectromet: Background count rate (/s)	Measured gross count rate (/s)	Net count rate (/s)	ROI */PR ratios	Calculated by the "knowledge library" model: Total mass thickness by model (kg/m²)	Shield mass thickness by model (kg/m²)	Deviation from observed (%)
A	644.88	1487.31	842.43	17.426	332.07	307.21	14.9
B	181.94	475.57	293.63	6.074	383.48	358.62	34.2
C	83.03	269.47	186.44	3.857	411.30	386.44	44.6
PL	31.84	151.24	119.40	2.470	689.04	664.18	148.5
PC	0.81	7.46	6.65				
PR	21.06	69.40	48.34	Average	453.97	429.11	60.5

Report from team:	DEMA
Describe shield mater	clay tiles, thickness 21.6 cm

Observed data without gamma spectrometry

Shield thickness observed (m)	Shield material density (kg/m³)	Shield mass thickness (kg/m²)	Source detector distance (m)	Air mass thickness (kg/m²)	Total mass thickness (kg/m²)
0.22	1650.00	356.40	20.00	24.86	381.26

ROI	Measured by gamma spectromet: Background count rate (/s)	Measured gross count rate (/s)	Net count rate (/s)	ROI */PR ratios	Calculated by the "knowledge library" model: Total mass thickness by model (kg/m²)	Shield mass thickness by model (kg/m²)	Deviation from observed (%)
A	644.88	1214.58	569.70	24.447	412.68	387.82	8.8
B	181.94	355.97	174.03	7.468	450.13	425.27	19.3
C	83.03	188.29	105.26	4.517	465.80	440.94	23.7
PL	31.84	94.74	62.90	2.699	777.83	752.97	111.3
PC	0.81	4.15	3.34				
PR	21.06	44.36	23.30	Average	526.61	501.75	40.8

Report from team:	DEMA
Describe shield mater	clay tiles, thickness 32,4 cm

Observed data without gamma spectrometry

Shield thickness observed (m)	Shield material density (kg/m³)	Shield mass thickness (kg/m²)	Source detector distance (m)	Air mass thickness (kg/m²)	Total mass thickness (kg/m²)
0.32	1650.00	534.60	20.00	24.86	559.46

ROI	Measured by gamma spectromet: Background count rate (/s)	Measured gross count rate (/s)	Net count rate (/s)	ROI */PR ratios	Calculated by the "knowledge library" model: Total mass thickness by model (kg/m²)	Shield mass thickness by model (kg/m²)	Deviation from observed (%)
A	644.88	996.54	351.66	52.437	594.37	569.51	6.5
B	181.94	258.63	76.69	11.436	587.59	562.73	5.3
C	83.03	117.98	34.95	5.212	515.14	490.28	-8.3
PL	31.84	51.11	19.26	2.873	840.12	815.26	52.5
PC	0.81	1.71	0.90				
PR	21.06	27.76	6.71	Average	634.30	609.44	14.0

Fig B.1.1 Tables comparing true shielding thickness values (denoted as observed data) with calculated values based on measured ROI net count rate ratios in the 4 litre DEMA detector when using the Lund University exponential model for a 4 litre NaI(Tl)-detector for the calculation (denoted as calculated by the "knowledge library" model). The ROIs (A, B, C, PL ad PR) are defined in Table B.1.2

The LU model calculation based on measured ROI count rate ratios using the energy ROIs A, B, and C in relation to the right side of the full energy peak area PR overestimated the clay shield thickness by 31 ± 12 percent for thicknesses 90 - 180 kg/m2 (5 - 10 cm), by 24 ± 5 percent for thicknesses 270 - 360 kg/m2 (15 - 20 cm), and by 1 ± 3 percent for thickness 530 kg/m2 (32 cm). So the model calculation got closer to the true value as the shield thickness was increased.

For the ratio of left side (PL) to right side (PR) full energy peak area the overestimation was much higher, but reduced with increasing shield thickness. Though, the method is very sensitive to exact selection of the PL and PR ROIs and to possible gain drifts, a possible explanation for the overestimation of calculated shield thickness using the PL and PR ROIs is that the FWHM peak width could have been different from the LU data that the model is based on.

Assuming that there is an exponential relationship between the shield thickness and the ratios between the count rates in the respective ROI, values of the coefficients *a* and *b* in the LU model have been recalculated from the DEMA measurement data for the DEMA 4 liter NaI(Tl)-spectrometer. The values are given in Table B.1.3 in comparison with the corresponding values for LU. There are some differences in the coefficients *b* between the LU model and DEMA data, while the coefficients *a*, which indicate the slope of the exponential curve, are approximately equal. This indicates that there may be some difference in the exact choice of limits for the different ROIs, while the main principle of an exponential relationship between mass thickness of the shield and the ratio of count rates in specified ROIs seems to apply.

Table B.1.3 Coefficients *a* and *b* in the expression for determining the shield mass thickness $x = \ln(q/a)/b$, where *q* is the respective measured count rate ratios of ROIs A/PR, B/PR, C/PR and PL/PR, as obtained in the experimental measurements by DEMA compared to the coefficients in the Lund University (LU) model.

		ROI A/PR		ROI B/PR		ROI C/PR		ROI PL/PR	
Team	NaI(Tl) detector volume	*a*	*b*	*a*	*b*	*a*	*b*	*a*	*b*
LU	4 litre	4.32	0.0042	1.85	0.0031	1.17	0.0029	1.24	0.0010
DEMA	4 litre	4.54	0.0045	2.27	0.0031	1.68	0.0023	1.75	0.0010

B.1.5 Conclusion

We found relatively large deviations between the shield mass thickness calculated by the LU exponential model, and the true shield mass thickness of the clay tiles used. The deviations from the model values decrease with increasing shield thickness. We speculate that this might be due to variations in ROI setup compared to the instructions, uncertainties in the system such as gain drift, or the geometrical setup.

It seems that the general principles of an exponential relationship between net count rates in specific ROIs seems reasonable to be used to determine mass thicknesses for building materials. However, measurement data are too limited to be able to draw far-reaching conclusions. The differences between the model coefficients for measurements with DEMA's detector and the LU model indicate that further measurement experiments under well-controlled conditions are necessary to more accurately verify the method.

B.2 Report from Icelandic Radiation Safety Authority (IRSA) Geislavarnir Ríkisins (GR) shielding measurements for SHIELDMORC 2020

B.2.1 Description of shielding set-up and geometry

A site with buildings with cast concrete walls was chosen for the shielding experiment. The source used was a Troxler 3440 density gauge that contained 40mCi Am-241 and 8 mCi Cs-137 (300 MBq) and the reference date is 16.02.2005. (Fig B.2.1). The Cs-137 source activity at the measurement date was 210 MBq. The source is also a neutron-emitting source by having beryllium alongside the Am-241.

The presence of a neutron source could somewhat complicate the measurements of a gamma spectrum with a NaI(Tl) detector because of thermal neutron capture in the detector and its surroundings. In addition an Am-241-Be source emits high-energy gamma-rays directly, which can further contribute to the signal in the detector, provided that the source is not shielded with a high-density material (Nilsson et al, 2015). Using this source is therefore not optimal for the experiment and special care has to be observed when analyzing the measured pulse height distribution.

The source was placed inside the building about 5-10 cm from the ground and also 5-10 cm from the concrete wall (Fig B.2.2 and B.2.3) when in shielded measurement position. When unshielded, the source was placed just outside the building at the same height about 40 cm from the wall (Fig B.2.4).

The concrete wall thickness was 20 cm. Its density could not be measured. The density of concrete varies with its water content. Wet concrete has higher density than dry concrete. Here the same density has been chosen as measured for dry concrete tiles in the shielding experiments made by Lund University, 2271 kg/m3.

B.2.2 Description of measuring equipment and analysis

The NaI(Tl) gamma spectrometer consisted of two 2 litre NaI(Tl)-crystals placed in the trunk of a car at 20 m distance from the source (Fig B.2.5 and B.2.6). The pulse height distributions were summed in the spectrometer to form a single pulse height distribution. Auto gain was turned on during the measurements, which means that the instrument tweaks the gain to hold the K-40 peak at a fixed channel. Both the individual 2 liter NaI(Tl) spectral results (denoted G01 and G02) and the summed results (denoted G01+G02) was recorded and extracted.

In the after analysis it turned out that the gain for the detectors G01 and G02 were somewhat different. Therefore, individual analysis were made for each pulse height distribution by readjusting the gain to a fixed energy calibration, using a numerical method, allowing a fixed selection of ROIs as given in Table B.2.2.

It also turned out that the measured background pulse height distribution had higher count rates over the whole spectrum than was reasonable when observing the count rates above 800 keV in the shielded source measurements. The reason for this has not been fully clarified, but it may have to do with high-energy gamma contribution from the neutron source. Anyhow it is not reasonable to use a higher background in the background subtraction, so it was reduced for all energies to match the background count rate in the energy region above 800 keV for the individual shielded measurements, which gave correction coefficients between 0.87 and 0.96.

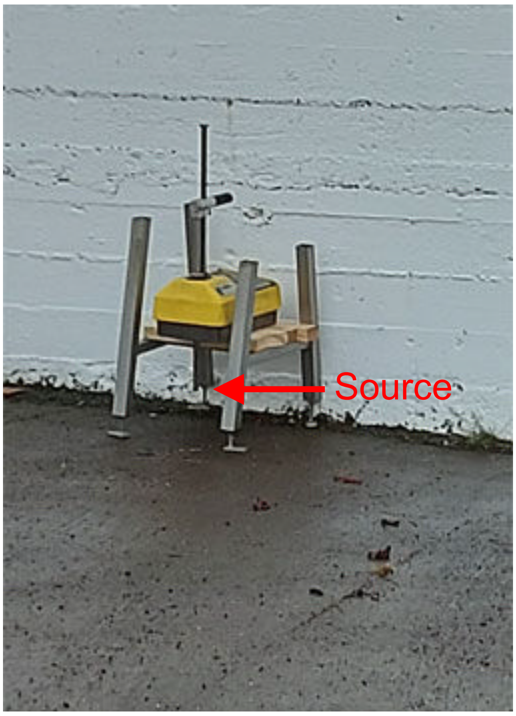

Fig B.2.1 The Troxler 3440 density gauge source, with the source in radiation position below the casing.

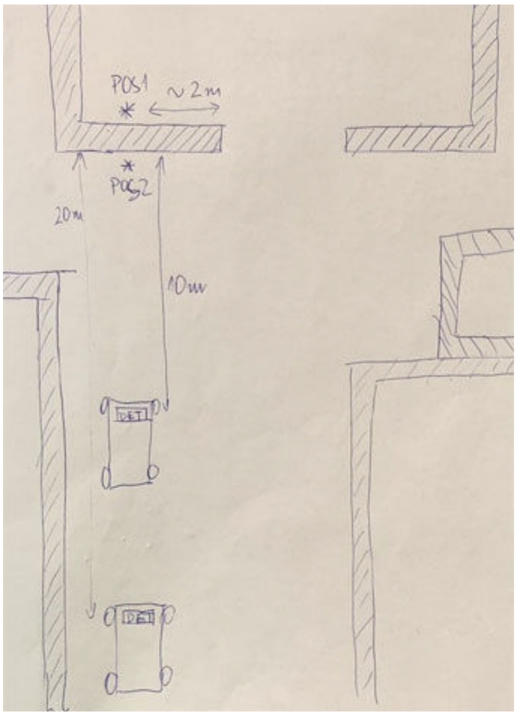

Fig B.2.2 Sketch of the positions of the radiation source and the detector.

Fig B.2.3 The density gauge source inside the building with 20 cm concrete walls.

Fig B.2.4 The density gauge outside the building.

Fig B.2.5 The two 2 litre NaI(Tl) spectrometers in a casing placed in the trunk of the measuring vehicle.

Fig B.2.6 The measuring vehicle and the building at 20 m distance where the source was placed.

Table B.2.1 Shielding thickness and measurement distance used in the shielding experiment by IRSA/GR. G01 and G02 are individual 2 litre NaI(Tl)-spectrometers. G01+G02 is the summed result from the spectrometers.

Detector	Source placement and shielding	Distance	Acquisition time
G01	Background, no source		4338 s
G02	Background, no source		4338 s
G01	Source behind 20 cm concrete wall	10 m	1075 s
G02	Source behind 20 cm concrete wall	10 m	1075 s
G01	Source behind 20 cm concrete wall	20 m	1745 s
G02	Source behind 20 cm concrete wall	20 m	1745 s
G01+G02	Source without shielding	20 m	735 s

B.2.3 ROI set-up

The ROI setup was chosen to as closely as possible match the setup used in the Lund University model. Depending on differences in the linearity of the energy calibration between individual gamma spectrometers it is not possible to exactly match the energy ROIs. The ROI setup for the experiment is listed in Table B.2.2.

Table B.2.2 The ROI setup for the IRSA/GR shielding experiment

ROI	Energy node (keV)	Energy interval (keV)	Channel interval	Number of channels
	74			
A		79 - 238	32 - 84	53
	242			
B		247 - 405	87 - 139	53
	410			
C		415 - 573	142 - 194	53
	578			
PL		582 - 659	197 - 222	26
PC	662	662	223	1
PR		665 - 741	224 - 249	26

B.2.4 Results

Background subtracted pulse height distributions from the shielded and unshielded measurements on the Cs-137 source are shown in Fig B.2.7. The full energy peaks at 662 keV are clearly seen in all measurements and so are the combined contributions at lower energies from Compton scattered radiation in the wall shielding, surrounding material and air and the scattering effects in the detector.

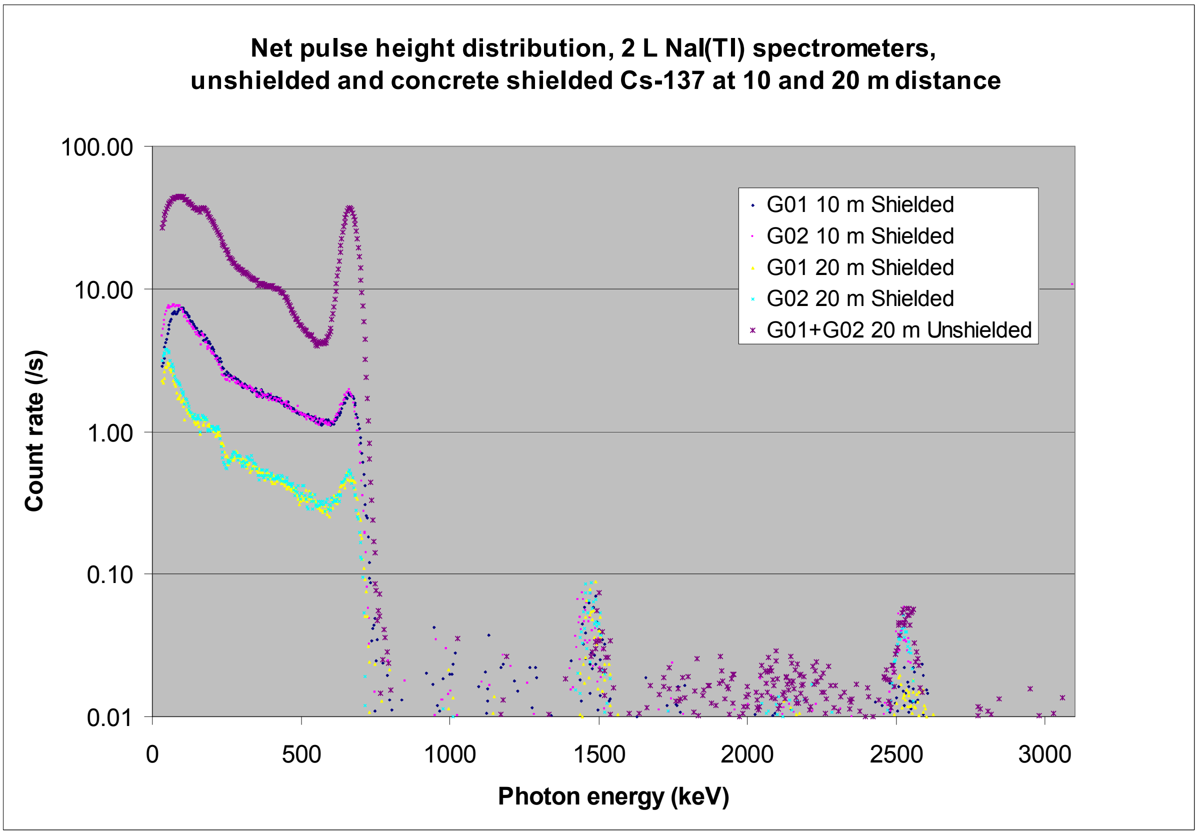

Fig B.2.7 Net (background subtracted) pulse height distribution count rates for concrete shielded measurements of a 210 MBq Cs-137 source placed inside a building behind a 20 cm concrete wall and unshielded outside the building. Measuring distances were 10 and 20 m. G01 and G02 were 2 litre NaI(Tl)-detectors. In the G01+G02 measurement spectral data from the two detectors was added.

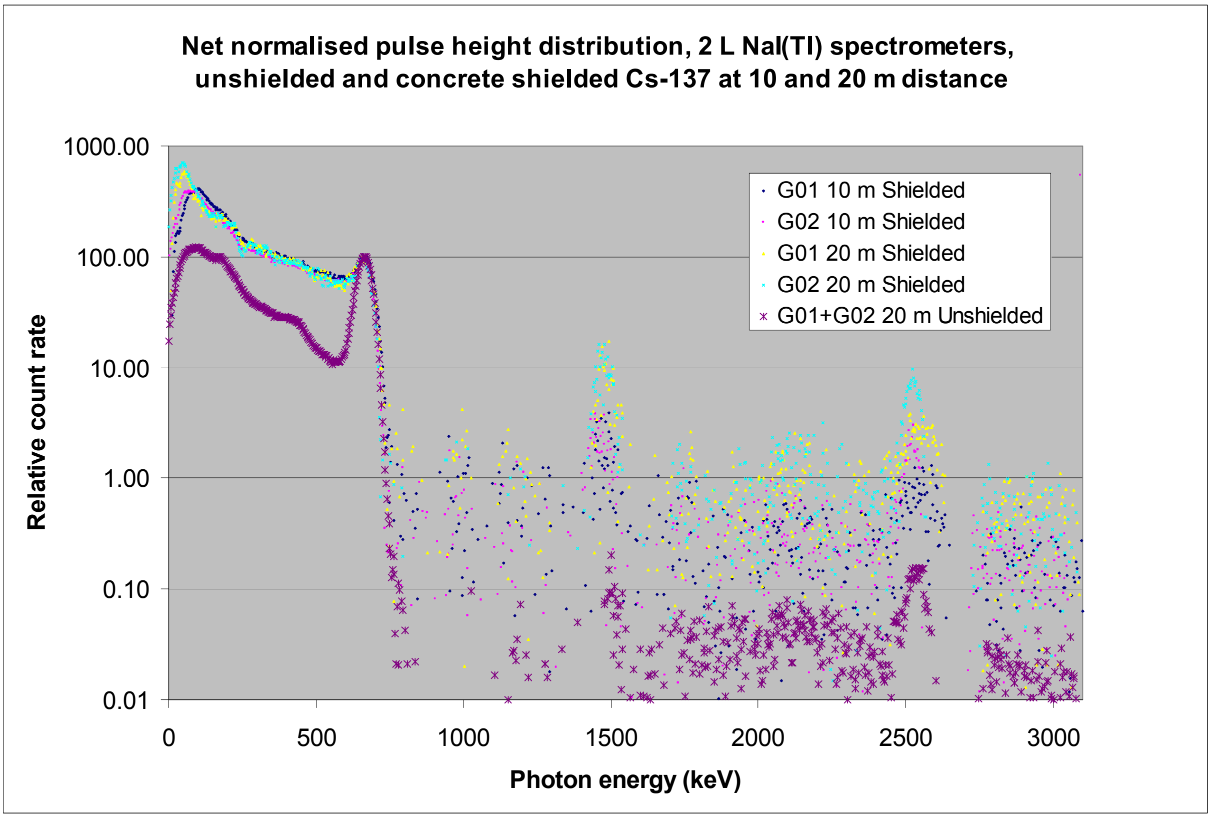

Fig B.2.8 Net (background subtracted) normalized (to 662 keV peak count rate) pulse height distribution count rates for concrete shielded measurements of a 210 MBq Cs-137 source placed inside a building behind a 20 cm concrete wall and unshielded outside the building. Measuring distances were 10 and 20 m. G01 and G02 were 2 litre NaI(Tl)-detectors. In the G01+G02 measurement spectral data from the two detectors was added. The background is not perfectly representative for the radiation situation, as some remnants from the full energy peaks of K-40 at 1460 keV and Tl-208 at 2615 keV (from the Th-232 decay series) can be seen in the net pulse height distribution after background subtraction.

When the detector is moved from 10 to 20 m distance from the Cs-137 source, the count rate of primary and scattered photons from the source is reduced as can be seen in Fig B.2.7. However, the relative contribution of count rates from scattered to primary photons is nearly the same because most of the Compton scattering occurs in the shielding wall and very little in the air between the source and the detector. This can be seen in Fig B.2.8 where the pulse height distribution is normalized to 100 for the channel with maximum count rate for the primary photons. The unshielded source, with only air scattering of the photons, produces much less scattered radiation in relation to the primary radiation

Results of the calculated wall shield thickness using the Lund University model with ROI A, B, C and PL in relation to ROI PR as defined in Table B.2.2 compared to true values is given in the Excel-tables shown in Fig B.2.9. For the 2 litre NaI(Tl)-detector G01 the wall thickness is underestimated by 34 - 38 %. For the G02 detector the wall thickness is underestimated by 11 - 22 % compared to the true value. The lower values (34 and 11%) are valid for the longer distance, 20 m, from the source. The reason for the deviation can be multiple. Lund University's model is based on measurement data from a detector with a volume of 4 liters. Detectors with 2-liter volumes have a slightly different relative efficiency over the energy range of the recorded photons. It affects the relationship between the count rates in the different ROIs. Furthermore, the shielding geometry in the experiment is somewhat different from the geometry for which the model was developed. Exactly how it may affect the validity of the model has not yet been possible to investigate.

Calculation of shield mass thickness from gamma spectrometry on a shielded Cs-137 point source with a mobile 4 litre NaI(Tl)-spectrometer. Comparison with observed data.

Report from team: IRSA 2 L NaI(Tl)-detector G01

Describe shield material: Simple full concrete wall 20 cm

Observed data without gamma spectrometry

Shield thickness observed (m)	Shield material density (kg/m^3)	Shield mass thickness (kg/m^2)	Source detector distance (m)	Air mass thickness (kg/m^2)	Total mass thickness (kg/m^2)
0.20	2271.00	454.20	10.00	12.43	466.63

Measured by gamma spectrometry / Calculated by the "knowledge library" model

ROI	Background count rate (/s)	Measured gross count rate (/s)	Net count rate (/s)	ROI */PR ratios	Total mass thickness by model (kg/m^2)	Shield mass thickness by model (kg/m^2)	Deviation from observed (%)
A			271.67	12.319	249.49	237.06	-47.8
B			109.26	4.954	317.75	305.32	-32.8
C			73.46	3.331	360.76	348.33	-23.3
PL			34.96	1.585	245.57	233.14	-48.7
PC			1.79				
PR			22.05	Average	293.39	280.96	-38.1

Calculation of shield mass thickness from gamma spectrometry on a shielded Cs-137 point source with a mobile 4 litre NaI(Tl)-spectrometer. Comparison with observed data.

Report from team: IRSA 2 L NaI(Tl)-detector G02

Describe shield material: Simple full concrete wall 20 cm

Observed data without gamma spectrometry

Shield thickness observed (m)	Shield material density (kg/m^3)	Shield mass thickness (kg/m^2)	Source detector distance (m)	Air mass thickness (kg/m^2)	Total mass thickness (kg/m^2)
0.20	2271.00	454.20	10.00	12.43	466.63

Measured by gamma spectrometry / Calculated by the "knowledge library" model

ROI	Background count rate (/s)	Measured gross count rate (/s)	Net count rate (/s)	ROI */PR ratios	Total mass thickness by model (kg/m^2)	Shield mass thickness by model (kg/m^2)	Deviation from observed (%)
A			262.35	13.901	278.26	265.83	-41.5
B			106.61	5.649	360.09	347.66	-23.5
C			73.13	3.875	412.95	400.52	-11.8
PL			35.77	1.896	424.38	411.95	-9.3
PC			1.96				
PR			18.87	Average	368.92	356.49	-21.5

Calculation of shield mass thickness from gamma spectrometry on a shielded Cs-137 point source with a mobile 4 litre NaI(Tl)-spectrometer. Comparison with observed data.

Report from team: IRSA 2 L NaI(Tl)-detector G01

Describe shield material: Simple full concrete wall 20 cm

Observed data without gamma spectrometry

Shield thickness observed (m)	Shield material density (kg/m^3)	Shield mass thickness (kg/m^2)	Source detector distance (m)	Air mass thickness (kg/m^2)	Total mass thickness (kg/m^2)
0.20	2271.00	454.20	20.00	24.86	479.06

Measured by gamma spectrometry / Calculated by the "knowledge library" model

ROI	Background count rate (/s)	Measured gross count rate (/s)	Net count rate (/s)	ROI */PR ratios	Total mass thickness by model (kg/m^2)	Shield mass thickness by model (kg/m^2)	Deviation from observed (%)
A			65.96	11.972	242.70	217.84	-52.0
B			30.47	5.531	353.30	328.44	-27.7
C			19.67	3.570	384.67	359.81	-20.8
PL			9.40	1.706	319.19	294.33	-35.2
PC			0.51				
PR			5.51	Average	324.96	300.10	-33.9

Calculation of shield mass thickness from gamma spectrometry on a shielded Cs-137 point source with a mobile 4 litre NaI(Tl)-spectrometer. Comparison with observed data.

Report from team: IRSA 2 L NaI(Tl)-detector G02

Describe shield material: Simple full concrete wall 20 cm

Observed data without gamma spectrometry

Shield thickness observed (m)	Shield material density (kg/m^3)	Shield mass thickness (kg/m^2)	Source detector distance (m)	Air mass thickness (kg/m^2)	Total mass thickness (kg/m^2)
0.20	2271.00	454.20	20.00	24.86	479.06

Measured by gamma spectrometry / Calculated by the "knowledge library" model

ROI	Background count rate (/s)	Measured gross count rate (/s)	Net count rate (/s)	ROI */PR ratios	Total mass thickness by model (kg/m^2)	Shield mass thickness by model (kg/m^2)	Deviation from observed (%)
A			71.59	15.659	306.62	281.76	-38.0
B			30.98	6.776	418.76	393.90	-13.3
C			20.41	4.465	461.81	436.95	-3.8
PL			9.65	2.111	532.13	507.27	11.7
PC			0.53				
PR			4.57	Average	429.83	404.97	-10.8

Fig B.2.9 Tables comparing true shielding thickness values (denoted as observed data) with calculated values based on measured ROI net count rate ratios in the 2×2 litre IRSA detector when using the Lund University exponential model for a 4 litre NaI(Tl)-detector for the calculation (denoted as calculated by the "knowledge library" model). The ROIs (A, B, C, PL ad PR) are defined in Table B.2.2.

Table B.2.3 Coefficients a and b in the expression for determining the shield mass thickness $x = \ln(q/a)/b$ where q is the respective measured count rate ratios of ROIs A/PR, B/PR, C/PR and PL/PR, as obtained in the experimental measurements by IRSA/GR compared to the coefficients in the Lund University (LU) model.

		ROI A/PR		ROI B/PR		ROI C/PR		ROI PL/PR	
Team	NaI(Tl) detector volume	a	b	a	b	a	b	a	b
LU	4 litre	4.32	0.0042	1.85	0.0031	1.17	0.0029	1.24	0.0010
IRSA	2 litre	4.65	0.0022	1.67	0.0026	0.82	0.0032	1.02	0.0012

The Lund University (LU) model thus does not appear to exactly reproduce the mass thickness of the shielded wall. There seems to be a systematic underestimation. Assuming that there is still an exponential relationship between the shield thickness and the ratios between the count rates in the respective ROI, values of the coefficients *a* and *b* in the LU model have been calculated from the measurement data for the IRSA/GR 2 liter NaI(Tl)-spectrometer. The values are given in Table B.2.3 in comparison with the corresponding values for LU.

The coefficient *b* given in Table B.2.3 indicates that the slope of the exponential is less sharp for the lower energy ROI ratios A/PR and B/PR for the 2-liter detectors, than for a 4 liter detector. For the ROI ratio PL/PR (left to right area) of the full energy peak, the slope *b* is about the same.

B.2.5 Conclusion

We seemed to find a certain underestimation (10 - 40%) in the determination of the mass thickness of the shielding wall when using the coefficients *a* and *b* from the LU model when measuring with 2-liter NaI(Tl) detectors. This may be due to several things, including the fact that the lower detector volume compared to 4 liters for the LU model has a slightly different efficiency distributed over the photon energies used. Based on the IRSA/GR measured pulse height distributions, new values of the coefficients *a* and *b* have been calculated, which indicates a slightly less sharp slope on the curve in the exponential model for a 2 liter NaI(Tl) detector. However, the experimental data are very limited. More experimental measurements under similar conditions for 2 liter and 4 liter detectors are required to verify this.

B.2.6 Reference

Jonas M.C. Nilsson, Robert R. Finck, Christopher Rääf, Investigation and optimization of mobile NaI(Tl) and 3H-based neutron detectors for finding point sources, Nuclear instruments and methods in Physical Research A 786, pp 127-134, 2015.

B.3 Report from Geological Survey of Norway (NGU) shielding measurements for SHIELDMORC 2020

The measurements were done by NGU at the Institute for Energy Technology (IFE) in Kjeller, Norway on Wednesday, October 21st, 2020.

B.3.1 Description of shielding set-up and geometry

The source used was Cs-137 with an activity of 2.4 GBq. The measuring equipment was kept 55 m away from the source. The detectors were oriented directly towards the source. Given the terrain topography roughness of the area, 2-3 m vertical variation from source to detector is estimated. It was a cold and foggy day with an average temperature of 4.5 ºC (1.1 – 7.6 ºC) with a wind speed of about 1 m/s and an air humidity of 80-85%. The concrete tiles used for shielding had a weight range between 9.39 – 9.66 kg and size 29.5×29.5×5 cm. We used their average weight 9.55 kg in the calculation of their density, which then was determined to 2195 kg/m^3.

B.3.2 Description of measuring equipment

We used a RSX-5 spectrometer with 16-litre (4×4) NaI(Tl) detector. The detector, consisting of four crystals, was directly looking towards the source. The spectrometer was installed vertically and recorded 1024-channel spectra. The sampling interval was 1 second. We measured for ca. 5 minutes for the source with shielding configurations and 39 minutes for the background without the source.

Table B.3.1 Shielding thickness and measurement distance used in the shielding experiment by NGU, using a 4x4 litre NaI(Tl) detector and a 1024-channel analyzer. The source was Cs-137 with an activity of 2.4 GBq.

Detector	Source placement and shielding	Distance	Acquisition time
16 L NaI(Tl)	Background, no source		2314 s
16 L NaI(Tl)	Source behind 5 cm concrete tiles	55 m	287 s
16 L NaI(Tl)	Source behind 10 cm concrete tiles	55 m	361 s
16 L NaI(Tl)	Source behind 15 cm concrete tiles	55 m	302 s
16 L NaI(Tl)	Source behind 20 cm concrete tiles	55 m	291 s
16 L NaI(Tl)	Source behind 25 cm concrete tiles	55 m	212 s
16 L NaI(Tl)	Source behind 30 cm concrete tiles	55 m	271 s

The area used for the measurements was not ideal. We conducted this experiment at the end of October when the spectrometer was available after our regular field season. We measured near an open area at IFE in Kjeller, Norway. Unfortunately, it snowed two days before the planned acquisition date. We had to postpone the measurements by a day. However, the ground remained wet, prohibiting us from driving the car inside the area. Therefore, we performed the measurements from the side of road, which had a slight inclination causing a vertical variation of 2-3 m of the detectors compared to the source. Few vehicles were driving occasionally around ten meters away from the source, but no jumps or artifacts were observed in any of the ROIs in the post processed data. We performed the measurement with concrete tiles shield of thickness from 5 cm to 35 cm (Table B.3.1). For the shielding configuration of 35-cm-thickness, the measurements were very similar to the background measurements. Therefore, we assumed the source was not detected by the instrument and we did not report the result.

B.3.3 ROI set-up

The ROI setup for the experiment using the Cs-137 source was chosen to match the setup used by the Lund University model. The setup is listed in Table B.3.2.

Table B.3.2 The ROI setup for the NGU shielding experiment

ROI	Energy node (keV)	Energy interval (keV)	Channel interval	Number of channels
	74			
A		77 - 239	26 - 80	55
	242			
B		245 - 407	82 - 136	55
	410			
C		413 - 575	138 - 192	55
	578			
PL		581 - 659	194 - 220	27
PC	662	662	221	1
PR		665 - 743	222 - 248	27
	746			

B.3.4 Results

Calculated wall shield thickness from the measurements with the 16 L NaI(Tl) detector compared to true values is given in the Excel-tables shown in Fig B.3.1. The calculation was based on the Lund University "knowledge library" model with ROI A, B, C and PL in relation to PR (the right part of the 662 keV full energy peak, see definition of the ROI windows in Fig 3 in the main report) where the ROI channel intervals were set according to Table B.3.2.

The 16 litre NaI(Tl) detector showed about 10% overestimation of the shield thickness for concrete blocks of thickness 10 - 20 cm compared to the true value when using the Lund University model for a 4 litre NaI(Tl) detector using ROI C.. For smaller (5 cm) and larger (25 - 30 cm) shield thickness, the overestimation was between 7 and 27% using ROI C. Other ROIs showed larger deviations in general. This may be caused by a somewhat different shape of the efficiency curve for the 16 liter detector as a function of energy compared to a single 4 liter detector. The 16 liter detector consists of four 4 liter detectors mounted close together. Compton photons that may escape from a single 4 liter detector may be absorbed to a greater extent in the combination of four detectors. This is, however, a hypothesis that has to be confirmed by more detailed efficiency measurements of the 16 liter system. There could also be some variations due to differences in the local weather condition and the terrain at Kjeller and Lund.

For all shield thickness, there seems to be a systematic overestimation when applying the LU model coefficients for the 16 liter detector. Assuming that an exponential relationship between the shield thickness and the ratios between the count rates in the respective ROI, still exist, new values of the coefficients *a* and *b* have been calculated from the measurement data for the NGU 16 liter NaI(Tl)-spectrometer. The values are given in Table B.3.3 in comparison with the corresponding values for LU.

The coefficients *b* for all four ratios (A/PR, B/PR, C/PR and PL/PR) given in Table B.3.3 is generally larger than the corresponding values for the LU model 4 liter detector, indicating that there is a difference in the detector efficiency between the two systems. Therefore, a 16 liter system should be calibrated separately if one wants to achieve a higher accuracy with the method for determining shield thickness.

Calculation of shield mass thickness from gamma spectrometry on a shielded Cs-137 point source with a mobile 16 litre NaI(Tl)-spectrometer. Comparison with observed data.

Report from team: NGU

Describe shield material: concrete tiles

Observed data without gamma spectrometry

Shield thickness observed (m)	Shield material density (kg/m³)	Shield mass thickness (kg/m²)	Source detector distance (m)	Air mass thickness (kg/m²)	Total mass thickness (kg/m²)
0.05	2195.00	109.75	55.00	68.37	178.12

Measured by gamma spectrometry / Calculated by the "knowledge library" model

ROI	Background count rate (/s)	Measured gross count rate (/s)	Net count rate (/s)	ROI */PR ratios	Total mass thickness by model (kg/m²)	Shield mass thickness by model (kg/m²)	Deviation from observed (%)
A	2722	4674	1952.00	7.450	129.76	61.40	-44.1
B	929	1829	900.00	3.435	199.63	131.27	19.6
C	459	996	537.00	2.050	193.33	124.96	13.9
PL	168	633	465.00	1.775	358.58	290.22	164.4
PC	5	35	30.00				
PR	117	379	262.00	Average	220.33	151.96	38.5

Calculation of shield mass thickness from gamma spectrometry on a shielded Cs-137 point source with a mobile 16 litre NaI(Tl)-spectrometer. Comparison with observed data.

Report from team: NGU

Describe shield material: concrete tiles

Observed data without gamma spectrometry

Shield thickness observed (m)	Shield material density (kg/m³)	Shield mass thickness (kg/m²)	Source detector distance (m)	Air mass thickness (kg/m²)	Total mass thickness (kg/m²)
0.10	2195.00	219.50	55.00	68.37	287.87

Measured by gamma spectrometry / Calculated by the "knowledge library" model

ROI	Background count rate (/s)	Measured gross count rate (/s)	Net count rate (/s)	ROI */PR ratios	Total mass thickness by model (kg/m²)	Shield mass thickness by model (kg/m²)	Deviation from observed (%)
A	2722	4009.00	1287.00	11.000	222.53	154.17	-29.8
B	929	1480.00	551.00	4.709	301.41	233.05	6.2
C	459	768.00	309.00	2.641	280.75	212.38	-3.2
PL	168	396.00	228.00	1.949	452.06	383.70	74.8
PC	5	18.00	13.00				
PR	117	234.00	117.00	Average	314.19	245.82	12.0

Calculation of shield mass thickness from gamma spectrometry on a shielded Cs-137 point source with a mobile 16 litre NaI(Tl)-spectrometer. Comparison with observed data.

Report from team: NGU

Describe shield material: concrete tiles

Observed data without gamma spectrometry

Shield thickness observed (m)	Shield material density (kg/m³)	Shield mass thickness (kg/m²)	Source detector distance (m)	Air mass thickness (kg/m²)	Total mass thickness (kg/m²)
0.15	2195.00	329.25	55.00	68.37	397.62

Measured by gamma spectrometry / Calculated by the "knowledge library" model

ROI	Background count rate (/s)	Measured gross count rate (/s)	Net count rate (/s)	ROI */PR ratios	Total mass thickness by model (kg/m²)	Shield mass thickness by model (kg/m²)	Deviation from observed (%)
A	2722	3682	960.00	18.824	350.44	282.08	-14.3
B	929	1298	369.00	7.235	439.93	371.57	12.9
C	459	633	174.00	3.412	369.04	300.68	-8.7
PL	168	278	110.00	2.157	553.54	485.18	47.4
PC	5	11	6.00				
PR	117	168	51.00	Average	428.24	359.87	9.3

Calculation of shield mass thickness from gamma spectrometry on a shielded Cs-137 point source with a mobile 16 litre NaI(Tl)-spectrometer. Comparison with observed data.

Report from team: NGU

Describe shield material: concrete tiles

Observed data without gamma spectrometry

Shield thickness observed (m)	Shield material density (kg/m³)	Shield mass thickness (kg/m²)	Source detector distance (m)	Air mass thickness (kg/m²)	Total mass thickness (kg/m²)
0.20	2195.00	439.00	55.00	68.37	507.37

Measured by gamma spectrometry / Calculated by the "knowledge library" model

ROI	Background count rate (/s)	Measured gross count rate (/s)	Net count rate (/s)	ROI */PR ratios	Total mass thickness by model (kg/m²)	Shield mass thickness by model (kg/m²)	Deviation from observed (%)
A	2722	3515	793.00	36.045	505.13	436.76	-0.5
B	929	1204	275.00	12.500	616.30	547.94	24.8
C	459	559	100.00	4.545	467.97	399.61	-9.0
PL	168	221	53.00	2.409	664.14	595.77	35.7
PC	5	7	2.00				
PR	117	139	22.00	Average	563.39	495.02	12.8

Calculation of shield mass thickness from gamma spectrometry on a shielded Cs-137 point source with a mobile 16 litre NaI(Tl)-spectrometer. Comparison with observed data.

Report from team: NGU

Describe shield material: concrete tiles

Observed data without gamma spectrometry

Shield thickness observed (m)	Shield material density (kg/m³)	Shield mass thickness (kg/m²)	Source detector distance (m)	Air mass thickness (kg/m²)	Total mass thickness (kg/m²)
0.25	2195.00	548.75	55.00	68.37	617.12

Measured by gamma spectrometry / Calculated by the "knowledge library" model

ROI	Background count rate (/s)	Measured gross count rate (/s)	Net count rate (/s)	ROI */PR ratios	Total mass thickness by model (kg/m²)	Shield mass thickness by model (kg/m²)	Deviation from observed (%)
A	2722	3434	712.00	89.000	720.33	651.96	18.8
B	929	1151	222.00	27.750	873.56	805.20	46.7
C	459	522	63.00	7.875	657.48	589.11	7.4
PL	168	192	24.00	3.000	883.50	815.14	48.5
PC	5	6	1.00				
PR	117	125	8.00	Average	783.72	715.35	30.4

Calculation of shield mass thickness from gamma spectrometry on a shielded Cs-137 point source with a mobile 16 litre NaI(Tl)-spectrometer. Comparison with observed data.

Report from team: NGU

Describe shield material: concrete tiles

Observed data without gamma spectrometry

Shield thickness observed (m)	Shield material density (kg/m³)	Shield mass thickness (kg/m²)	Source detector distance (m)	Air mass thickness (kg/m²)	Total mass thickness (kg/m²)
0.30	2195.00	658.50	55.00	68.37	726.87

Measured by gamma spectrometry / Calculated by the "knowledge library" model

ROI	Background count rate (/s)	Measured gross count rate (/s)	Net count rate (/s)	ROI */PR ratios	Total mass thickness by model (kg/m²)	Shield mass thickness by model (kg/m²)	Deviation from observed (%)
A	2722	3392	670.00	223.333	939.38	871.02	32.3
B	929	1129	200.00	66.667	1156.30	1087.93	65.2
C	459	507	48.00	16.000	901.93	833.56	26.6
PL	168	179	11.00	3.667	1084.17	1015.81	54.3
PC	5	5	0.00				
PR	117	120	3.00	Average	1020.44	952.08	44.6

Fig B.3.1 Tables comparing true shielding thickness values (denoted as observed data) with calculated values based on measured ROI net count rate ratios in the 16 litre NGU detector when using the Lund University exponential model for a 4 litre NaI(Tl)-detector for the calculation (denoted as calculated by the "knowledge library" model). The ROIs (A, B, C, PL ad PR) are defined in Table B.3.2

Table B.3.3 Coefficients *a* and *b* in the expression for determining the shield mass thickness $x = \ln(q/a)/b$ where *q* is the respective measured count rate ratios of ROIs A/PR, B/PR, C/PR and PL/PR, as obtained in the experimental measurements by NGU using a 16 litre NaI(Tl)-detector compared to the coefficients in the Lund University (LU) model.

		ROI A/PR		ROI B/PR		ROI C/PR		ROI PL/PR	
Team	NaI(Tl) detector volume	*a*	*b*	*a*	*b*	*a*	*b*	*a*	*b*
LU	4 litre	4.32	0.0042	1.85	0.0031	1.17	0.0029	1.24	0.0010
NGU	16 litre	1.92	0.0062	1.03	0.0054	0.92	0.0036	1.33	0.0013

B.3.5 Conclusion

We observed that average deviation from the true shield mass thickness against Lund University knowledge library is larger (30 to 45 %) for 5 cm, 25 cm and 30 cm shields than for 10 - 20 cm. The shields of 10, 15 and 20-cm thickness yield around 10 % average deviation for actual shield mass thickness. PL window (left part of the full energy peak) always gave the largest deviation and the C window (the energy part with Compton scattering 27-58 degrees) gave the smallest deviation.

The *b* coefficient in the exponential expression for determining shield thickness from ROI net count rate measurements is generally somewhat larger when calculated for the 16 liter NaI(Tl) detector than the coefficient given in the Lund University “knowledge library” model for a 4 liter detector. This indicates that the 16 liter system should use coefficients *a* and *b* that are individually determined for this system.

B.4 Report from Radiation and Nuclear Safety Authority, Finland (STUK) shielding measurements for SHIELDMORC 2020

The Radiation and Nuclear Safety Authority, STUK, Finland made the measurements in November-December 2020.

B.4.1 Description of shielding set-up and geometry

The source used was Cs-137 with an activity of 18500 MBq. The shield was made from 50 × 50 × 5 cm concrete slabs with increasing number of slabs towards the detector and one slab thick on the sides and the back. Inner dimensions were 40 × 50 × 50 cm (W x L x H) and the source was placed 5 cm away from the inner front wall. (Fig B.4.1). The shield was built on a wooden pallet for easy movement between various distances. The density of the concrete slabs was 2196 kg/m^3.

Fig B.4.1. The concrete 5 cm slabs used by STUK as shielding material in the SHIELDMORC 2020 experiment. The front shielding wall is facing left. The shielding construction was mounted on wheels so that it could be moved to different distances from the detector. In the picture the shielding wall is built with 6 concrete slabs to a thickness of 30 cm.

B.4.2 Description of measuring equipment

A 4 litre NaI(Tl)-spectrometer (Environics RanidPort Mobile) with 1024 channels was used in the experiment. The NaI(Tl) crystal was oriented with its long side towards the source location. The sampling interval was 1 second. Consecutive measurements were summed to achieve higher statistical accuracy. The distance between the detector and the source varied from 10 to 40 m in steps of 10 m. The combination of shield thickness and source distance used in the experiment is summarized in Table B.4.1.

Table B.4.1 Shielding thickness and measurement distance used in the shielding experiment by STUK, using a 4 liter NaI(Tl) spectrometer. The source was Cs-137 with an activity of 18500 MBq. The acquisition times given in the table will provide less than 1% statistical uncertainty in the full energy peak area. Actual acquisition times in the experiment were longer than those given.

Detector	Source placement and shielding	Distance	Acquisition time
4 L NaI(Tl)	Background, no source		-
4 L NaI(Tl)	Source behind 10 cm concrete tiles	10 m	2.3 s
4 L NaI(Tl)	Source behind 20 cm concrete tiles	10 m	32.5 s
4 L NaI(Tl)	Source behind 30 cm concrete tiles	10 m	46.5 s
4 L NaI(Tl)	Source behind 10 cm concrete tiles	20 m	9.3 s
4 L NaI(Tl)	Source behind 20 cm concrete tiles	20 m	146.5 s
4 L NaI(Tl)	Source behind 30 cm concrete tiles	20 m	209.2 s
4 L NaI(Tl)	Source behind 10 cm concrete tiles	30 m	23.2 s
4 L NaI(Tl)	Source behind 20 cm concrete tiles	30 m	372.0 s
4 L NaI(Tl)	Source behind 30 cm concrete tiles	30 m	511.5 s
4 L NaI(Tl)	Source behind 10 cm concrete tiles	40 m	46.5 s
4 L NaI(Tl)	Source behind 20 cm concrete tiles	40 m	720.7 s
4 L NaI(Tl)	Source behind 30 cm concrete tiles	40 m	999.7 s

B.4.3 ROI set-up

The ROI setup for the experiment was chosen to match the setup used by the Lund University model. The setup is listed in Table B.4.2.

Table B.4.2 The ROI setup for the STUK shielding experiment. The channel values represent photon energies with an uncertainty of ± 1.5 keV in relation to the energy nodes recommended by for Lund University model.

ROI	Energy node (keV)	Energy interval (keV) ± 1.5 keV	Channel interval	Number of channels
	74			
A		74 - 242	22 - 69	48
	242			
B		242 - 410	69 - 116	68
	410			
C		410 - 578	116 – 163	48
	578			
PL		578 - 662	163-186	24
PC	662	662	1	1
PR		662 - 746	186 – 209	24
	746			

B.4.4 Results

Results of the calculated concrete shield thickness from the measurements with the 4 NaI(Tl) detector by STUK, using the Lund University model with ROI A, B, C and PL in relation to ROI PR (the right part of the 662 keV full energy peak) compared to the true values is shown in the Excel-tables, Fig B.4.1.

The calculated shielding thickness values from the measured ratios ROI A/PR, B/PR, C/PR and PL/PR showed 5 - 25% underestimation of the shield thickness for concrete blocks of thickness 20 - 30 cm compared to the true value. For 10 cm shielding thickness the underestimation was 5 - 60%, with the largest value obtained at the shortest distance 10 m from the source. This may be explained by the relatively high activity of the source, producing about 10% dead-time at this distance with 10 cm concrete shielding, as it may have distorted the pulse height distribution to some extent at this high count rate.

Calculation of shield mass thickness from gamma spectrometry on a shielded Cs-137 point source with a mobile 4 litre NaI(Tl)-spectrometer. Comparison with observed data.

Report from team: STUK

Describe shield material: concrete garden path slab 50 x 50 x 5 cm x n to thickness

Observed data without gamma spectrometry

Shield thickness observed (m)	Shield material density (kg/m^3)	Shield mass thickness (kg/m^2)	Source detector distance (m)	Air mass thickness (kg/m^2)	Total mass thickness (kg/m^2)
0.10	2196.00	219.60	10.00	12.43	232.03

Measured by gamma spectrometry / Calculated by the "knowledge library" model

ROI	Background count rate (/s)	Measured gross count rate (/s)	Net count rate (/s)	ROI */PR ratios	Total mass thickness by model (kg/m^2)	Shield mass thickness by model (kg/m^2)	Deviation from observed (%)
A	1331.80	126857.70	125525.90	3.936	-22.18	-34.61	-115.8
B	514.00	97357.00	96843.00	3.036	159.84	147.41	-32.9
C	232.50	67318.70	67086.20	2.103	202.27	189.84	-13.6
PL	90.40	42326.00	42235.60	1.324	65.76	53.33	-75.7
PC	2.50	3222.10	3219.60				
PR	58.70	31952.00	31893.30	Average	101.42	88.99	-59.5

Calculation of shield mass thickness from gamma spectrometry on a shielded Cs-137 point source with a mobile 4 litre NaI(Tl)-spectrometer. Comparison with observed data.

Report from team: STUK

Describe shield material: concrete garden path slab 50 x 50 x 5 cm x n to thickness

Observed data without gamma spectrometry

Shield thickness observed (m)	Shield material density (kg/m^3)	Shield mass thickness (kg/m^2)	Source detector distance (m)	Air mass thickness (kg/m^2)	Total mass thickness (kg/m^2)
0.20	2196.00	439.20	10.00	12.43	451.63

Measured by gamma spectrometry / Calculated by the "knowledge library" model

ROI	Background count rate (/s)	Measured gross count rate (/s)	Net count rate (/s)	ROI */PR ratios	Total mass thickness by model (kg/m^2)	Shield mass thickness by model (kg/m^2)	Deviation from observed (%)
A	1331.80	56769.00	55437.20	12.630	255.42	242.99	-44.7
B	514.00	27564.00	27050.00	6.162	388.16	375.73	-14.5
C	232.50	14637.30	14404.80	3.282	355.64	343.21	-21.9
PL	90.40	7906.40	7816.00	1.781	361.85	349.42	-20.4
PC	2.50	532.00	529.50				
PR	58.70	4448.20	4389.50	Average	340.27	327.84	-25.4

Calculation of shield mass thickness from gamma spectrometry on a shielded Cs-137 point source with a mobile 4 litre NaI(Tl)-spectrometer. Comparison with observed data.

Report from team: STUK

Describe shield material concrete garden path slab 50 x 50 x 5 cm x n to thickness

Observed data without gamma spectrometry

Shield thickness observed (m)	Shield material density (kg/m^3)	Shield mass thickness (kg/m^2)	Source detector distance (m)	Air mass thickness (kg/m^2)	Total mass thickness (kg/m^2)
0.30	2196.00	658.80	10.00	12.43	671.23

Measured by gamma spectrometry / Calculated by the "knowledge library" model

ROI	Background count rate (/s)	Measured gross count rate (/s)	Net count rate (/s)	ROI */PR ratios	Total mass thickness by model (kg/m^2)	Shield mass thickness by model (kg/m^2)	Deviation from observed (%)
A	1331.80	36737.30	35405.50	43.944	552.30	539.87	-18.1
B	514.00	12997.40	12483.40	15.494	685.57	673.14	2.2
C	232.50	4880.40	4647.90	5.769	550.16	537.73	-18.4
PL	90.40	1933.50	1843.10	2.288	612.38	599.95	-8.9
PC	2.50	105.50	103.00				
PR	58.70	864.40	805.70	Average	600.10	587.67	-10.8

Calculation of shield mass thickness from gamma spectrometry on a shielded Cs-137 point source with a mobile 4 litre NaI(Tl)-spectrometer. Comparison with observed data.

Report from team: STUK

Describe shield material: concrete garden path slab 50 x 50 x 5 cm x n to thickness

Observed data without gamma spectrometry

Shield thickness observed (m)	Shield material density (kg/m^3)	Shield mass thickness (kg/m^2)	Source detector distance (m)	Air mass thickness (kg/m^2)	Total mass thickness (kg/m^2)
0.10	2196.00	219.60	20.00	24.86	244.46

Measured by gamma spectrometry / Calculated by the "knowledge library" model

ROI	Background count rate (/s)	Measured gross count rate (/s)	Net count rate (/s)	ROI */PR ratios	Total mass thickness by model (kg/m^2)	Shield mass thickness by model (kg/m^2)	Deviation from observed (%)
A	1331.80	31376.40	30044.60	6.243	87.66	62.80	-71.4
B	514.00	16286.30	15772.30	3.277	184.46	159.60	-27.3
C	232.50	9841.00	9608.50	1.997	184.28	159.42	-27.4
PL	90.40	7605.30	7514.90	1.562	230.54	205.68	-6.3
PC	2.50	655.20	652.70				
PR	58.70	4871.30	4812.60	Average	171.74	146.88	-33.1

Calculation of shield mass thickness from gamma spectrometry on a shielded Cs-137 point source with a mobile 4 litre NaI(Tl)-spectrometer. Comparison with observed data.

Report from team: STUK

Describe shield material: concrete garden path slab 50 x 50 x 5 cm x n to thickness

Observed data without gamma spectrometry

Shield thickness observed (m)	Shield material density (kg/m^3)	Shield mass thickness (kg/m^2)	Source detector distance (m)	Air mass thickness (kg/m^2)	Total mass thickness (kg/m^2)
0.20	2196.00	439.20	20.00	24.86	464.06

Measured by gamma spectrometry / Calculated by the "knowledge library" model

ROI	Background count rate (/s)	Measured gross count rate (/s)	Net count rate (/s)	ROI */PR ratios	Total mass thickness by model (kg/m^2)	Shield mass thickness by model (kg/m^2)	Deviation from observed (%)
A	1331.80	14638.70	13306.90	15.817	309.01	284.15	-35.3
B	514.00	5583.20	5069.20	6.025	380.90	356.04	-18.9
C	232.50	2834.10	2601.60	3.092	335.15	310.29	-29.4
PL	90.40	1694.20	1603.80	1.906	430.07	405.21	-7.7
PC	2.50	123.60	121.10				
PR	58.70	900.00	841.30	Average	363.78	338.92	-22.8

Calculation of shield mass thickness from gamma spectrometry on a shielded Cs-137 point source with a mobile 4 litre NaI(Tl)-spectrometer. Comparison with observed data.

Report from team: STUK

Describe shield material concrete garden path slab 50 x 50 x 5 cm x n to thickness

Observed data without gamma spectrometry

Shield thickness observed (m)	Shield material density (kg/m^3)	Shield mass thickness (kg/m^2)	Source detector distance (m)	Air mass thickness (kg/m^2)	Total mass thickness (kg/m^2)
0.30	2196.00	658.80	20.00	24.86	683.66

Measured by gamma spectrometry / Calculated by the "knowledge library" model

ROI	Background count rate (/s)	Measured gross count rate (/s)	Net count rate (/s)	ROI */PR ratios	Total mass thickness by model (kg/m^2)	Shield mass thickness by model (kg/m^2)	Deviation from observed (%)
A	1331.80	10347.00	9015.20	55.684	608.67	583.81	-11.4
B	514.00	2985.10	2471.10	15.263	680.73	655.87	-0.4
C	232.50	1104.30	871.80	5.385	526.41	501.55	-23.9
PL	90.40	496.80	406.40	2.510	705.25	680.39	3.3
PC	2.50	26.70	24.20				
PR	58.70	220.60	161.90	Average	630.26	605.40	-8.1

Calculation of shield mass thickness from gamma spectrometry on a shielded Cs-137 point source with a mobile 4 litre NaI(Tl)-spectrometer. Comparison with observed data.

Report from team: STUK

Describe shield material: concrete garden path slab 50 x 50 x 5 cm x n to thickness

Observed data without gamma spectrometry					
Shield thickness observed (m)	Shield material density (kg/m^3)	Shield mass thickness (kg/m^2)	Source detector distance (m)	Air mass thickness (kg/m^2)	Total mass thickness (kg/m^2)
0.10	2196.00	219.60	30.00	37.29	256.89

	Measured by gamma spectrometry				Calculated by the "knowledge library" model		
ROI	Background count rate (/s)	Measured gross count rate (/s)	Net count rate (/s)	ROI */PR ratios	Total mass thickness by model (kg/m^2)	Shield mass thickness by model (kg/m^2)	Deviation from observed (%)
A	1331.80	14065.10	12733.30	7.835	141.75	104.46	-52.4
B	514.00	6582.20	6068.20	3.734	226.53	189.24	-13.8
C	232.50	3831.20	3598.70	2.214	219.98	182.69	-16.8
PL	90.40	3070.50	2980.10	1.834	391.21	353.92	61.2
PC	2.50	257.40	254.90				
PR	58.70	1683.90	1625.20	Average	244.87	207.58	-5.5

Calculation of shield mass thickness from gamma spectrometry on a shielded Cs-137 point source with a mobile 4 litre NaI(Tl)-spectrometer. Comparison with observed data.

Report from team: STUK

Describe shield material: concrete garden path slab 50 x 50 x 5 cm x n to thickness

Observed data without gamma spectrometry					
Shield thickness observed (m)	Shield material density (kg/m^3)	Shield mass thickness (kg/m^2)	Source detector distance (m)	Air mass thickness (kg/m^2)	Total mass thickness (kg/m^2)
0.20	2196.00	439.20	30.00	37.29	476.49

	Measured by gamma spectrometry				Calculated by the "knowledge library" model		
ROI	Background count rate (/s)	Measured gross count rate (/s)	Net count rate (/s)	ROI */PR ratios	Total mass thickness by model (kg/m^2)	Shield mass thickness by model (kg/m^2)	Deviation from observed (%)
A	1331.80	7222.40	5890.60	17.796	337.08	299.79	-31.7
B	514.00	2578.90	2064.90	6.238	392.11	354.82	-19.2
C	232.50	1275.00	1042.50	3.150	341.47	304.18	-30.7
PL	90.40	746.10	655.70	1.981	468.47	431.18	-1.8
PC	2.50	51.00	48.50				
PR	58.70	389.70	331.00	Average	384.78	347.49	-20.9

Calculation of shield mass thickness from gamma spectrometry on a shielded Cs-137 point source with a mobile 4 litre NaI(Tl)-spectrometer. Comparison with observed data.

Report from team: STUK

Describe shield material concrete garden path slab 50 x 50 x 5 cm x n to thickness

Observed data without gamma spectrometry					
Shield thickness observed (m)	Shield material density (kg/m^3)	Shield mass thickness (kg/m^2)	Source detector distance (m)	Air mass thickness (kg/m^2)	Total mass thickness (kg/m^2)
0.30	2196.00	658.80	30.00	37.29	696.09

	Measured by gamma spectrometry				Calculated by the "knowledge library" model		
ROI	Backgroun d count rate (/s)	Measured gross count rate (/s)	Net count rate (/s)	ROI */PR ratios	Total mass thickness by model (kg/m^2)	Shield mass thickness by model (kg/m^2)	Deviation from observed (%)
A	1331.80	5524.80	4193.00	62.303	635.42	598.13	-9.2
B	514.00	1556.20	1042.20	15.486	685.40	648.11	-1.6
C	232.50	589.90	357.40	5.311	521.62	484.33	-26.5
PL	90.40	264.20	173.80	2.582	733.63	696.34	5.7
PC	2.50	13.40	10.90				
PR	58.70	126.00	67.30	Average	644.02	606.73	-7.9

Calculation of shield mass thickness from gamma spectrometry on a shielded Cs-137 point source with a mobile 4 litre NaI(Tl)-spectrometer. Comparison with observed data.

Report from team: STUK

Describe shield material: concrete garden path slab 50 x 50 x 5 cm x n to thickness

Observed data without gamma spectrometry					
Shield thickness observed (m)	Shield material density (kg/m^3)	Shield mass thickness (kg/m^2)	Source detector distance (m)	Air mass thickness (kg/m^2)	Total mass thickness (kg/m^2)
0.10	2196.00	219.60	40.00	49.72	269.32

	Measured by gamma spectrometry				Calculated by the "knowledge library" model		
ROI	Background count rate (/s)	Measured gross count rate (/s)	Net count rate (/s)	ROI */PR ratios	Total mass thickness by model (kg/m^2)	Shield mass thickness by model (kg/m^2)	Deviation from observed (%)
A	1331.80	8139.00	6807.20	7.489	131.01	81.29	-63.0
B	514.00	3650.80	3136.80	3.451	201.14	151.42	-31.0
C	232.50	2127.40	1894.90	2.085	199.20	149.48	-31.9
PL	90.40	1527.20	1436.80	1.581	242.83	193.11	-12.1
PC	2.50	132.40	129.90				
PR	58.70	967.60	908.90	Average	193.55	143.83	-34.5

Calculation of shield mass thickness from gamma spectrometry on a shielded Cs-137 point source with a mobile 4 litre NaI(Tl)-spectrometer. Comparison with observed data.

Report from team: STUK

Describe shield material: concrete garden path slab 50 x 50 x 5 cm x n to thickness

Observed data without gamma spectrometry					
Shield thickness observed (m)	Shield material density (kg/m^3)	Shield mass thickness (kg/m^2)	Source detector distance (m)	Air mass thickness (kg/m^2)	Total mass thickness (kg/m^2)
0.20	2196.00	439.20	40.00	49.72	488.92

	Measured by gamma spectrometry				Calculated by the "knowledge library" model		
ROI	Background count rate (/s)	Measured gross count rate (/s)	Net count rate (/s)	ROI */PR ratios	Total mass thickness by model (kg/m^2)	Shield mass thickness by model (kg/m^2)	Deviation from observed (%)
A	1331.80	4603.90	3272.10	20.124	366.34	316.62	-27.9
B	514.00	1602.00	1088.00	6.691	414.72	365.00	-16.9
C	232.50	781.20	548.70	3.375	365.26	315.54	-28.2
PL	90.40	429.90	339.50	2.088	521.07	471.35	7.3
PC	2.50	27.60	25.10				
PR	58.70	221.30	162.60	Average	416.85	367.13	-16.4

Calculation of shield mass thickness from gamma spectrometry on a shielded Cs-137 point source with a mobile 4 litre NaI(Tl)-spectrometer. Comparison with observed data.

Report from team: STUK

Describe shield material concrete garden path slab 50 x 50 x 5 cm x n to thickness

Observed data without gamma spectrometry					
Shield thickness observed (m)	Shield material density (kg/m^3)	Shield mass thickness (kg/m^2)	Source detector distance (m)	Air mass thickness (kg/m^2)	Total mass thickness (kg/m^2)
0.30	2196.00	658.80	40.00	49.72	708.52

	Measured by gamma spectrometry				Calculated by the "knowledge library" model		
ROI	Backgroun d count rate (/s)	Measured gross count rate (/s)	Net count rate (/s)	ROI */PR ratios	Total mass thickness by model (kg/m^2)	Shield mass thickness by model (kg/m^2)	Deviation from observed (%)
A	1331.80	4450.20	3118.40	80.371	696.05	646.33	-1.9
B	514.00	1187.50	673.50	17.358	722.22	672.50	2.1
C	232.50	442.00	209.50	5.399	527.34	477.62	-27.5
PL	90.40	190.80	100.40	2.588	735.63	685.91	4.1
PC	2.50	8.60	6.10				
PR	58.70	97.50	38.80	Average	670.31	620.59	-5.8

Fig B.4.2 Tables comparing true shielding thickness values (denoted as observed data) with calculated values based on measured ROI net count rate ratios in the 4 liter STUK detector when using the Lund University exponential model for a 4 liter NaI(Tl)-detector for the calculation (denoted as calculated by the “knowledge library” model). The ROIs (A, B, C, PL ad PR) are defined in Table B.4.2

For all shield thickness, there seems to be a systematic underestimation when applying the LU model coefficients for the STUK detector. Assuming that an exponential relationship between the shield thickness and the ratios between the count rates in the respective ROI exist, new values of the coefficients *a* and *b* have been calculated from the measurement data for the STUK 4 liter NaI(Tl)-spectrometer. The values are given in Table B.4.3 in comparison with the corresponding values for LU. The coefficient *b* values are somewhat higher for the STUK detector, except for the ROI ratio C/PR, but too far-reaching conclusions about differences in the coefficient *b* cannot be drawn because the experimental data from STUK is not sufficiently extensive.

Table B.4.3 Coefficients *a* and *b* in the expression for determining the shield mass thickness $x = \ln(q/a)/b$ where *q* is the respective measured count rate ratios of ROIs A/PR, B/PR, C/PR and PL/PR, as obtained in the experimental measurements by STUK using a 4 litre NaI(Tl)-detector compared to the coefficients in the Lund University (LU) model.

		ROI A/PR		ROI B/PR		ROI C/PR		ROI PL/PR	
Team	NaI(Tl) detector volume	*a*	*b*	*a*	*b*	*a*	*b*	*a*	*b*
LU	4 litre	4.32	0.0042	1.85	0.0031	1.17	0.0029	1.24	0.0010
STUK	4 litre	1.57	0.0052	1.32	0.0035	1.20	0.0022	1.18	0.0011

B.4.5 Conclusion

The LU model applied on measurement data from the STUK 4 litre NaI(Tl) spectrometer gave an underestimation 5 - 25% underestimation of the shield thickness for concrete blocks of thickness 20 - 30 cm compared to the true value when the dead time of the spectrometer was kept low.

The *b* coefficient in the exponential expression for determining shield thickness from ROI net count rate measurements, when calculated for the STUK 4 litre NaI(Tl) spectrometer seams to be just a little larger than the coefficient given in the Lund University model for the same type of detector. This indicates that the principle of using a “knowledge library” with an exponential expression can be used to determine approximate values of shield thickness if the gamma spectrometers pulse height distribution is calibrated for the situation in question.

B.5 Report from Swedish Radiation Safety Authority, (SSM) shielding measurements for SHIELDMORC 2020

The Swedish Radiation Safety Authority made the shielding measurements in Barsebäck in Sweden in October 2020.

B.5.1 Shielding set-up and geometry

Three Cs-137 point sources with a total activity of 1070 MBq were used together for the shielding experiment. Wood shielding in 9 cm thick beams and concrete tile shielding with tile dimensions 20 × 13.3 × 5 cm (W x L x H) were used. The densities were 526 kg/m^3 for the wood beam and 2270 kg/m^3 for the concrete tiles. The shields were built in a trailer (Fig B.5.1).

The wood shielding wall thickness was built to 9, 18, 27 and 36 cm. The concrete wall thickness was built to 5, 10, 15, 20, 25 and 30 cm. Fig B.5.2 shows the set up before the shielding wall was built, showing the position of the three point sources placed in a plastic cup. When the shielding wall was built, the sources ended up about 3 cm behind the wall. Fig B.5.3 shows the concrete wall built with tiles to 5 cm thickness.

Fig B.5.1. The trailer in which the radiation sources and the shielding material was set up for the SSM SHIELDMORC 2020 experiment.

Fig B.5.2. Concrete 5 cm tiles used around the three Cs-137 point sources and four clay tiles above the sources before the front wall was set up. The sources are placed in the plastic cup.

Fig B.5.3. A shielding wall built with five concrete slabs of thickness 5 cm in front of the Cs-137 sources. Up to six layers of concrete tiles were used in the experiment to a total thickness of 30 cm.

B.5.2 Measuring equipment

Two 4 liter NaI(Tl)-spectrometers with 1024 channels and one 120% HPGe-spectrometer with 8192 channels were used in the experiment. The NaI(Tl) detectors were oriented with their long sides towards the source location. The acquisition intervals were in the order of 600 - 2300 s. The source - detector distance was 50 m in all set-ups. The combinations of shield material, shield thickness, detectors and acquisition times are given in Table B.5.1.

Table B.5.1 Detectors, shielding material and thickness, distance between source and detector and acquisition times applied in the shielding experiment by SSM. The total activity of the three Cs-137 sources used in all experiments was 1070 MBq.

Detector	Source placement and shielding	Distance	Acquisition time
4L NaI(Tl) (L)	Background, no source		1422 s
4L NaI(Tl) (L))	Source, unshielded	50 m	2073 s
4L NaI(Tl) (L)	Source behind 9 cm wood	50 m	842 s
4L NaI(Tl) (L)	Source behind 18 cm wood	50 m	951 s
4L NaI(Tl) (L)	Source behind 27 cm wood	50 m	931 s
4L NaI(Tl) (L)	Source behind 36 cm wood	50 m	1543 s
4L NaI(Tl) (L)	Source behind 5 cm concrete tiles	50 m	934 s
4L NaI(Tl) (L))	Source behind 10 cm concrete tiles	50 m	2862 s
4L NaI(Tl) (L))	Source behind 15 cm concrete tiles	50 m	1636 s
4L NaI(Tl) (L)	Source behind 20 cm concrete tiles	50 m	2067 s
4L NaI(Tl) (L))	Source behind 25 cm concrete tiles	50 m	2307 s
4L NaI(Tl) (L)	Source behind 30 cm concrete tiles	50 m	1556 s
4L NaI(Tl) (R)	Background, no source		1458 s
4L NaI(Tl) (R)	Source, unshielded	50 m	2202 s
4L NaI(Tl) (R)	Source behind 9 cm wood	50 m	832 s
4L NaI(Tl) (R)	Source behind 18 cm wood	50 m	954 s
4L NaI(Tl) (R)	Source behind 27 cm wood	50 m	931 s
4L NaI(Tl) (R)	Source behind 36 cm wood	50 m	1548 s
4L NaI(Tl) (R)	Source behind 5 cm concrete tiles	50 m	953 s
4L NaI(Tl) (R)	Source behind 10 cm concrete tiles	50 m	1654 s
4L NaI(Tl) (R)	Source behind 15 cm concrete tiles	50 m	1631 s
4L NaI(Tl) (R)	Source behind 20 cm concrete tiles	50 m	1935 s
4L NaI(Tl) (R)	Source behind 25 cm concrete tiles	50 m	2286 s
4L NaI(Tl) (R)	Source behind 30 cm concrete tiles	50 m	1562 s
120 % HPGe	Background, no source		1346 s
120 % HPGe	Source unshielded	50 m	3784 s
120 % HPGe	Source behind 9 cm wood	50 m	787 s
120 % HPGe	Source behind 18 cm wood	50 m	891 s
120 % HPGe	Source behind 27 cm wood	50 m	901 s
120 % HPGe	Source behind 36 cm wood	50 m	1501 s
120 % HPGe	Source behind 5 cm concrete tiles	50 m	667 s
120 % HPGe	Source behind 10 cm concrete tiles	50 m	1630 s
120 % HPGe	Source behind 15 cm concrete tiles	50 m	1566 s
120 % HPGe	Source behind 20 cm concrete tiles	50 m	1996 s
120 % HPGe	Source behind 25 cm concrete tiles	50 m	2210 s
120 % HPGe	Source behind 30 cm concrete tiles	50 m	1520 s

B.5.3 ROI set-up

The ROI setup for the experiment was chosen to match the setup used by the Lund University model. The setups for the detectors are is listed in Table B.5.2 - B.5.4

Table B.5.2 The ROI setup for the SSM shielding experiment using a 4 liter NaI(Tl) detector (L).

ROI	Energy node (keV)	Energy interval (keV) ± 1.5 keV	Channel interval	Number of channels
	74		34	
A		78 – 238	35 - 90	56
	242		91	
B		244 – 408	92 - 148	57
	410		149	
C		414 – 576	150 - 205	56
	578		206	
PL		582 – 659	207 - 233	27
PC	662	662	234	1
PR		665 – 742	235 - 261	27
	745			

Table B.5.3 The ROI setup for the SSM shielding experiment using a 4 liter NaI(Tl) detector (R).

ROI	Energy node (keV)	Energy interval (keV) ± 1.5 keV	Channel interval	Number of channels
	74		34	
A		76 – 240	35 - 91	57
	242		92	
B		246 – 407	93 - 148	56
	410		149	
C		413 – 575	150 - 205	56
	578		206	
PL		581 – 658	207 - 233	27
PC	662	661	234	1
PR		664 – 741	235 - 261	27
	745			

Table B.5.4 The ROI setup for the SSM shielding experiment using a 120% HPGe detector.

ROI	Energy node (keV)	Energy interval (keV) ± 1.5 keV	Channel interval	Number of channels
	74.1		204	
A		74.5 – 241.8	205 - 663	459
	242.2		664	1
B		242.6 – 409.5	665 - 1122	458
	409.9		1123	1
C		410.2 – 577.6	1124 – 1582	459
	577.9		1583	1
P		653.5 -669.6	1790 - 1834	45

B.5.4 Results

The calculated concrete shield thickness values based on SSM measurements with the two 4 NaI(Tl) detectors (L) and (R) and using the Lund University "knowledge-library" model compared to the true values are shown in the Excel tables, Fig B.5.2a and B.5.2c. The correspondence between the calculated shield thicknesses from the net count rate ratios ROI A/PR, B/PR, C/PR and PL/PR and the true values improved as the shield thickness increased. The calculated values showed about 25 - 30% underestimation of the shield thickness for a single layer of 5 cm concrete tiles. For 10 - 20 cm thickness the underestimation was about 10%. For 25 - 30 cm the calculated thickness values from the ROI ratio measurements were close to the true values.

The calculated wood shield thickness values from the ROI count rate ratios measurements in the two 4 liter NaI(Tl) detectors (L) and (R) compared to the true values are shown in the Excel tables, Fig B.5.2b and B.5.2d. For 9 - 18 cm wood shielding there is an underestimation of 50 - 100%. For 27 - 36 cm wood shielding the underestimation is 25 - 30%.

The calculated concrete shield thickness values from the measurements with the 120% HPGe detector using the Lund University "knowledge-library" model with net count rate ratios ROI A/P, B/P, C/P compared to the true values are shown in Fig B.5.2e. The calculated values showed an overestimation of about 20% for 5 cm thickness and about ±5% for 10 - 30 cm thickness.

The calculated wood shield thickness values from the measurements with the 120% HPGe detector compared to the true values are shown in Fig B.5.2f. The shielding thickness values obtained from measurements were within about ±10% of the true values for all wood thickness 9 - 36 cm.

For both wood and concrete, there seems to be a systematic underestimation when applying the Lund University "knowledge-library" model coefficients for the two SSM 4 liter NaI(Tl) detectors(L) and (R) for the thinner shields. As the shield thickness increases, the correspondence between calculated and true values becomes better. For the 120% HPGe detector there seems not to be any systematic deviation using the Lund University model compared to the true shield thickness.

Assuming that an exponential relationship between the shield thickness and the ratios between the count rates in the respective ROI exist, new values of the coefficients *a* and *b* have been calculated from the measurement data for the SSM detectors. The values are given in Table B.5.5 for the NaI(Tl) detectors (L) and (R) and in Table B.5.6 for the 120% HPGe detector in comparison to the corresponding values for the Lund University "knowledge-library" model.

Calculation of shield mass thickness from gamma spectrometry on a shielded Cs-137 point source with a mobile 4 litre NaI(Tl)-spectrometer. Comparison with observed data.

Report from team: SSM

Describe shield material: concrete blocks

Observed data without gamma spectrometry

Shield thickness observed (m)	Shield material density (kg/m^3)	Shield mass thickness (kg/m^2)	Source detector distance (m)	Air mass thickness (kg/m^2)	Total mass thickness (kg/m^2)
0.05	2271.00	113.55	50.00	62.15	175.70

Measured by gamma spectrometry | Calculated by the "knowledge library" model

ROI	Background count rate (/s)	Measured gross count rate (/s)	Net count rate (/s)	ROI */PR ratios	Total mass thickness by model (kg/m^2)	Shield mass thickness by model (kg/m^2)	Deviation from observed (%)
A	668.09	1221.50	553.41	6.926	112.38	50.23	-55.8
B	254.71	500.53	245.82	3.076	164.05	101.90	-10.3
C	122.60	275.58	152.98	1.915	169.83	107.68	-5.2
PL	47.33	159.40	112.07	1.403	123.17	61.02	-46.3
PC			0.00				
PR	32.86	112.77	79.91	Average	142.36	80.21	-29.4

Calculation of shield mass thickness from gamma spectrometry on a shielded Cs-137 point source with a mobile 4 litre NaI(Tl)-spectrometer. Comparison with observed data.

Report from team: SSM

Describe shield material: concrete blocks

Observed data without gamma spectrometry

Shield thickness observed (m)	Shield material density (kg/m^3)	Shield mass thickness (kg/m^2)	Source detector distance (m)	Air mass thickness (kg/m^2)	Total mass thickness (kg/m^2)
0.10	2271.00	227.10	50.00	62.15	289.25

Measured by gamma spectrometry | Calculated by the "knowledge library" model

ROI	Background count rate (/s)	Measured gross count rate (/s)	Net count rate (/s)	ROI */PR ratios	Total mass thickness by model (kg/m^2)	Shield mass thickness by model (kg/m^2)	Deviation from observed (%)
A	668.09	1015.60	347.51	10.338	207.75	145.60	-35.9
B	254.71	399.38	144.67	4.304	272.35	210.20	-7.4
C	122.60	211.30	88.70	2.639	280.43	218.28	-3.9
PL	47.33	102.20	54.87	1.632	274.88	212.73	-6.3
PC			0.00				
PR	32.86	66.48	33.62	Average	258.85	196.70	-13.4

Calculation of shield mass thickness from gamma spectrometry on a shielded Cs-137 point source with a mobile 4 litre NaI(Tl)-spectrometer. Comparison with observed data.

Report from team: SSM

Describe shield material: concrete blocks

Observed data without gamma spectrometry

Shield thickness observed (m)	Shield material density (kg/m^3)	Shield mass thickness (kg/m^2)	Source detector distance (m)	Air mass thickness (kg/m^2)	Total mass thickness (kg/m^2)
0.15	2271.00	340.65	50.00	62.15	402.80

Measured by gamma spectrometry | Calculated by the "knowledge library" model

ROI	Background count rate (/s)	Measured gross count rate (/s)	Net count rate (/s)	ROI */PR ratios	Total mass thickness by model (kg/m^2)	Shield mass thickness by model (kg/m^2)	Deviation from observed (%)
A	668.09	898.13	230.04	16.115	313.45	251.30	-26.2
B	254.71	340.69	85.97	6.023	380.76	318.61	-6.5
C	122.60	168.84	46.24	3.240	351.18	289.03	-15.2
PL	47.33	73.52	26.19	1.835	391.76	329.61	-3.2
PC			0.00				
PR	32.86	47.14	14.28	Average	359.29	297.14	-12.8

Calculation of shield mass thickness from gamma spectrometry on a shielded Cs-137 point source with a mobile 4 litre NaI(Tl)-spectrometer. Comparison with observed data.

Report from team: SSM

Describe shield material: concrete blocks

Observed data without gamma spectrometry

Shield thickness observed (m)	Shield material density (kg/m^3)	Shield mass thickness (kg/m^2)	Source detector distance (m)	Air mass thickness (kg/m^2)	Total mass thickness (kg/m^2)
0.20	2271.00	454.20	50.00	62.15	516.35

Measured by gamma spectrometry | Calculated by the "knowledge library" model

ROI	Background count rate (/s)	Measured gross count rate (/s)	Net count rate (/s)	ROI */PR ratios	Total mass thickness by model (kg/m^2)	Shield mass thickness by model (kg/m^2)	Deviation from observed (%)
A	668.09	840.79	172.70	28.726	451.08	388.93	-14.4
B	254.71	310.22	55.51	9.233	518.59	456.44	0.5
C	122.60	146.84	24.24	4.032	426.63	364.48	-19.8
PL	47.33	59.76	12.43	2.068	511.24	449.09	-1.1
PC			0.00				
PR	32.86	38.88	6.01	Average	476.89	414.74	-8.7

Calculation of shield mass thickness from gamma spectrometry on a shielded Cs-137 point source with a mobile 4 litre NaI(Tl)-spectrometer. Comparison with observed data.

Report from team: SSM

Describe shield material: concrete blocks

Observed data without gamma spectrometry

Shield thickness observed (m)	Shield material density (kg/m^3)	Shield mass thickness (kg/m^2)	Source detector distance (m)	Air mass thickness (kg/m^2)	Total mass thickness (kg/m^2)
0.25	2271.00	567.75	50.00	62.15	629.90

Measured by gamma spectrometry | Calculated by the "knowledge library" model

ROI	Background count rate (/s)	Measured gross count rate (/s)	Net count rate (/s)	ROI */PR ratios	Total mass thickness by model (kg/m^2)	Shield mass thickness by model (kg/m^2)	Deviation from observed (%)
A	668.09	815.84	147.75	60.429	628.15	566.00	-0.3
B	254.71	295.26	40.54	16.583	707.47	645.32	13.7
C	122.60	135.69	13.09	5.354	524.43	462.28	-18.6
PL	47.33	52.99	5.66	2.315	624.26	562.11	-1.0
PC			0.00				
PR	32.86	35.31	2.45	Average	621.08	558.93	-1.6

Calculation of shield mass thickness from gamma spectrometry on a shielded Cs-137 point source with a mobile 4 litre NaI(Tl)-spectrometer. Comparison with observed data.

Report from team: SSM

Describe shield material: concrete blocks

Observed data without gamma spectrometry

Shield thickness observed (m)	Shield material density (kg/m^3)	Shield mass thickness (kg/m^2)	Source detector distance (m)	Air mass thickness (kg/m^2)	Total mass thickness (kg/m^2)
0.30	2271.00	681.30	50.00	62.15	743.45

Measured by gamma spectrometry | Calculated by the "knowledge library" model

ROI	Background count rate (/s)	Measured gross count rate (/s)	Net count rate (/s)	ROI */PR ratios	Total mass thickness by model (kg/m^2)	Shield mass thickness by model (kg/m^2)	Deviation from observed (%)
A	668.09	803.48	135.39	124.207	799.69	737.54	8.3
B	254.71	289.87	35.16	32.253	922.07	859.92	26.2
C	122.60	130.58	7.98	7.320	632.28	570.13	-16.3
PL	47.33	50.24	2.91	2.670	766.83	704.68	3.4
PC			0.00				
PR	32.86	33.96	1.09	Average	780.22	718.07	5.4

Fig B.5.2a Tables comparing true shielding thickness values for concrete tiles 5, 10, 15, 20, 25 and 30 cm (denoted as observed data) with calculated values based on measured ROI net count rate ratios in the 4 liter SSM NaI(Tl)-detector (L) when using the Lund University exponential model for a 4 liter NaI(Tl)-detector for the calculation (denoted as calculated by the “knowledge library” model). The ROIs (A, B, C, PL and PR) are defined in Table B.5.2

Calculation of shield mass thickness from gamma spectrometry on a shielded Cs-137 point source with a mobile 4 litre NaI(Tl)-spectrometer. Comparison with observed data.

Report from team: SSM

Describe shield material: Wood

Observed data without gamma spectrometry

Shield thickness observed (m)	Shield material density (kg/m^3)	Shield mass thickness (kg/m^2)	Source detector distance (m)	Air mass thickness (kg/m^2)	Total mass thickness (kg/m^2)
0.09	526.00	47.34	50.00	62.15	109.49

Measured by gamma spectrometry / Calculated by the "knowledge library" model

ROI	Background count rate (/s)	Measured gross count rate (/s)	Net count rate (/s)	ROI */PR ratios	Total mass thickness by model (kg/m^2)	Shield mass thickness by model (kg/m^2)	Deviation from observed (%)
A	668.09	1369.40	701.31	5.317	49.43	-12.72	-126.9
B	254.71	570.66	315.95	2.395	83.32	21.17	-55.3
C	122.60	311.70	189.10	1.434	70.07	7.92	-83.3
PL	47.33	216.94	169.61	1.286	36.31	-25.84	-154.6
PC			0.00				
PR	32.86	164.77	131.91	Average	59.78	-2.37	-105.0

Calculation of shield mass thickness from gamma spectrometry on a shielded Cs-137 point source with a mobile 4 litre NaI(Tl)-spectrometer. Comparison with observed data.

Report from team: SSM

Describe shield material: Wood

Observed data without gamma spectrometry

Shield thickness observed (m)	Shield material density (kg/m^3)	Shield mass thickness (kg/m^2)	Source detector distance (m)	Air mass thickness (kg/m^2)	Total mass thickness (kg/m^2)
0.18	526.00	94.68	50.00	62.15	156.83

Measured by gamma spectrometry / Calculated by the "knowledge library" model

ROI	Background count rate (/s)	Measured gross count rate (/s)	Net count rate (/s)	ROI */PR ratios	Total mass thickness by model (kg/m^2)	Shield mass thickness by model (kg/m^2)	Deviation from observed (%)
A	668.09	1218.97	550.88	6.110	82.53	20.38	-78.5
B	254.71	498.56	243.85	2.704	122.49	60.34	-36.3
C	122.60	274.40	151.80	1.684	125.48	63.33	-33.1
PL	47.33	171.47	124.14	1.377	104.66	42.51	-55.1
PC			0.00				
PR	32.86	123.03	90.17	Average	108.79	46.64	-50.7

Calculation of shield mass thickness from gamma spectrometry on a shielded Cs-137 point source with a mobile 4 litre NaI(Tl)-spectrometer. Comparison with observed data.

Report from team: SSM

Describe shield material: Wood

Observed data without gamma spectrometry

Shield thickness observed (m)	Shield material density (kg/m^3)	Shield mass thickness (kg/m^2)	Source detector distance (m)	Air mass thickness (kg/m^2)	Total mass thickness (kg/m^2)
0.27	526.00	142.02	50.00	62.15	204.17

Measured by gamma spectrometry / Calculated by the "knowledge library" model

ROI	Background count rate (/s)	Measured gross count rate (/s)	Net count rate (/s)	ROI */PR ratios	Total mass thickness by model (kg/m^2)	Shield mass thickness by model (kg/m^2)	Deviation from observed (%)
A	668.09	1109.10	441.01	7.229	122.58	60.43	-57.4
B	254.71	442.86	188.14	3.084	164.86	102.71	-27.7
C	122.60	242.26	119.66	1.961	178.17	116.02	-18.3
PL	47.33	137.13	89.80	1.472	171.52	109.37	-23.0
PC			0.00				
PR	32.86	93.87	61.01	Average	159.28	97.13	-31.6

Calculation of shield mass thickness from gamma spectrometry on a shielded Cs-137 point source with a mobile 4 litre NaI(Tl)-spectrometer. Comparison with observed data.

Report from team: SSM

Describe shield material: Wood

Observed data without gamma spectrometry

Shield thickness observed (m)	Shield material density (kg/m^3)	Shield mass thickness (kg/m^2)	Source detector distance (m)	Air mass thickness (kg/m^2)	Total mass thickness (kg/m^2)
0.36	526.00	189.36	50.00	62.15	251.51

Measured by gamma spectrometry / Calculated by the "knowledge library" model

ROI	Background count rate (/s)	Measured gross count rate (/s)	Net count rate (/s)	ROI */PR ratios	Total mass thickness by model (kg/m^2)	Shield mass thickness by model (kg/m^2)	Deviation from observed (%)
A	668.09	1035.11	367.02	8.303	155.57	93.42	-50.7
B	254.71	405.29	150.57	3.406	196.93	134.78	-28.8
C	122.60	219.63	97.03	2.195	216.98	154.83	-18.2
PL	47.33	115.62	68.29	1.545	219.86	157.71	-16.7
PC			0.00				
PR	32.86	77.07	44.20	Average	197.33	135.18	-28.6

Fig B.5.2b Tables comparing true shielding thickness values for wood blocks of thickness 9, 18, 27 and 36 cm (denoted as observed data) with calculated values based on measured ROI net count rate ratios in the 4 liter SSM NaI(Tl)-detector (L) when using the Lund University exponential model for a 4 liter NaI(Tl)-detector for the calculation (denoted as calculated by the "knowledge library" model). The ROIs (A, B, C, PL and PR) are defined in Table B.5.2

Calculation of shield mass thickness from gamma spectrometry on a shielded Cs-137 point source with a mobile 4 litre NaI(Tl)-spectrometer. Comparison with observed data.

Report from team: SSM

Describe shield material: concrete blocks

Observed data without gamma spectrometry

Shield thickness observed (m)	Shield material density (kg/m^3)	Shield mass thickness (kg/m^2)	Source detector distance (m)	Air mass thickness (kg/m^2)	Total mass thickness (kg/m^2)
0.05	2271.00	113.55	50.00	62.15	175.70

ROI	Background count rate (/s)	Measured gross count rate (/s)	Net count rate (/s)	ROI */PR ratios	Total mass thickness by model (kg/m^2)	Shield mass thickness by model (kg/m^2)	Deviation from observed (%)
	Measured by gamma spectrometry				Calculated by the "knowledge library" model		
A	631.10	1217.40	586.30	7.339	126.17	64.02	-43.6
B	226.11	470.87	244.76	3.064	162.72	100.57	-11.4
C	111.50	265.37	153.87	1.926	171.88	109.73	-3.4
PL	42.97	154.95	111.98	1.402	122.56	60.41	-46.8
PC			0.00				
PR	29.25	109.14	79.89	Average	145.83	83.68	-26.3

Calculation of shield mass thickness from gamma spectrometry on a shielded Cs-137 point source with a mobile 4 litre NaI(Tl)-spectrometer. Comparison with observed data.

Report from team: SSM

Describe shield material: concrete blocks

Observed data without gamma spectrometry

Shield thickness observed (m)	Shield material density (kg/m^3)	Shield mass thickness (kg/m^2)	Source detector distance (m)	Air mass thickness (kg/m^2)	Total mass thickness (kg/m^2)
0.10	2271.00	227.10	50.00	62.15	289.25

ROI	Background count rate (/s)	Measured gross count rate (/s)	Net count rate (/s)	ROI */PR ratios	Total mass thickness by model (kg/m^2)	Shield mass thickness by model (kg/m^2)	Deviation from observed (%)
	Measured by gamma spectrometry				Calculated by the "knowledge library" model		
A	631.10	1000.47	369.37	10.797	218.10	155.95	-31.3
B	226.11	370.28	144.17	4.214	265.57	203.42	-10.4
C	111.50	201.14	89.64	2.620	278.03	215.88	-4.9
PL	42.97	99.02	56.05	1.638	278.61	216.46	-4.7
PC			0.00				
PR	29.25	63.46	34.21	Average	260.08	197.93	-12.8

Calculation of shield mass thickness from gamma spectrometry on a shielded Cs-137 point source with a mobile 4 litre NaI(Tl)-spectrometer. Comparison with observed data.

Report from team: SSM

Describe shield material: concrete blocks

Observed data without gamma spectrometry

Shield thickness observed (m)	Shield material density (kg/m^3)	Shield mass thickness (kg/m^2)	Source detector distance (m)	Air mass thickness (kg/m^2)	Total mass thickness (kg/m^2)
0.15	2271.00	340.65	50.00	62.15	402.80

ROI	Background count rate (/s)	Measured gross count rate (/s)	Net count rate (/s)	ROI */PR ratios	Total mass thickness by model (kg/m^2)	Shield mass thickness by model (kg/m^2)	Deviation from observed (%)
	Measured by gamma spectrometry				Calculated by the "knowledge library" model		
A	631.10	874.18	243.08	17.293	330.25	268.10	-21.3
B	226.11	310.36	84.25	5.994	379.22	317.07	-6.9
C	111.50	158.87	47.37	3.370	364.79	302.64	-11.2
PL	42.97	69.47	26.50	1.885	418.94	356.79	4.7
PC			0.00				
PR	29.25	43.31	14.06	Average	373.30	311.15	-8.7

Calculation of shield mass thickness from gamma spectrometry on a shielded Cs-137 point source with a mobile 4 litre NaI(Tl)-spectrometer. Comparison with observed data.

Report from team: SSM

Describe shield material: concrete blocks

Observed data without gamma spectrometry

Shield thickness observed (m)	Shield material density (kg/m^3)	Shield mass thickness (kg/m^2)	Source detector distance (m)	Air mass thickness (kg/m^2)	Total mass thickness (kg/m^2)
0.20	2271.00	454.20	50.00	62.15	516.35

ROI	Background count rate (/s)	Measured gross count rate (/s)	Net count rate (/s)	ROI */PR ratios	Total mass thickness by model (kg/m^2)	Shield mass thickness by model (kg/m^2)	Deviation from observed (%)
	Measured by gamma spectrometry				Calculated by the "knowledge library" model		
A	631.10	809.88	178.78	29.502	457.43	395.28	-13.0
B	226.11	280.10	53.99	8.909	507.07	444.92	-2.0
C	111.50	135.18	23.68	3.907	415.76	353.61	-22.1
PL	42.97	55.91	12.94	2.135	543.50	481.35	6.0
PC			0.00				
PR	29.25	35.31	6.06	Average	480.94	418.79	-7.8

Calculation of shield mass thickness from gamma spectrometry on a shielded Cs-137 point source with a mobile 4 litre NaI(Tl)-spectrometer. Comparison with observed data.

Report from team: SSM

Describe shield material: concrete blocks

Observed data without gamma spectrometry

Shield thickness observed (m)	Shield material density (kg/m^3)	Shield mass thickness (kg/m^2)	Source detector distance (m)	Air mass thickness (kg/m^2)	Total mass thickness (kg/m^2)
0.25	2271.00	567.75	50.00	62.15	629.90

ROI	Background count rate (/s)	Measured gross count rate (/s)	Net count rate (/s)	ROI */PR ratios	Total mass thickness by model (kg/m^2)	Shield mass thickness by model (kg/m^2)	Deviation from observed (%)
	Measured by gamma spectrometry				Calculated by the "knowledge library" model		
A	631.10	785.45	154.35	60.097	626.84	564.69	-0.5
B	226.11	267.55	41.44	16.134	698.63	636.48	12.1
C	111.50	124.85	13.35	5.198	514.26	452.11	-20.4
PL	42.97	49.20	6.23	2.426	671.00	608.85	7.2
PC			0.00				
PR	29.25	31.82	2.57	Average	627.68	565.53	-0.4

Calculation of shield mass thickness from gamma spectrometry on a shielded Cs-137 point source with a mobile 4 litre NaI(Tl)-spectrometer. Comparison with observed data.

Report from team: SSM

Describe shield material: concrete blocks

Observed data without gamma spectrometry

Shield thickness observed (m)	Shield material density (kg/m^3)	Shield mass thickness (kg/m^2)	Source detector distance (m)	Air mass thickness (kg/m^2)	Total mass thickness (kg/m^2)
0.30	2271.00	681.30	50.00	62.15	743.45

ROI	Background count rate (/s)	Measured gross count rate (/s)	Net count rate (/s)	ROI */PR ratios	Total mass thickness by model (kg/m^2)	Shield mass thickness by model (kg/m^2)	Deviation from observed (%)
	Measured by gamma spectrometry				Calculated by the "knowledge library" model		
A	631.10	770.70	139.60	139.600	827.51	765.36	12.3
B	226.11	259.86	33.75	33.747	936.68	874.53	28.4
C	111.50	118.84	7.34	7.337	633.10	570.95	-16.2
PL	42.97	45.63	2.66	2.660	763.21	701.06	2.9
PC			0.00				
PR	29.25	30.25	1.00	Average	790.12	727.97	6.9

Fig B.5.2c Tables comparing true shielding thickness values for concrete tiles of thickness 5, 10, 15, 20, 25 and 30 cm (denoted as observed data) with calculated values based on measured ROI net count rate ratios in the 4 liter SSM NaI(Tl)-detector (R) when using the Lund University exponential model for a 4 liter NaI(Tl)-detector for the calculation (denoted as calculated by the "knowledge library" model). The ROIs (A, B, C, PL and PR) are defined in Table B.5.3

Calculation of shield mass thickness from gamma spectrometry on a shielded Cs-137 point source with a mobile 4 litre NaI(Tl)-spectrometer. Comparison with observed data.

Report from team: SSM

Describe shield material: Wood

Observed data without gamma spectrometry

Shield thickness observed (m)	Shield material density (kg/m^3)	Shield mass thickness (kg/m^2)	Source detector distance (m)	Air mass thickness (kg/m^2)	Total mass thickness (kg/m^2)
0.09	526.00	47.34	50.00	62.15	109.49

	Measured by gamma spectrometry				Calculated by the "knowledge library" model		
ROI	Background count rate (/s)	Measured gross count rate (/s)	Net count rate (/s)	ROI */PR ratios	Total mass thickness by model (kg/m^2)	Shield mass thickness by model (kg/m^2)	Deviation from observed (%)
A	631.10	1377.96	746.86	5.572	60.61	-1.54	-103.3
B	226.11	542.49	316.38	2.361	78.61	16.46	-65.2
C	111.50	301.56	190.06	1.418	66.30	4.15	-91.2
PL	42.97	213.66	170.69	1.274	26.67	-35.48	-174.9
PC			0.00				
PR	29.25	163.28	134.03	Average	58.05	-4.10	-108.7

Calculation of shield mass thickness from gamma spectrometry on a shielded Cs-137 point source with a mobile 4 litre NaI(Tl)-spectrometer. Comparison with observed data.

Report from team: SSM

Describe shield material: Wood

Observed data without gamma spectrometry

Shield thickness observed (m)	Shield material density (kg/m^3)	Shield mass thickness (kg/m^2)	Source detector distance (m)	Air mass thickness (kg/m^2)	Total mass thickness (kg/m^2)
0.18	526.00	94.68	50.00	62.15	156.83

	Measured by gamma spectrometry				Calculated by the "knowledge library" model		
ROI	Background count rate (/s)	Measured gross count rate (/s)	Net count rate (/s)	ROI */PR ratios	Total mass thickness by model (kg/m^2)	Shield mass thickness by model (kg/m^2)	Deviation from observed (%)
A	631.10	1216.51	585.41	6.357	91.96	29.81	-68.5
B	226.11	468.29	242.18	2.630	113.45	51.30	-45.8
C	111.50	263.83	152.33	1.654	119.39	57.24	-39.5
PL	42.97	169.34	126.37	1.372	101.31	39.16	-58.6
PC			0.00				
PR	29.25	121.34	92.09	Average	106.53	44.38	-53.1

Calculation of shield mass thickness from gamma spectrometry on a shielded Cs-137 point source with a mobile 4 litre NaI(Tl)-spectrometer. Comparison with observed data.

Report from team: SSM

Describe shield material: Wood

Observed data without gamma spectrometry

Shield thickness observed (m)	Shield material density (kg/m^3)	Shield mass thickness (kg/m^2)	Source detector distance (m)	Air mass thickness (kg/m^2)	Total mass thickness (kg/m^2)
0.27	526.00	142.02	50.00	62.15	204.17

	Measured by gamma spectrometry				Calculated by the "knowledge library" model		
ROI	Background count rate (/s)	Measured gross count rate (/s)	Net count rate (/s)	ROI */PR ratios	Total mass thickness by model (kg/m^2)	Shield mass thickness by model (kg/m^2)	Deviation from observed (%)
A	631.10	1099.00	467.90	7.432	129.17	67.02	-52.8
B	226.11	413.95	187.84	2.984	154.18	92.03	-35.2
C	111.50	232.70	121.20	1.925	171.71	109.56	-22.9
PL	42.97	134.87	91.90	1.460	163.07	100.92	-28.9
PC			0.00				
PR	29.25	92.21	62.96	Average	154.53	92.38	-35.0

Calculation of shield mass thickness from gamma spectrometry on a shielded Cs-137 point source with a mobile 4 litre NaI(Tl)-spectrometer. Comparison with observed data.

Report from team: SSM

Describe shield material: Wood

Observed data without gamma spectrometry

Shield thickness observed (m)	Shield material density (kg/m^3)	Shield mass thickness (kg/m^2)	Source detector distance (m)	Air mass thickness (kg/m^2)	Total mass thickness (kg/m^2)
0.36	526.00	189.36	50.00	62.15	251.51

	Measured by gamma spectrometry				Calculated by the "knowledge library" model		
ROI	Background count rate (/s)	Measured gross count rate (/s)	Net count rate (/s)	ROI */PR ratios	Total mass thickness by model (kg/m^2)	Shield mass thickness by model (kg/m^2)	Deviation from observed (%)
A	631.10	1016.50	385.40	8.411	158.64	96.49	-49.0
B	226.11	377.25	151.14	3.299	186.56	124.41	-34.3
C	111.50	208.52	97.02	2.117	204.55	142.40	-24.8
PL	42.97	112.14	69.17	1.510	196.74	134.59	-28.9
PC			0.00				
PR	29.25	75.07	45.82	Average	186.62	124.47	-34.3

Fig B.5.2d Tables comparing true shielding thickness values for wood blocks of thickness 9, 18, 27 and 36 cm (denoted as observed data) with calculated values based on measured ROI net count rate ratios in the 4 liter SSM NaI(Tl)-detector (R) when using the Lund University exponential model for a 4 liter NaI(Tl)-detector for the calculation (denoted as calculated by the "knowledge library" model). The ROIs (A, B, C, PL and PR) are defined in Table B.5.3

Calculation of shield mass thickness from gamma spectrometry on a shielded Cs-137 point source with a 120% HPGe-spectrometer. Comparison with observed data.

Report from team: SSM

Describe shield material:

Observed data without gamma spectrometry

Shield thickness observed (m)	Shield material density (kg/m^3)	Shield mass thickness (kg/m^2)	Source detector distance (m)	Air mass thickness (kg/m^2)	Total mass thickness (kg/m^2)
0.05	2271.00	113.55	50.00	62.15	175.70

ROI	Background count rate (/s)	Measured gross count rate (/s)	Net count rate (/s)	ROI */PR ratios	Total mass thickness by model (kg/m^2)	Shield mass thickness by model (kg/m^2)	Deviation from observed (%)
	Measured by gamma spectrometry			Calculated by the "knowledge library" model			
A	136.59	257.59	121.00	8.430	184.20	122.05	7.5
B	39.95	81.05	41.10	2.863	204.25	142.10	25.1
C	18.33	40.11	21.78	1.517	198.48	136.33	20.1
P	1.25	15.60	14.35	1.000			-100.0
			0.00	Average	195.64	133.49	17.6

Calculation of shield mass thickness from gamma spectrometry on a shielded Cs-137 point source with a 120% HPGe-spectrometer. Comparison with observed data.

Report from team: SSM

Describe shield material:

Observed data without gamma spectrometry

Shield thickness observed (m)	Shield material density (kg/m^3)	Shield mass thickness (kg/m^2)	Source detector distance (m)	Air mass thickness (kg/m^2)	Total mass thickness (kg/m^2)
0.10	2271.00	227.10	50.00	62.15	289.25

ROI	Background count rate (/s)	Measured gross count rate (/s)	Net count rate (/s)	ROI */PR ratios	Total mass thickness by model (kg/m^2)	Shield mass thickness by model (kg/m^2)	Deviation from observed (%)
	Measured by gamma spectrometry			Calculated by the "knowledge library" model			
A	136.59	211.70	75.11	12.532	272.30	210.15	-7.5
B	39.95	63.39	23.44	3.910	304.78	242.63	6.8
C	18.33	30.11	11.78	1.965	327.74	265.59	17.0
P	1.25	7.24	5.99	1.000			
			0.00	Average	301.61	239.46	5.4

Calculation of shield mass thickness from gamma spectrometry on a shielded Cs-137 point source with a 120% HPGe-spectrometer. Comparison with observed data.

Report from team: SSM

Describe shield material:

Observed data without gamma spectrometry

Shield thickness observed (m)	Shield material density (kg/m^3)	Shield mass thickness (kg/m^2)	Source detector distance (m)	Air mass thickness (kg/m^2)	Total mass thickness (kg/m^2)
0.15	2271.00	340.65	50.00	62.15	402.80

ROI	Background count rate (/s)	Measured gross count rate (/s)	Net count rate (/s)	ROI */PR ratios	Total mass thickness by model (kg/m^2)	Shield mass thickness by model (kg/m^2)	Deviation from observed (%)
	Measured by gamma spectrometry			Calculated by the "knowledge library" model			
A	136.59	186.00	49.41	20.303	379.52	317.37	-6.8
B	39.95	52.68	12.73	5.229	398.54	336.39	-1.3
C	18.33	24.01	5.68	2.332	413.45	351.30	3.1
P	1.25	3.68	2.43	1.000			
			0.00	Average	397.17	335.02	-1.7

Calculation of shield mass thickness from gamma spectrometry on a shielded Cs-137 point source with a 120% HPGe-spectrometer. Comparison with observed data.

Report from team: SSM

Describe shield material:

Observed data without gamma spectrometry

Shield thickness observed (m)	Shield material density (kg/m^3)	Shield mass thickness (kg/m^2)	Source detector distance (m)	Air mass thickness (kg/m^2)	Total mass thickness (kg/m^2)
0.20	2271.00	454.20	50.00	62.15	516.35

ROI	Background count rate (/s)	Measured gross count rate (/s)	Net count rate (/s)	ROI */PR ratios	Total mass thickness by model (kg/m^2)	Shield mass thickness by model (kg/m^2)	Deviation from observed (%)
	Measured by gamma spectrometry			Calculated by the "knowledge library" model			
A	136.59	172.56	35.97	35.838	505.80	443.65	-2.3
B	39.95	47.57	7.62	7.587	518.62	456.47	0.5
C	18.33	20.87	2.54	2.526	453.40	391.25	-13.9
P	1.25	2.25	1.00	1.000			
			0.00	Average	492.61	430.46	-5.2

Calculation of shield mass thickness from gamma spectrometry on a shielded Cs-137 point source with a 120% HPGe-spectrometer. Comparison with observed data.

Report from team: SSM

Describe shield material:

Observed data without gamma spectrometry

Shield thickness observed (m)	Shield material density (kg/m^3)	Shield mass thickness (kg/m^2)	Source detector distance (m)	Air mass thickness (kg/m^2)	Total mass thickness (kg/m^2)
0.25	2271.00	567.75	50.00	62.15	629.90

ROI	Background count rate (/s)	Measured gross count rate (/s)	Net count rate (/s)	ROI */PR ratios	Total mass thickness by model (kg/m^2)	Shield mass thickness by model (kg/m^2)	Deviation from observed (%)
	Measured by gamma spectrometry			Calculated by the "knowledge library" model			
A	136.59	167.31	30.72	80.058	684.41	622.26	9.6
B	39.95	44.97	5.02	13.070	694.06	631.91	11.3
C	18.33	19.52	1.19	3.089	554.01	491.86	-13.4
P	1.25	1.63	0.38	1.000			
			0.00	Average	644.16	582.01	2.5

Calculation of shield mass thickness from gamma spectrometry on a shielded Cs-137 point source with a 120% HPGe-spectrometer. Comparison with observed data.

Report from team: SSM

Describe shield material:

Observed data without gamma spectrometry

Shield thickness observed (m)	Shield material density (kg/m^3)	Shield mass thickness (kg/m^2)	Source detector distance (m)	Air mass thickness (kg/m^2)	Total mass thickness (kg/m^2)
0.30	2271.00	681.30	50.00	62.15	743.45

ROI	Background count rate (/s)	Measured gross count rate (/s)	Net count rate (/s)	ROI */PR ratios	Total mass thickness by model (kg/m^2)	Shield mass thickness by model (kg/m^2)	Deviation from observed (%)
	Measured by gamma spectrometry			Calculated by the "knowledge library" model			
A	136.59	164.80	28.21	183.501	868.73	806.58	18.4
B	39.95	43.41	3.46	22.476	868.94	806.79	18.4
C	18.33	18.58	0.25	1.596	223.80	161.65	-76.3
P	1.25	1.40	0.15	1.000			
			0.00	Average	653.83	591.68	-13.2

Fig B.5.2e Tables comparing true shielding thickness values for concrete tiles of thickness 5, 10, 15, 20, 25 and 30 cm (denoted as observed data) with calculated values based on measured ROI net count rate ratios in the SSM 120% HPGe-detector when using the Lund University exponential model for a 123% HPGe-detector for the calculation (denoted as calculated by the "knowledge library" model). The ROIs (A, B, C and P) are defined in Table B.5.4

Calculation of shield mass thickness from gamma spectrometry on a shielded Cs-137 point source with a 120% HPGe-spectrometer. Comparison with observed data.

Report from team: SSM

Describe shield material:

Observed data without gamma spectrometry

Shield thickness observed (m)	Shield material density (kg/m^3)	Shield mass thickness (kg/m^2)	Source detector distance (m)	Air mass thickness (kg/m^2)	Total mass thickness (kg/m^2)
0.09	526.00	47.34	50.00	62.15	109.49

Measured by gamma spectrometry / Calculated by the "knowledge library" model

ROI	Background count rate (/s)	Measured gross count rate (/s)	Net count rate (/s)	ROI */PR ratios	Total mass thickness by model (kg/m^2)	Shield mass thickness by model (kg/m^2)	Deviation from observed (%)
A	136.59	290.02	153.43	6.313	119.94	57.79	22.1
B	39.95	95.86	55.91	2.300	133.65	71.50	51.0
C	18.33	47.73	29.40	1.209	85.20	23.05	-51.3
P	1.25	25.55	24.30	1.000			
			0.00	Average	112.93	50.78	7.3

Calculation of shield mass thickness from gamma spectrometry on a shielded Cs-137 point source with a 120% HPGe-spectrometer. Comparison with observed data.

Report from team: SSM

Describe shield material:

Observed data without gamma spectrometry

Shield thickness observed (m)	Shield material density (kg/m^3)	Shield mass thickness (kg/m^2)	Source detector distance (m)	Air mass thickness (kg/m^2)	Total mass thickness (kg/m^2)
0.18	526.00	94.68	50.00	62.15	156.83

Measured by gamma spectrometry / Calculated by the "knowledge library" model

ROI	Background count rate (/s)	Measured gross count rate (/s)	Net count rate (/s)	ROI */PR ratios	Total mass thickness by model (kg/m^2)	Shield mass thickness by model (kg/m^2)	Deviation from observed (%)
A	136.59	259.10	122.51	7.428	156.07	93.92	-0.8
B	39.95	81.48	41.53	2.518	162.78	100.63	6.3
C	18.33	41.28	22.95	1.391	155.17	93.02	-1.8
P	1.25	17.74	16.49	1.000			
			0.00	Average	158.00	95.85	1.2

Calculation of shield mass thickness from gamma spectrometry on a shielded Cs-137 point source with a 120% HPGe-spectrometer. Comparison with observed data.

Report from team: SSM

Describe shield material:

Observed data without gamma spectrometry

Shield thickness observed (m)	Shield material density (kg/m^3)	Shield mass thickness (kg/m^2)	Source detector distance (m)	Air mass thickness (kg/m^2)	Total mass thickness (kg/m^2)
0.27	526.00	142.02	50.00	62.15	204.17

Measured by gamma spectrometry / Calculated by the "knowledge library" model

ROI	Background count rate (/s)	Measured gross count rate (/s)	Net count rate (/s)	ROI */PR ratios	Total mass thickness by model (kg/m^2)	Shield mass thickness by model (kg/m^2)	Deviation from observed (%)
A	136.59	233.88	97.29	8.554	187.44	125.29	-11.8
B	39.95	72.00	32.05	2.817	199.08	136.93	-3.6
C	18.33	35.22	16.89	1.485	187.67	125.52	-11.6
P	1.25	12.62	11.37	1.000			
			0.00	Average	191.40	129.25	-9.0

Calculation of shield mass thickness from gamma spectrometry on a shielded Cs-137 point source with a 120% HPGe-spectrometer. Comparison with observed data.

Report from team: SSM

Describe shield material:

Observed data without gamma spectrometry

Shield thickness observed (m)	Shield material density (kg/m^3)	Shield mass thickness (kg/m^2)	Source detector distance (m)	Air mass thickness (kg/m^2)	Total mass thickness (kg/m^2)
0.36	526.00	189.36	50.00	62.15	251.51

Measured by gamma spectrometry / Calculated by the "knowledge library" model

ROI	Background count rate (/s)	Measured gross count rate (/s)	Net count rate (/s)	ROI */PR ratios	Total mass thickness by model (kg/m^2)	Shield mass thickness by model (kg/m^2)	Deviation from observed (%)
A	136.59	216.40	79.81	10.098	224.32	162.17	-14.4
B	39.95	65.21	25.26	3.195	239.68	177.53	-6.2
C	18.33	31.62	13.29	1.681	249.76	187.61	-0.9
P	1.25	9.15	7.90	1.000			
			0.00	Average	237.92	175.77	-7.2

Fig B.5.2f Tables comparing true shielding thickness values for wood blocks of thickness 9, 18, 27 and 36 cm (denoted as observed data) with calculated values based on measured ROI net count rate ratios in the SSM 120% HPGe-detector when using the Lund University exponential model for a 123% HPGe-detector for the calculation (denoted as calculated by the “knowledge library” model). The ROIs (A, B, C, and P) are defined in Table B.5.4

Table B.5.5 Coefficients a and b in the expression for determining the shield mass thickness $x = \ln(q/a)/b$ where q is the respective measured count rate ratios of ROIs A/PR, B/PR, C/PR and PL/PR, as obtained in the experimental measurements by SSM using two 4 liter NaI(Tl)-detectors (L) and (R) compared to the coefficients in the Lund University (LU) “knowledge-library” model.

		ROI A/PR		ROI B/PR		ROI C/PR		ROI PL/PR	
Team	NaI(Tl) detector volume	a	b	a	b	a	b	a	b
LU	4 liter	4.32	0.0042	1.85	0.0031	1.17	0.0029	1.24	0.0010
SSM (L)	4 liter	2.81	0.0048	1.42	0.0039	1.11	0.0026	1.14	0.0012
SSM (R)	4 liter	2.92	0.0048	1.38	0.0040	1.10	0.0026	1.13	0.0012

Table B.5.6. Coefficients *a* and *b* in the expression for determining the shield mass thickness $x = \ln(q/a)/b$ where *q* is the respective measured count rate ratios of ROIs A/P, B/P and C/P, as obtained in the experimental measurements by SSM using a 120% HPGe-detector compared to the coefficients in the Lund University (LU) "knowledge-library" model for a 123% HPGe-detector.

		ROI A/P		ROI B/P		ROI C/P	
Team	HPGe detector efficiency	*a*	*b*	*a*	*b*	*a*	*b*
LU model	123%	3.68	0.0045	1.52	0.0031	1.02	0.0020
SSM	120%	3.50	0.0047	1.50	0.0033	1.01	0.0019

B.5.5 Conclusion

Results for the HPGe detector agrees surprisingly well with the data supplied from the Lund University "knowledge library" model. The deviation between the model and observed results were generally less than 10 per cent in all measurements (slightly more for 5 cm and 30 cm concrete shielding). However, the detector used is very similar to the detector used by Lund University in the development of the knowledge library.

The discrepancies between model and measurement results were larger for the NaI(Tl) detectors, and in particular when less shielding was applied.

Bibliographic Data Sheet **NKS-448**

Title	Detection of orphan gamma radiation sources in shielded building geometries by mobile gamma spectrometry. A method of using Compton scattered radiation to estimate the shielding mass thickness of common building material.
Author(s)	Christopher L. Rääf[1], Robert R. Finck[1], Vikas C. Baranwal[5], Jonas Boson[6], Antanas Bukartas[1], Marie-Andrée Dumais[5], Kjartan Guðnason[4], Marjan Ilkov[4], Gísli Jónsson[4], Mattias Jönsson1, Simon Karlsson[6], Marie Lundgaard Davidsdóttir[2], Frode Ofstad[5], Jan Steinar Rønning[5], Petri Smolander[3], Mikael Westin[6]
Affiliation(s)	[1]Medical Radiation Physics, ITM, Lund University, Sweden [2]Danish Emergency Management Agency, Denmark [3]Radiation and Nuclear Safety Authority, Finland [4]Icelandic Radiation Safety Authority, Iceland [5]Geological Survey of Norway, Norway [6]Swedish Radiation Safety Authority, Sweden
ISBN	978-87-7893-540-3
Date	June 2021
Project	NKS-B / SHIELDMORC, Contract: AFT/B(20)1
No. of pages	73
No. of tables	48
No. of illustrations	28
No. of references	11
Abstract max. 2000 characters	If nuclear or radioactive materials are out of control (materials out of regulatory control, MORC), authorities must deal with the threatening situation. Gamma-ray sources out of control can have various degrees of shielding. When located in a building the building material shields the source. Information on the shielding of an identified source will provide data to estimate the radiation hazard and assist in securing the source. In a Nordic joint project, a method to assess shielding mass thickness of common building materials in cases with hidden Cs-137 point sources have been studied and experimentally investigated using mobile gamma spectrometry. The method uses detection of Compton scatted photons of different energies in relation to primary photons to obtain approximate information about the mass thickness of shielding material between the source and the detector. These ratios follow the expression of exponential functions of shield mass thickness, provided the shield is composed mainly of materials where Compton interaction dominates. The shielding thickness assessment method is based on previous detector response

calibration measurements for well-known shielding geometries, thus determining function parameters. In the experiments, attempts to determine shield thickness from a measured pulse height distribution using various NaI(Tl) spectrometers and applying the exponential function produced values within ±50% of the true value. When applying the method to a HPGe spectrometer, the difference between measured and actual values was less than ±10%.

Key words Mobile gamma spectrometry, orphan sources, shielding